NASA CR-135125
TE 4202-12-77

HIGH EFFICIENCY
THERMIONIC CONVERTER STUDIES

REPRODUCIBLE COPY
(FACILITY CASEFILE COPY)

by F. N. Huffman, A.H. Sommer, C.L. Balestra
T.R. Briere, D.P. Lieb and P.E. Oettinger

THERMO ELECTRON CORPORATION

prepared for

NATIONAL AERONAUTICS AND SPACE ADMINISTRATION

1. Report No. NASA CR-135125	2. Government Accession No.	3. Recipient's Catalog No.
4. Title and Subtitle HIGH EFFICIENCY THERMIONIC CONVERTER STUDIES		5. Report Date November 1976
		6. Performing Organization Code
7. Author(s) F. N. Huffman, A. H. Sommer, C. L. Balestra, T. R. Briere, D. P. Lieb, P. E. Oettinger		8. Performing Organization Report No. TE4202-12-77
		10. Work Unit No.
9. Performing Organization Name and Address Thermo Electron Corporation 85 First Avenue Waltham, Mass. 02154		
		11. Contract or Grant No. NAS3-19866
12. Sponsoring Agency Name and Address National Aeronautics and Space Administration Washington, DC 20546		13. Type of Report and Period Covered Contractor Report 7/1/75 - 6/30/76
		14. Sponsoring Agency Code

15. Supplementary Notes

Project Manager, James Morris, Thermionics and Heat Pipe Section, NASA Lewis Research Center, Cleveland, Ohio

16. Abstract

This report summarizes the NASA sponsored studies conducted at Thermo Electron Corporation during FY1976 relevant to the development of high efficiency thermionic converters. The objective of these studies is to improve thermionic converter performance by means of reduced interelectrode losses, greater emitter capabilities and lower collector work functions until the converter performance level is suitable for out-of-core space reactors and radioisotope generators. Electrode screening experiments have identified several promising collector materials. Back emission work function measurements of a ZnO collector in a thermionic diode have given values less than 1.3 eV. Diode tests have been conducted over the range of temperatures of interest for space power applications. Enhanced mode converter experiments have included triodes operated in both the surface ionization and plasmatron modes. Pulsed triodes have been studied as a function of pulse length, pulse potential, inert gas fill pressure, cesium pressure, spacing, emitter temperature and collector temperature. Current amplifications (i.e., mean output current/mean grid current) of several hundred have been observed up to output current densities of one amp/cm^2. These data correspond to an equivalent arc drop less than 0.1 eV.

17. Key Words (Suggested by Author(s)) Thermionic converter Emitter Collector Plasma arc drop Barrier Index	18. Distribution Statement Unclassified - unlimited	
19. Security Classif. (of this report) Unclassified	20. Security Classif. (of this page) Unclassified	21. No. of Pages 123	22. Price* 3.00

Page
Intentionally
Left Blank

TABLE OF CONTENTS

TABLE OF CONTENTS (Continued)

TABLE OF CONTENTS (Continued)

SUMMARY

In order to provide design flexibility for space missions, thermionic converters must operate efficiently at reduced emitter temperatures. Maintaining converter efficiency while operating at reduced temperatures requires improved emitter and collector electrodes as well as decreased potential losses in the plasma as the electrons flow across the interelectrode space. The effort described in the report addresses both the electrode and plasma problems.

Electrode screening studies have identified several candidate materials (e. g., LaB_6, BaO and ZnO) that have passed short term chemical compatibility tests. These materials are being incorporated into thermionic diodes. A ZnO collector has given a back emission work function of less than 1.3 eV. However, coating resistance and cesium vapor pressure mismatches with the emitter have thus far prevented the realization of the corresponding diode performance. A diode with a carbon emitter indicates that this material may be useful for applications requiring low emitter vaporization.

Diodes with LaB_6 collectors have been constructed to study controlled oxygen addition via a heated silver tube. Triode converters utilizing a grid between the emitter and collectors have been built to investigate plasma loss reduction. Plasmatron operation is more promising than operation in the surface ionization mode.

Pulsed operation of the triode gives better performance than steady potentials because it enables higher voltages to be applied in the cesium-xenon atmosphere without breakdown. The higher grid potential provides more favorable collision cross sections, improved ionization efficiency and higher converter performance. Equivalent arc drops less than 0.1 eV have been measured at load current densities less than one amp/cm^2. An alternate means of attacking the arc drop problem is to eliminate the need for the plasma by spacing the emitter and collector close enough to overcome the electron space charge. Although such spacings present difficult mechanical problems, a design concept for a particulate spaced diode has been formulated which may be practical.

1

Page
Intentionally
Left Blank

I. INTRODUCTION

Thermionic energy conversion is well suited for space applications. The conversion efficiency and high temperature of heat rejection minimize the size and weight of the radiator. Consequently, thermionic systems with high power-to-weight ratios are possible. In addition to the inherent reliability potential of static conversion, thermionics can be designed to eliminate single point system failures. The feasibility of thermionic conversion for space applications has been demonstrated by a variety of reactor and radioisotope systems.

To date, most of the thermionic reactor development has been concentrated on in-core systems. The U.S. program in the sixties as well as the U.S.S.R. TOPAZ reactors were based on thermionic converters inside the core. However, lower temperature out-of-core designs have the advantages of reduced shield weight and increased program flexibility. In order to obtain as low a specific weight system out-of-core as in-core, it is necessary to maintain thermionic performance (i.e., efficiency and power density) at lower operating temperatures. This goal requires advances in thermionic converter technology. The avenues to better thermionic performance are improved electrodes (emitter and collector) and reduced plasma arc drop.

This report summarizes the NASA-sponsored studies at Thermo Electron Corporation during FY 1976 for the development of high efficiency thermionic converters. The objective of these studies is to improve thermionic converter performance by means of reduced interelectrode losses, greater emitter capabilities and lower collector work functions until the converter performance level is suitable for space reactors and radioisotope generators. This program complements an ERDA advanced thermionic technology effort which has the development of thermionic topped fossil fuel powerplants as its primary objective.

This report describes the basic surface experiments in Section II, the thermionic diode tests in Section III, the triode converter investigations in Section IV, and the Powder Puff Diode experiments in Section V. The results of these studies are discussed in Section VI and conclusions are drawn in Section VII.

3

Page
Intentionally
Left Blank

II. BASIC SURFACE EXPERIMENTS

A. ACTIVATION CHAMBER STUDIES

1. General Considerations

a. Introduction

The purpose of the experiments described in this section is to find
a collector material having a work function below 1.4 eV and, preferably,
below 1.3 eV. It is well known that many cesium-activated semiconductors
have a work function in the desired range. The difficulty of finding a suitable
collector material arises from the fact that low work function is a nec-
essary, but not a sufficient, requirement for a collector material. The
three most important additional requirements are:

- Chemical stability in converter environment (i. e., at high
  temperatures and in a cesium atmosphere).

- Low bulk and contact resistance to permit current flow of
  at least 10 amp/cm^2 with potential drops less than 0.05
  volt.

- Compatibility with emitter material. It is important
  that the lowest work function be obtained at a cesium
  vapor pressure (cesium reservoir temperature) at
  which the work function of the emitter gives current
  densities of the order of 10 amp/cm^2.

Other desirable characteristics of a collector material include low
thermal emissivity, low electron reflectivity, low cost of material and
ease of fabrication.

The time and effort required to test a large number of prospective
collector materials in experimental diodes would be prohibitive. In
principle, there are two ways of screening materials. First, solid
state theory may be of help in choosing promising materials.
Second, simple experimental procedures relative to thermionic diode
evaluation can be used to quickly test many materials. These two
approaches are discussed briefly below.

b. Qualitative Theoretical Considerations

The thermionic work function of a semiconductor depends on so
many factors and is so sensitive to the chemical nature of the monatomic
surface layer that no theory is, at this time, quantitative enough to

predict the absolute value of the work function of a semiconductor. However, there exist some qualitative considerations which deserve a brief discussion because they have produced useful results.

Every semiconductor can be described in terms of an energy band model. Figure 1 shows the most simplified band model of an "intrinsic" semiconductor. The thermionic work function is given by the energy difference between Fermi level and vacuum level. It is apparent from the figure that low work function requires: (1) a small energy difference between Fermi level and conduction band edge, and (2) a low electron affinity.

The position of the Fermi level is a bulk property of the material. The Fermi level is in the center of the "forbidden gap" only in an intrinsic semiconductor. It is closer to the valence band in a p-type material and closer to the conduction band in an n-type material. Hence, n-type materials appear most promising for thermionic electrodes with low work function.

The value of the electron affinity is predominantly a surface property. There are theoretical considerations which indicate the position of the vacuum level is lowered by forming a surface layer consisting of a monolayer (or less) of an electropositive element adsorbed on an electronegative element. Experiments have abundantly confirmed this emission model. All materials that are known to have a work function less than 1.3 eV contain cesium (the most electropositive element) in combination with oxygen (the most electronegative element next to fluorine). There are reasons why oxygen is more effective than fluorine, but this subject is beyond the scope of this report. Moreover, theoretical and experimental evidence indicates that the electron affinity decreases with increasing binding forces between the oxygen and the cesium.

In summary, it appears that strongly n-type semiconductors with an oxygen-cesium surface layer are the most promising for low work function collectors.

c.   Experimental Methods

Confining ourselves to a consideration of the four main requirements stated previously; vis., low work function, chemical stability, low resistance and compatibility with the emitter — it appears that valid data on the two last-named requirements can be obtained only in an operating thermionic diode. Therefore, the experimental work reported in this section has been concerned primarily with the first two requirements.
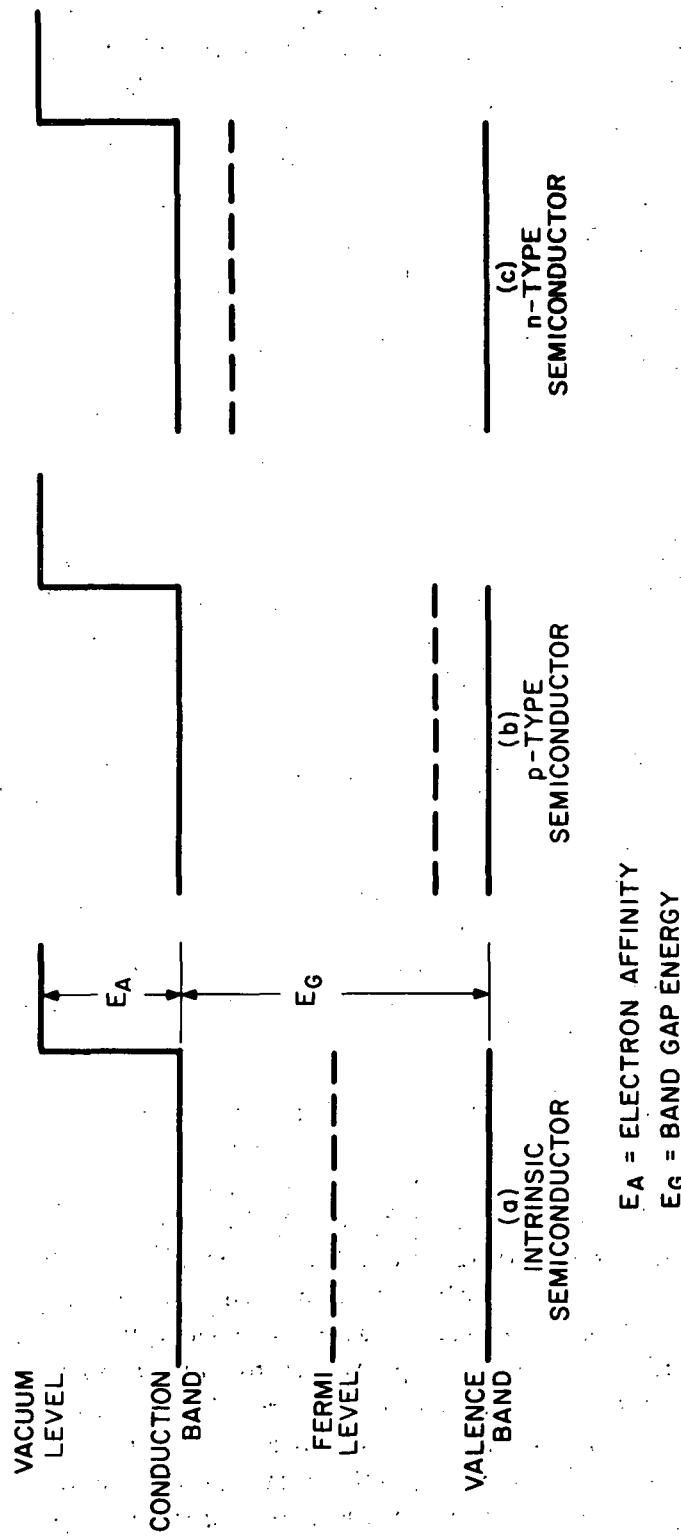
Figure 1. Band Gap Diagrams

768-3

VACUUM LEVEL

CONDUCTION BAND

FERMI LEVEL

VALENCE BAND

E_A

E_G

(a)
INTRINSIC
SEMICONDUCTOR

(b)
p-TYPE
SEMICONDUCTOR

(c)
n-TYPE
SEMICONDUCTOR

E_A = ELECTRON AFFINITY
E_G = BAND GAP ENERGY

7

Stability tests were performed in a "simulated" converter in which the material to be studied can be exposed to high cesium vapor pressure of several torr at temperatures up to 1000 K. In this simple device it is not possible to make electron emission or other electrical measurements. The main purpose is to observe changes in the material after exposure to cesium (usually about 100 hours) at high temperature. This test has proven valuable in eliminating potential collector materials. Typical examples, described in earlier reports, are single crystal gallium arsenide and germanium which emerged from the test in the form of a black powder, obviously the result of chemical reaction with cesium.

The emphasis of the experimental work described in this chapter is on work function measurements of materials that have passed the preliminary chemical stability test. The "Activation Chamber" used for these tests has been described before, so a brief summary of the essential features of this equipment will suffice.

Figure 2 is a diagrammatic representation of the Activation Chamber. The sample is mounted in such a way that it can be heated indirectly by a filament while the temperature is measured with a thermocouple spot-welded to the support. The cesium source consists of a cesium "channel" from which well controlled amounts of cesium are released by resistance heating. Oxygen is introduced through a silver tube by heating the tube to a temperature where it passes oxygen. For emission measurements, an electrode close to the sample is maintained at a positive potential relative to the sample. Useful information about the effect of cesium is obtained from photoemission measurements because these can be performed at room temperature where thermionic emission is immeasurably low. Therefore the vacuum system is provided with a window to admit light to the sample. Where desirable, the photoemission measurements can be refined by using monochromatic light.

Since the Activation Chamber is continuously pumped, the cesium pressure can never be raised to the values typical for an operational thermionic converter. This characteristic leads to three limitations. First, the cesium pressure may not reach the value required for lowest work function. This is a minor limitation because it means that, at worst, the measured value is higher than would be obtainable in a diode. Also, as will be discussed later, in some cases optimum cesium pressure is definitely obtained because, on pumping out the cesium, the work function decreases. Second, the work function cannot be measured at temperatures above approximately 550 K because the surface is destroyed by cesium evaporation. Third, the material, while stable at the low cesium pressures of the Activation Chamber, may suffer a chemical change at the higher

752-2A

CERAMIC GUARD

THERMOCOUPLE

SILVER TUBE
HEATER } OXYGEN SOURCE

LIGHT SOURCE

CESIUM CHANNEL

COLLECTING RING

SAMPLE

SAMPLE HOLDER

SAMPLE HEATER

TO VAC-ION SYSTEM
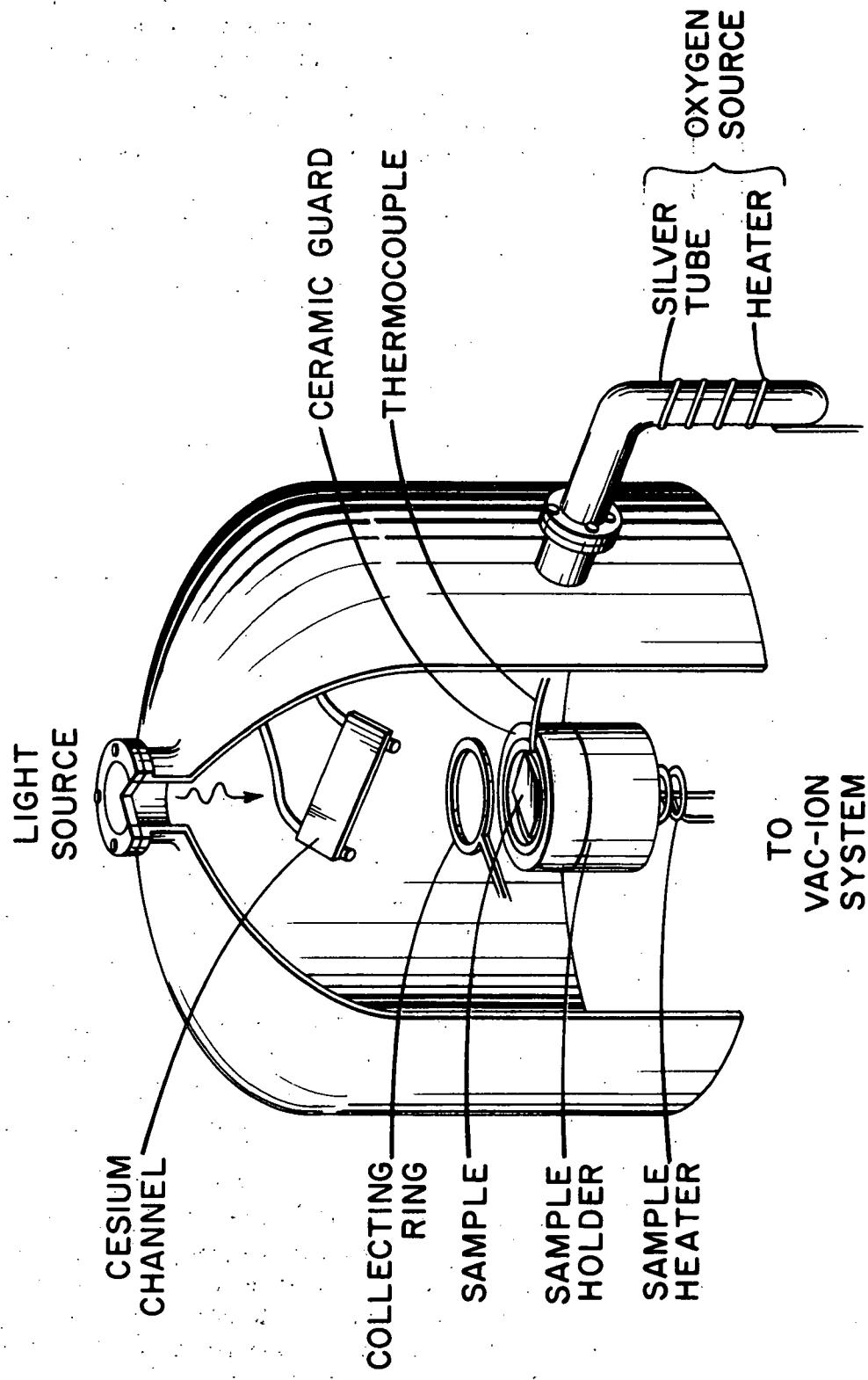
Figure 2. Cutaway View of the Activation Chamber

pressures prevailing in the diode. Another disadvantage of the Activation Chamber is that the operation of the cesium channel during the current measurement confuses the data (due to thermal radiation from the hot channel). Consequently, the data from this equipment is nonequilibrium and does not permit a determination of T/T_R (i. e., electrode temperature/ effective cesium reservoir temperature) for a given work function.

The limitations of the Activation Chamber are more than balanced by its two great advantages. First, the system is so simple that it takes only one to two days to test a sample (including mounting, pumping and degassing). Second, while some materials that look promising in the Activation Chamber may not be stable in the converter, no material with too high a work function in the Activation Chamber need be considered for a diode. Thus, the combination of the Activation Chamber work function tests and the "simulated converter" chemical compatibility evaluations reduces the number of materials worth investigating in a thermionic diode to a manageable size.

Before discussing the results obtained with experiments in the Activation Chamber, one specific problem must be mentioned, which does not arise in the Activation Chamber, but is important for use of a material as a collector in the thermionic converter. As discussed previously, best results are obtained with an oxygen-cesium surface film.

In the diode configuration, the cesium is introduced from a cesium reservoir, and a constant pressure is maintained by holding the reservoir at the appropriate temperature. Oxygen can be supplied by two methods. The first consists of using an oxide as the basic material, a typical example is barium oxide. The second method used for materials that do not contain oxygen (e. g., lanthanum hexaboride) requires the introduction of gaseous oxygen into the interelectrode space. The controlled admission of oxygen into the Activation Chamber is easy because the Activation Chamber is evacuated after release of cesium so that oxygen diffusing through the heated silver tube can reach the cesiated sample and react with the cesiated electrode. Moreover, admission of cesium and oxygen can be alternated to produce the optimum cesium-oxygen surface film.

Controlled admission of oxygen in the diode presents two difficulties. First, any oxygen entering the diode will immediately react with the ever-present cesium vapor. To maintain constant optimum cesium and oxygen pressures, it is therefore necessary to continuously replenish both cesium and oxygen at a critical rate. Second, the close spacing of the electrodes makes it difficult to obtain a uniform Cs:O ratio within the interelectrode space, assuming the oxygen enters from outside this space. In principle,

this difficulty is avoided if the oxygen is produced from one of the electrodes. Our best diode performance has been achieved by using a tungsten oxide collector which dispenses oxygen during operation. However, optimization is difficult because the temperature of the collector is a compromise that must simultaneously: (1) dispense oxygen to the emitter, (2) provide a low collector work function, and (3) be low enough to limit back emission.

The most satisfactory solution to supplying oxygen to a thermionic converter would be a cesium oxide reservoir that would supply an equilibrium cesium and oxygen atmosphere of the proper composition. Experiments by Pigford, et al., have indicated that such a reservoir may be feasible.

Another alternative, tried with limited success in the past, consists of diffusing oxygen to the collector surface through a silver membrane. Again, this technique requires that the collector be held at the critical temperature that produces optimum Cs:O ratio. Moreover, the mechanical problems associated with the silver membrane are formidable because the membrane has little strength at temperatures at which appreciable oxygen permeation takes place.

The preceding discussion leads to the conclusion that, until an improved method for introducing gaseous oxygen into the converter has been developed, it is appropriate to explore oxides as potential collector materials. The following section of this report will show that this conclusion was acted upon during the past year. Nonoxide materials were investigated primarily for their potential use as emitter materials. A brief discussion of emitter material problems will be given in Section 3.

2. Experimental Results

To illustrate the versatility and simplicity of the Activation Chamber, Table I lists in chronological order all 65 work function tests carried out during the year. It would be confusing and of little interest to describe the individual experiments in detail. Therefore, the most significant results are summarized briefly in tabular form. Some materials were studied for other aspects of the converter project and will not be discussed (Nos. 75, 85, 86, 88, 90, 92, 120). As is apparent from this table, the two most thoroughly investigated materials were barium oxide (BaO) and zinc oxide (ZnO). These materials will be discussed more fully after a brief survey of the other materials that were tested only once or twice. All the work function values in the tables in this report were obtained by determining the thermionic emission current at a measured temperature and computing the work function from the Richardson equation by assuming the Richardson constant, A, to be 120 $amp/(cm^2-K^2)$.

TABLE I

EXPERIMENTS IN ACTIVATION CHAMBER
JULY 1, 1975 TO July 1, 1976

7612-1a

No.	Material	Chemical Formula of base material	Activated with
72	Sprayed Europium Carbonate reduced to oxide	Eu_2O_3	Cs and O_2
73	Sprayed Ytterbium Carbonate, reduced to oxide	Yb_2O_3	Cs and O_2
74	Repeat of #73	Yb_2O_3	
75	Magnesium Oxide (for triode grid)	MgO	Cs and O_2
76	Sprayed Barium Carbonate, reduced to oxide	BaO	for use in diode
77	Sprayed Lanthanum Carbonate, reduced to oxide	La_2O_3	Cs and O_2
78	Sprayed Europium Carbonate, reduced to oxide	Eu_2O_3	Cs and O_2
79	Sprayed Lanthanum Sulfide	La_2S_3	Cs and O_2
80	Sprayed Lanthanum Hexaboride	LaB_6	Cs and O_2
83	Sprayed Strontium Oxide	SrO	Cs and O_2
84	Sprayed Strontium Carbonate, reduced to oxide	SrO	Cs and O_2
85	Philips Dispenser Cathode	BeO	Cs and O_2
86	Philips Dispenser Cathode	BaO	Cs
87	Repeat of #84	SrO	
88	Repeat of #86	BaV	
89	Sprayed Calcium Carbonate, reduced to oxide	CaO	Cs and O_2

12

TABLE I (Continued)

7612-1b

No.	Material	Chemical Formula of base material	Activated with
90	Repeat of #86	BaO	
91	Evaporated Barium Oxide	BaO	Cs
92	Repeat of #86	BaO	
93	Repeat of #91	Bao	
94	Evaporated Strontium Oxide	SrO	Cs
95	Internally evaporated Barium Oxide	BaO	Cs and O_2
96	Repeat of #95	BaO	
97	Barium Oxide evaporated onto Silver substrate	BaO	Cs
98	Repeat of #97	BaO	
99	Evaporated Barium Oxide	BaO	Ag, Cs and O_2
100	Evaporated Zinc Oxide	ZnO	Cs
102	Evaporated Zinc Oxide	ZnO	Cs and O_2
103	Pre-evaporated Zinc Oxide (exposed to air)	ZnO	Cs and O_2
106	Repeat of #100	ZnO	
107	Sprayed Zinc Oxide	ZnO	Cs
108	Pre-evaporated Zinc Oxide	ZnO	Cs
109	Repeat of #105	ZnO	
110	Sprayed Zinc Oxide, exposed to air after heating	ZnO	Cs and O_2
111	Repeat of #105	ZnO	
112	Repeat of #100	ZnO	

TABLE I (Continued)

No.	Material	Chemical Formula of base material	Activated with
113	Repeat of #100	ZnO	
114	Repeat of #100	ZnO	
115	Repeat of #100	ZnO	
116	Repeat of #107	ZnO	
117	Single crystal Zinc Oxide (Oxygen face)	ZnO	Cs
118	Repeat of #117	ZnO	
119	Single crystal Zinc Oxide (Zinc face)	ZnO	Cs
120	Zirconium Oxide	ZrO	Cs and O_2

a. <u>Rare Earth Oxides</u> (Table II)

In the absence of cesium, the work functions of lanthanum oxide, europium oxide, and ytterbium oxide are above 3 eV. Cesium reduces these work functions to the 1.4 to 1.5 eV range and cesium-oxygen alternation to the 1.1 eV range.

b. <u>Rare Earth Sulfides and Hexaborides</u> (Table III)

Lanthanum sulfide was evaluated because of its high electrical conductivity and thermal stability. As Table III shows, no thermionic emission was measurable even after Cs/O activation. The lanthanum hexaboride result is in agreement with earlier measurements. Cerium hexaboride had a high work function in all stages, but the results of this single experiment should not be accepted as final.

c. <u>Transition Metal Diborides</u> (Table IV)

In a recent publication from the Soviet Union (ref. 1), it was reported that cesiated diborides of some transition metals have work functions as low as 1.25 eV. In an attempt to duplicate these results, the diborides of tantalum, zirconium and titanium were studied in the Activation Chamber. In all three cases, cesium activation produced work functions above 1.7 eV, although cesium-oxygen alternations reduced the work functions to very low values. Since only one experiment was performed with each material, the differences in the minimum values of the three diborides may not be significant. All materials were deposited on a nickel substrate by spraying an emulsion of the powders.

d. <u>Refractory Metals</u> (Table V)

The main purpose of these experiments was to find out whether the minimum work functions in the 1.0 to 1.1 eV region obtained after cesium-oxygen alternations with most semiconducting substrates were a characteristic of cesium oxide or of the substrate material. Table V shows that after cesium-oxygen alternations the minimum work function of all four metals was about 0.2 eV higher than that of many semiconductors. These data indicate that the substrate material does influence the minimum work function value. Of course, the cesium-oxygen surface is still essential for the work function to be below 1.3 eV. As indicated in Table V, the relatively low work function values after activation with only cesium are probably explained by incomplete heat-cleaning of the surface (i.e., by the presence of small amounts of oxygen).

7612-2

TABLE II

WORK FUNCTION (eV) OF RARE EARTH OXIDES

MATERIAL	BARE	MINIMUM CESIUM	MINIMUM CESIUM/ OXYGEN
Lanthanum Oxide	> 3 (1200 K)	> 1.50 (450 K)	1.12 (450 K)
Europium Oxide	> 3 (1200 K)	1.43 (525 K)	1.14 (450 K)
Ytterbium Oxide	> 3 (1000 K)	1.52 (600 K)	1.05 (450 K)

16

TABLE III

WORK FUNCTION (eV) OF RARE EARTH SULFIDES AND HEXABORIDES

MATERIAL	BARE	MINIMUM CESIUM	MINIMUM CESIUM/ OXYGEN
Lanthanum Sulfide	> 3	> 3	> 3
Lanthanum Hexaboride	2.57 (900 K)	1.68 (600 K)	1.12 (450 K)
Cerium Hexaboride	2.75 (1100 K)	>1.8 (600 K)	1.24 (450 K)

7612-4

TABLE IV

WORK FUNCTION (eV) OF TRANSITION METAL BORIDES

MATERIAL	BARE	MINIMUM CESIUM	MINIMUM CESIUM/ OXYGEN
Tantalum Diboride	> 3	> 1.7 (550 K)	1.06 (450 K)
Zirconium Diboride	> 3	> 1.7 (550 K)	1.25 (450 K)
Titanium Diboride	> 3	> 1.7 (550 K)	1.10 (450 K)

7612-5

TABLE V

WORK FUNCTION (eV) OF REFRACTORY METALS*

MATERIAL	MINIMUM CESIUM	MINIMUM CESIUM/ OXYGEN
Tungsten	1.40 (500 K)	1.21 (450 K)
Titanium	1.47 (500 K)	1.23 (450 K)
Tantalum	>1.5 (500 K)	1.25 (450 K)
Molybdenum	1.43 (500 K)	1.25 (450 K)

*Surfaces Not Atomically Clean

e. <u>Gallium Oxide</u> (Ga_2O_3)

Two samples of sprayed gallium oxide were activated. This material was chosen because it is known from the activation of GaAs negative affinity photocathodes that it is very difficult to reduce surface films of gallium oxide. This tight binding of the oxygen indicates that a stable surface film with cesium may be obtainable. There is no information in the literature about the work function of cesiated Ga_2O_3.

After heat-cleaning the Ga_2O_3 deposit at 870 K, exposure to cesium vapor produced work functions in the range of 1.4 to 1.5 eV. Subsequent alternation of cesium and oxygen produced work function values as low as 1.04 eV at 400 K.

f. <u>Silicon</u>

Because of the promising results reported by Jet Propulsion Laboratory (K. M. Chang and K. Shimada at the ERDA/NASA TEC-ART Program Review held in Austin, Texas, May 1976) for cesium activation of polycrystalline silicon, a preliminary experiment was performed. Silicon powder was sprayed in the conventional way onto a nickel substrate and exposed to cesium vapor after degassing at 700 C. A work function of 1.43 eV was obtained, quite similar to that reported some time ago for single crystal silicon. In both cases the surface was not atomically clean because residual oxygen is not removed at temperatures below 1300 C. A single exposure to oxygen did not – as reported by JPL – reduce the work function, but repeated cesium-oxygen alternations reduced the work function to 1.09 eV.

g. <u>Alkaline Earth Oxides</u> (Table VI)

The barium oxide (more correctly the barium-strontium-calcium oxide) thermionic cathode has been in commercial use for many decades because of its low work function, low cost and ease of fabrication. Therefore, from the start of the surface study program, this and related materials have been given a great deal of attention.

The first experiments were performed with sprayed commercial BaO (i. e., (BaSrCa) O) (RCA type AG 010170) and indicated that, with cesium activation, work functions in the 1.3 - 1.4 eV range can be obtained. Initial diode experiments indicated that the resistance of sprayed layers of this material may be too high for the large currents required for diode operation. Therefore, it now seems advisable to work with evaporated materials which can be produced in much thinner films so that their bulk resistance will be much lower than sprayed deposits. Of course, interface (or "junction") resistance effects may still be a problem. It would be difficult to evaporate films of the mixed oxides but, from work done at the Naval Research

TABLE VI

WORK FUNCTION (eV) OF ALKALINE EARTH OXIDES

7612-6

MATERIAL	BARE	MINIMUM CESIUM	MINIMUM CESIUM/ OXYGEN
Commercial Barium Oxide* (Ba, Sr, Ca)O (Sprayed)	1.56 (600 K)	1.34 (500 K)	1.16 (450 K)
Barium Oxide (Evaporated)	1.50 (600 K)	1.38 (500 K)	No Change
Strontium Oxide (Sprayed)	2.0 (800 K)	1.4 (?) (500 K)	
Strontium Oxide (Evaporated)	2.0 (800 K)	1.4 (?) (500 K)	
Calcium Oxide (Sprayed)	2.6 (1000 K)	1.4 (?) (500 K)	

*RCA Type AG 010170

21

Laboratory (private communication, R. E. Thomas), it is known that the work function of evaporated barium oxide without cesium activation can be as low as 1.3 eV (at room temperature). Before expending too much effort on BaO thermionic diodes it seemed worthwhile to also investigate the work function of the other alkaline earth oxides, SrO and CaO.

The results obtained with alkaline earth oxides can be summarized as follows (see, also, Table VI).

(1) Commercial (Ba, Sr, Ca) Oxide

A large number of sprayed deposits of this type were investigated. This material is complex and was developed empirically. From commercial use as a thermionic cathode, the material is known not to be strictly reproducible in performance from sample to sample. Our experience confirmed this behavior. Hence, the work function given in the first line of Table VI must be considered as a typical value.

As this table shows, the work function is reduced by about 0.2 eV by exposure to cesium vapor. At the temperature at which measurements are possible, the cesium is so loosely bound that the minimum work function is not stable. From preliminary experiments with a more complex Dual Beam Chamber in which the cesium pressure can be controlled, it appears that at higher cesium pressures the work function is reduced to below 1.3 eV. Thus the use of the material for a diode collector looks promising because, in the diode, any desired cesium pressure can be obtained. The last column of Table VI shows that additional cesium-oxygen activation further reduces the work function.

(2) Barium Oxide

The study of evaporated pure barium oxide (i. e., not the mixed oxides) is still in an early stage but will be pursued more vigorously in the future because, as indicated, there are reasons to believe that the relatively thick sprayed films are too resistive. As shown in Table VI, the bare work function of the evaporated material was relatively low. The lower values reported by NRL may be, at least in part, due to the fact that they were measured at lower temperatures. Typically, the work function of BaO increases with temperature.

Two experiments with BaO, which are not shown in Table VI, deserve brief mention. From work with photoemissive materials, it is observed that the combination silver-oxygen-cesium has a lower work function than any other known material. Although this material is thermally unstable,

it was thought that the corresponding composition silver-oxygen-barium might combine higher stability with low work function. Attempts were made to produce such a compound either by depositing BaO on an evaporated silver substrate or by evaporating silver on top of a BaO deposit. Both experiments failed (i. e., the silver base was ineffective and the silver surface layer raised the work function). On heating, the silver layer seemed to diffuse into the BaO and the usual BaO work function was obtained. A single negative result is, of course, not conclusive and the experiments may be repeated with evaporated BaO films if these show promise as diode collectors.

(3) Strontium Oxide and Calcium Oxide

A few experiments were made with strontium oxide and calcium oxide (see Table VI) to check whether the rule "higher bare work function produces lower cesiated work function" that generally holds for metals is also valid for semiconductors. The bare work functions shown in Table VI agree well with published values and the incremental improvement with cesium was indeed greater than that for barium oxide. However, the absolute values after cesium activation were still higher than those for barium oxide. Moreover, the cesiated surfaces were even less stable at elevated temperature than on barium oxide. To establish the minimum work function value, the experiments will have to be repeated in the system that allows higher cesium vapor pressures. Of course, the potential use of SrO and CaO for diode collectors may be even more limited by resistance effects than that of BaO.

(4) Zinc Oxide (Table VII)

The possibility that cesium-activated zinc oxide, (Cs) ZnO, might have a low work function was suggested by the recently published work on this material by Hopkins, et al. (refs. 2 and 3). These authors studied cesiated surfaces of single-crystal ZnO with Auger spectroscopy and with low energy electron diffraction (LEED). They noted that cesium was bound much more tightly to the oxygen face than to the zinc face. Even at 1100 K, they observed that cesium is not completely desorbed from the oxygen face. In view of the previously mentioned correlation between electron affinity and binding forces, it appeared likely that cesium adsorbed on the oxygen face of ZnO would have a low electron affinity. Moreover, it is known that a stoichiometric excess of Zn makes pure ZnO a strongly n-type material with a Fermi level typically about 0.2 eV below the conduction band edge. These two considerations indicated that (Cs) ZnO might have a low work function. The following experiments were performed to establish the work function of (Cs) ZnO.

TABLE VII

WORK FUNCTION OF (Cs) ZnO

7612-7

MATERIAL	ACTIVATED WITH	ϕ (eV)
Sprayed	Cs	1.28
Evaporated	Cs	1.32
Single Crystal (Oxygen Surface)	Cs	1.4
Single Crystal (Zinc Surface)	Cs	>1.4
Sprayed	Ba	>1.5
Sprayed	K	>1.5

(a) Since single-crystal ZnO was not immediately available, the first experiments were performed with polycrystalline ZnO powder. It was assumed that if promising work-function values were obtained, cesium activation of the oxygen face of single-crystal ZnO should produce a further reduction.

Two methods were used to produce thin ZnO films on a nickel substrate. The first consisted of spraying a suspension of ZnO powder in butyl acetate and nitrocellulose onto a nickel substrate to a thickness of about 0.01 cm. The binder was removed by heating in vacuum to 900 K. Auger analysis of this surface showed that the ZnO surface was remarkably clean; in particular, the carbon content was negligible. In the second method, the same ZnO suspension was sprayed onto a platinum ribbon filament and evaporated onto the nickel substrate.

After exposure to cesium vapor the work function of both types of ZnO film was measured in the temperature range from 450 to 600 K. The work function of a large number of sprayed samples was close to 1.28 eV with remarkable reproducibility. Moreover, the work function did not change significantly over the range of measured temperatures. This characteristic compares favorably with the previously mentioned temperature dependence of the barium oxide work function.

The work function of the evaporated ZnO, after cesiation, was in the same range as that of the sprayed ZnO. This similarity is surprising because ZnO evaporates as zinc and oxygen, rather than in the form of ZnO molecules.

(b) Experiments were performed with single crystals (supplied by Professor Peter Mark of Princeton University) in the expectation that the cesiated oxygen face should have a lower work function than the poly-crystalline material. However, so far it has not been possible to reduce the work function of the oxygen face below 1.4 eV. One possible explanation for this surprising result would be an increased energy difference between Fermi level and conduction band edge in the single crystal, due to a difference in the n-type defects. Cesiation of the zinc face produced work functions in excess of 1.5 eV. This result was anticipated because the cesium is less tightly bound.

(c) Some experiments were made to replace cesium with barium and potassium. It was expected that these metals would produce somewhat higher work functions but it seemed to be of interest to establish whether the lower vapor pressure metals would lead to better thermal stability. As shown in Table VII, the work functions were, indeed, considerably higher. A surprising result was that the potassium surface was thermally

less stable than the cesium surface. Qualitatively this probably means that the greater binding force for cesium on ZnO more than compensates for the lower vapor pressure of potassium.

The potential usefulness of (Cs) ZnO as a collector material is apparent from the following summary of its characteristics.

(1) The work function is below 1.3 eV without additional cesium-oxygen activation. Thus, it is lower than that of any other material tested to date. It is interesting to note, though difficult to explain, that attempts at such additional activation produced only a negligible improvement.

(2) The work function appears to be less temperature dependent than barium oxide.

(3) Pure ZnO is strongly n-type, due to a stoichiometric excess of Zn. Therefore, it is a relatively good conductor of electricity. If the resistance of sprayed films should be too high, much thinner evaporated films appear to be a promising solution.

(4) ZnO is much easier to handle than BaO because it is stable in air. It forms neither a carbonate with the CO_2 in the air nor a hydroxide with water vapor.

While the described characteristics are individually and in combination superior to those of any other investigated material, one must not ignore the possible problems that may arise, or have arisen, in thermionic converters. The main problems are:

(1) There are indications that the resistivity of the sprayed material may be too high. If this is due to bulk resistance it is reasonable to expect that evaporated films will be satisfactory.

(2) The cesium vapor pressure required for minimum work function is probably lower than that required for optimum emitter performance in a diode.

(3) At high temperatures and cesium pressures a reaction

$$ZnO + Cs \rightarrow Zn + Cs\text{-}O$$
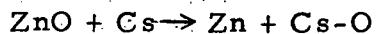
may gradually remove the ZnO from the collector because both zinc and cesium oxides have low vapor pressures.

Items (2) and (3) seem to be unavoidable at high cesium pressures, but the problems may be irrelevant if it turns out that high cesium pressure must be avoided in any case because of the unfavorable effect on the arc drop. Thus, for alternative designs, such as triodes and pulsed diodes which operate at low cesium pressure – (Cs) ZnO appears to be an attractive collector material.

3. Emitter Materials

The primary purpose of the Activation Chamber experiments was the study of potential collector materials. However, since collector and emitter must operate in the same environment, some thought must be given to the problem of compatibility of the two materials.

With regard to work function, the requirements for the emitter are, of course, much less stringent than for the collector because the optimum value lies in the 2 eV range, which can be obtained with a variety of materials. However, there are two important compatibility problems which seriously limit the choice of emitter material. First, the emitter must provide current densities around 10 amp/cm^2 at a cesium pressure which is consistent with low collector work function and low plasma losses. Second, it is desirable that the vapor pressure of the emitter at operating temperature be low enough to prevent evaporation onto the collector.

Evaporation of emitter material onto the collector would be relatively harmless if collector and emitter materials were identical. In principle, this should be feasible because, at optimum cesium pressure for the collector work function, the pressure will be automatically below optimum for the hotter emitter work function. The disadvantage of having the same material for both electrodes is that it limits the number of possible materials. The available collector materials with the lowest work functions are volatile at emitter temperature and the thermally stable emitter materials tend to have undesirably high work functions.

If emitter and collector materials are not identical, one can make an order-of-magnitude estimate of the permissible vapor pressure of the emitter material. If the system is operating in vacuum, the estimate can be derived as follows. The geometry of the converter (i. e., relatively close spacing of two large areas) permits the assumption that practically all, say 90 percent, of the material evaporating from the emitter will condense on the collector. At a pressure of 10^{-6} torr, a monolayer is deposited in one second. Since 1/10 monolayer is likely to increase the work function of the collector significantly, a vapor pressure of the emitter material of 10^{-7} torr will harm the collector within one second. Hence, an operating lifetime of 100 days (10^7 seconds) requires that the vapor pressure of the emitter at operating temperature be below 10^{-14} torr.

The vapor pressures of metals at high temperatures are well known. From these data, it is clear that few metals have the estimated required low vapor pressure in the 1400 K-and-over range. One unknown factor is the degree to which the cesium atmosphere may reduce the deposition on the collector, but this reduction is not likely to be more than a factor of ten.

The conclusion from the preceding discussion is that, until or unless one finds a material suitable for both emitter and collector, one is limited to refractory metals such as tungsten, molybdenum, rhenum, osmium and tantalum for the emitter. However, one other element seems to be in the required vapor pressure range; namely, carbon.

Since it is known that carbon in the form of graphite tends to bind cesium and is also a good conductor, some measurements were made of the work function of cesium activated graphite. The graphite was deposited on a nickel substrate in the form of Aquadag. Exposure to cesium vapor produced work functions in the 1.5 to 1.6 eV range. This result looked promising because it showed that, at nonoptimum cesium pressures, it should still be possible to get into the desired range of around 2 eV. The material is now being investigated in thermionic diodes.

B.   SURFACE CHARACTERIZATION CHAMBER

1.   Introduction

The Surface Characterization Chamber, described in Figures 3 and 4, is used for analytical support of thermionic research activities at Thermo Electron and for the fundamental characterization of low work function surfaces. Samples can be introduced to the chamber by an interlock which permits ultrahigh vacuum to be maintained in the chamber while the interlock is open to the laboratory atmosphere for sample loading. Inside the chamber, a sample is transferred from the tray onto a rotatable manipulator by means of a hook or by means of pneumatically activated jaws. The inboard jaw constitutes a hot/cold stage, inside of which hot or cold gases can flow to maintain sample temperatures from liquid nitrogen up to 300 C.

A sample admitted to the chamber can be cleaned thermally by electron bombardment from behind or can be cleaned by sputter etching from above (see Figure 4). A sample surface can be exposed to cesium vapor from heated elemental cesium and oxygen (from a silver diffusion tube) when positioned in front of the station at the left.

SAPPHIRE
WINDOW

PROTECTIVE
SHUTTER

LEED
ELECTRON
OPTICS

WINDOW

MANIPULATABLE
HOT/COLD STAGE

E.B. HEATER AND
PHOTO/THERMIONIC
EMISSION
STATION

KELVIN PROBE

METERING
VALVE

O₂

AUGER SPECTROMETER

Cs

HOOK

SHUT-OFF
VALVE

JAWS

SAMPLE
TRAY

VIEW PORT

FERP
GUN

IN-LINE
VALVE

STAGING
PLATFORM

VACUUM INTERLOCK

LOAD/UNLOAD
STATION

RACK AND PINION
DRIVE FOR
SAMPLE TRAY

RACK
MAGAZINE

Figure 3.   Surface Characterization Chamber
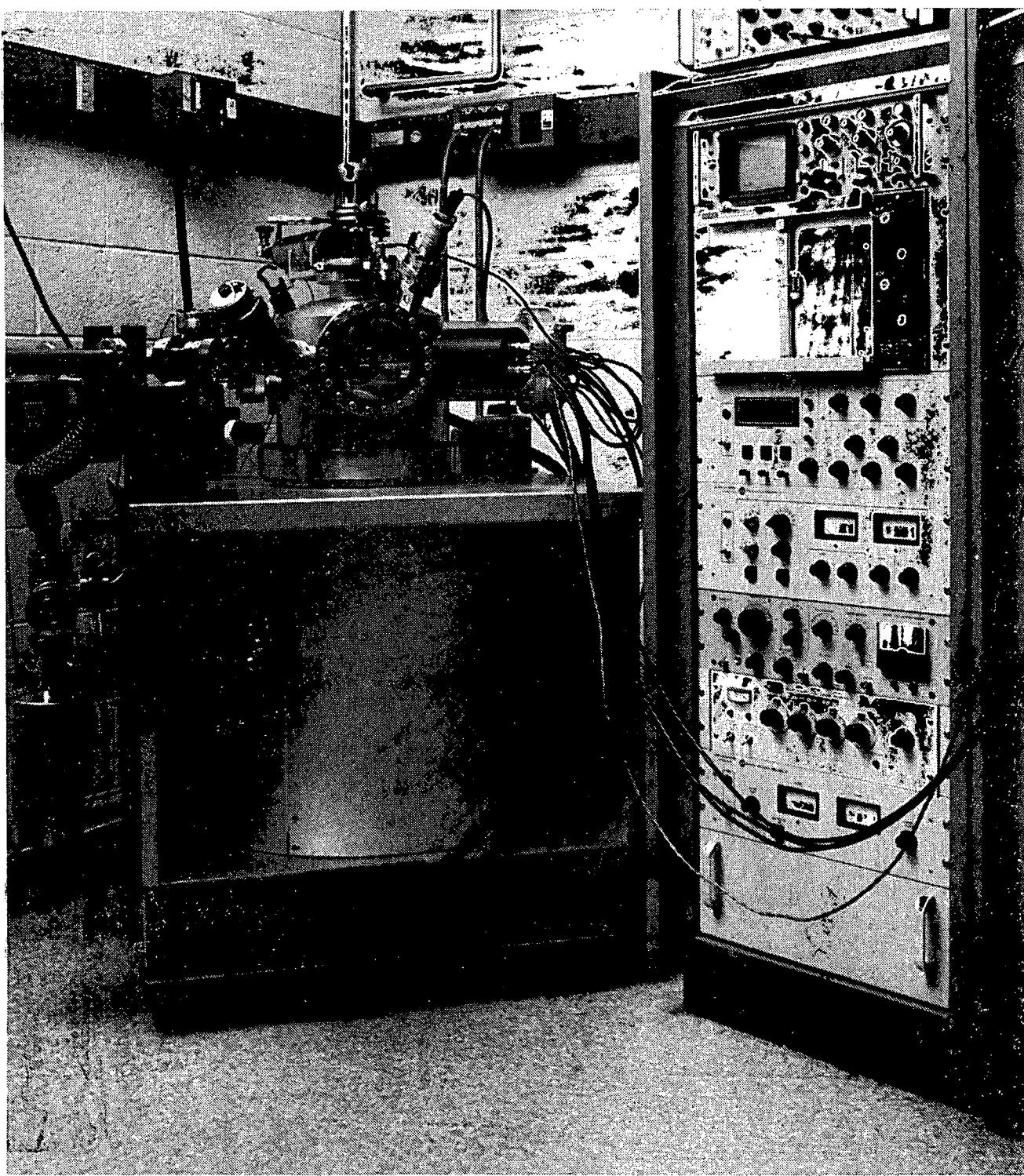
Figure 4. Surface Characterization Chamber and
Support Electronics

Sample work function can be measured by photoemission, thermionic emission, Kelvin probe, and by Field Emission Retarding Potential (FERP) methods. The physical principle underlying the FERP technique is illustrated in Figure 5. This method is especially valuable in characterizing collector surfaces in that it not only provides an absolute measurement of work function, but it also provides a measurement of the sample electron reflectivity spectrum. The field emitter electron source gives a fairly mono-energetic (~0.06 eV full width half maximum) probe beam which is independent of contact potential. Should finer resolution be desired, the experimentally obtained FERP spectrum may be deconvolved by computer calculation. For semiconductor surfaces the electronic structure of surface traps can be determined by the Kelvin probe by surface photovoltage spectroscopy. This method provides for determination of the position of surface states in the band gap. Such traps cause energy band bending at the surface of a semiconductor and therefore play a role in determining work function.

At practically any stage of sample processing, an ordered surface can be structurally characterized by means of low energy electron diffraction (LEED) and chemically characterized by means of Auger spectroscopy. Special holders are available for mounting simulated converter tests and reference surface samples as well as for mounting entire emitter and collector assemblies from thermionic converters. Other holders can be made for almost any sample that can fit through the 1.4-inch opening of the interlock's inline valve.

The sample support system, which is suspended from the top of the chamber, is made up of a series of three electrically isolated sections. The triaxial cable which electronically links the sample to laboratory instrumentation also permits guarded mode measurements to be made on the sample. This feature has proven essential to obtaining FERP data after a number of cesium exposures.

2. Surface Analyses of Diode Elements

Postmortem Auger analyses have been performed on the emitters and collectors of tested converters to establish a surface chemical composition data base to be correlated with device performance.

Converter No. 108 had a tungsten emitter and a (Ba, Sr, Ca) O collector sprayed onto an evaporated platinum film deposited on a conventional 201 nickel collector assembly. The collector's surface composition is summarized in Table VIII.

31

ENERGY

ϕ_e

$E_e = E_c - eV_c$

E_{FERMI}

$\dfrac{dI_e}{dE_e}$

V_c

E_c

EMITTER

ϕ_c

E_{FERMI}

$I_c = \displaystyle\int_{\phi_c}^{\infty} t(E_c)\,\dfrac{dI_e}{dE_e}\,dE_c$

ANODE
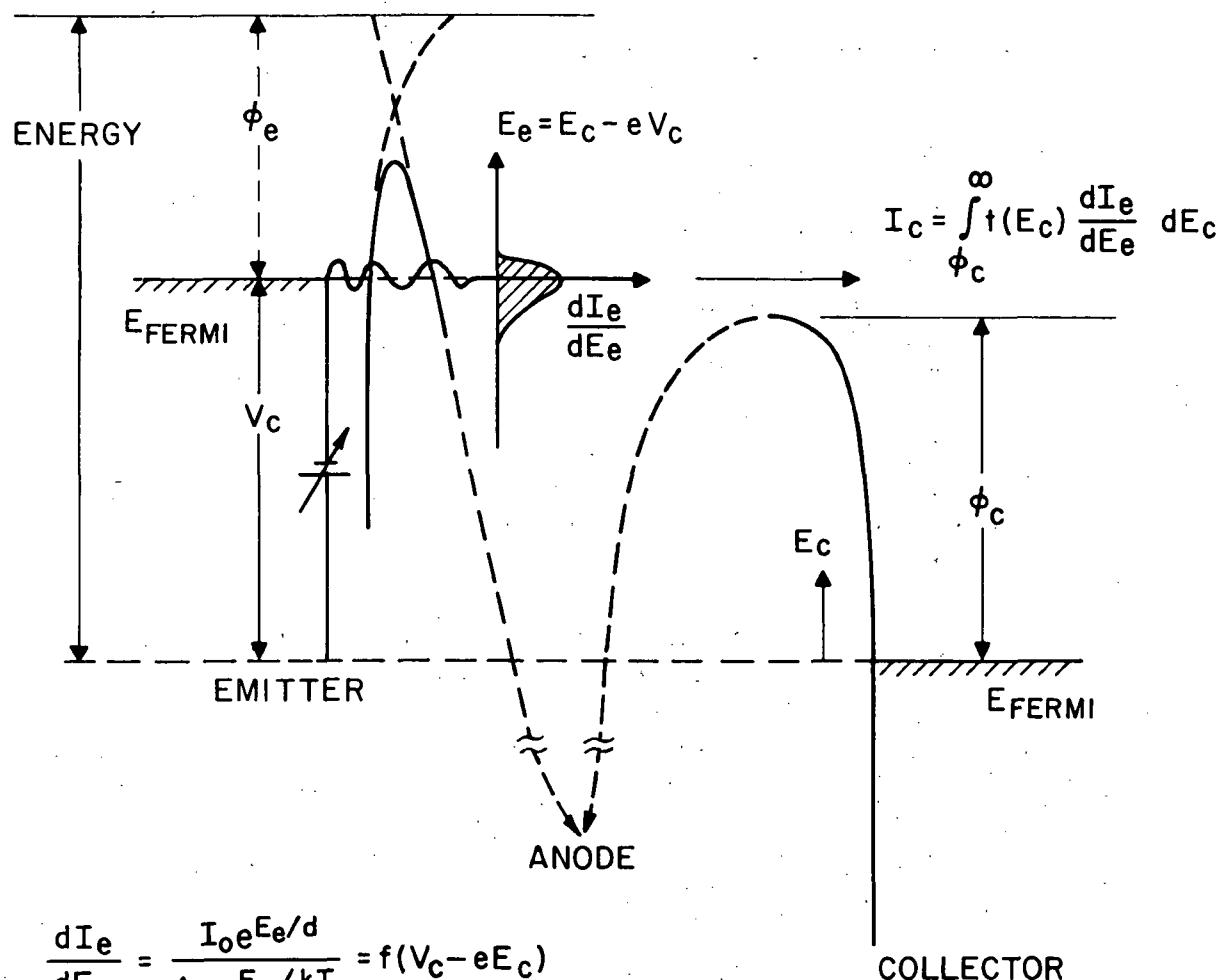
COLLECTOR

$$\dfrac{dI_e}{dE_e} = \dfrac{I_o e^{E_e/d}}{1 + e^{E_e/kT}} = f(V_c - eE_c)$$

$$\dfrac{d^2 I_e}{dE_e^2} = 0, \quad E_e = kT \ln \dfrac{kT}{d - kT}$$

$$I_c(V_c) = \int_{-\infty}^{\infty} t(E_c)\, f(V_c - eE_c)\, dE_c$$

Figure 5.   Field Emission Retarding Potential (FERP) Diagram

TABLE VIII

CHEMICAL COMPOSITION OF COLLECTOR SURFACE OF
CONVERTER NO. 108

7612-8

Chemical Specie		%
C	-	6. 3
O	-	16
S	-	0. 2
Ca	-	6. 0
Ni	-	2. 4
Sr	-	11
Cs	-	8. 0
Ba	-	46
W	-	4. 5

Carbon is a contaminant typically introduced by exposure of a surface to laboratory atmosphere. Oxygen, cadmium, strontium and barium are components of the sprayed coating. Cesium is a residue of the diode's atmosphere. Nickel is introduced by the underlying support and sulfur is a typical contaminant found in nickel. Platinum, the intermediate layer of the collector's sandwich-like configuration, is ostensibly absent. Since platinum and nickel readily alloy, it is likely that the former diffused in the much larger volume of the latter. Tungsten is present by virtue of either evaporation from the emitter or contact between emitter and collector.

Converter No. 116 consisted of a tungsten emitter and a (Ba, Sr, Ca)O collector supported by a standard nickel assembly. The collector had a white-to-gray appearance. The gray area was closest to where the cesium reservoir communicated with the interelectrode space. Three small (approximately 1 mm diameter) black spots were apparent underneath the surface of the coating. As shown in Table IX, Auger analyses indicated that the center and gray area were clean except for traces of nickel and copper. Carbon was present only at the black spots. The gray area was found to have slightly higher concentrations of nickel and copper.

A scanning electron microprobe investigation found nickel but no copper. This technique probes from 1000 $\overset{\circ}{A}$ to 10,000 $\overset{\circ}{A}$ of the surface layer. The nickel concentration was also higher in the sample's gray area. Nickel concentration between the grains of the coating was found to be higher than on the grains.

It appeared that evaporation of material from the (Ba, Sr, Ca) O coating had occurred during converter testing. The surface contamination by copper probably originated from the connecting tube to the cesium reservoir.

Converter No. 119 had a tungsten emitter and (Ba, Ca, Sr) O spray-coated nickel collector. After converter operation, the emitter had dull white, filmy areas which were opposed by gray patches on the collector. The collector also had a few smaller black spots. The Auger analyses of these electrodes are summarized in Table X. The emitter was heavily contaminated with graphitic carbon, some of which may have been incurred during atmospheric handling between dissection and Auger analysis. Atmospheric handling is also a possible source of sodium. The fact that the dull area was higher in carbon and lower in tungsten is indicative of carbon contamination occurring during converter operation. The outstanding features of the gray area of the collector are its high strontium concentration, its lower cesium and oxygen concentrations, and its absence of tungsten contamination. These observations indicate that physical contact of the emitter and collector occurred at some

TABLE IX

CHEMICAL COMPOSITION OF COLLECTOR SURFACE OF
CONVERTER No. 116

7612-9

Chemi-cal Specie	Center %	Black Spot %	Gray Area %
C		7.6	
Ca	4.1	4.0	3.5
O	18	17	17
Ni	0.3	0.4	0.5
Cu	0.3	0.3	0.8
Sr	17	15	17
Ba	60	55	60

TABLE X

CHEMICAL COMPOSITION OF ELECTRODE SURFACES OF CONVERTER NO. 119

7612-10

Chemical Specie	Collector			Emitter	
	Black Spot %	Gray Area %	White Area %	Dull Area %	Shiny Area %
C	9.9	0.5	6.1	72	55
N				0.6	0.8
O	22	6.3	16	4.4	5.6
Na	2.2	0.7	1.3	11	3.7
S	0.5		0.4	0.3	
Ca	1.0	0.6	1.6	0.4	1.1
Ni		0.1	2.2		
Sr	26	64	12		
Ba	1.0	21	34		
Cs	31	4.8	21	2.1	16
W	6.6		4.4	8.9	18

time during converter operation. The (Ba, Sr, Ca)O precursor is a mixture of the carbonates of these materials suspended in an organic vehicle. According to Zalm (ref. 4), strontium atoms constitute the top monolayer of an active coating. If this interpretation is correct, one can expect the surface of such a coating to give a high strontium Auger signal, even though this element is not necessarily in stoichiometric excess. The gray area is the cleanest region of the collector surface. Apparently, at some time the electrodes touched, with the result that tungsten was transferred from the shiny emitter area to the white collector area and the collector coating material was transferred at the gray area of the collector to the dull area of the emitter.

Converter No. 121 utilized a tungsten emitter and a lanthanum hexaboride collector. The collector had a 1/8-inch diameter hole which led to a silver tube for oxygen diffusion. The surface chemical compositions of Converter No. 121's electrodes are summarized in Table XI.

Auger data taken for five points on the emitter and five points on the collector did not show a spatial variation. Because of the overlap of boron and tungsten Auger spectra, the values obtained for boron concentration are approximate. Lanthanum concentrations, if present, are not given because the lanthanum Auger spectrum is buried beneath the secondary cesium spectrum. Aluminum and nitrogen occurred typically in sintered lanthanum hexaboride. The presence of silicon, sulfur, calcium and nickel is attributable to the diode structure.

Converter No. 123 consisted of a tungsten emitter and a titanium oxide collector. The collector structure was made up of a 0.010-inch-thick sheet of titanium which had been nickel-brazed to a molybdenum cap which, in turn, had been copper-nickel-brazed to a nickel collector assembly. The oxide was formed by heating the completed collector structure in air to 200 C. The Auger analyses of this converter are summarized in Table XII-A. Titanium contamination of the emitter indicates that the electrodes had made physical contact. Since the oxides of titanium are quite stable, it is highly unlikely that any evaporation or decomposition took place. Aluminum has been detected on the electrode surfaces of several converters which have undergone testing. The simultaneous presence of sulfur and nickel, as mentioned previously, is typical.

Table XII-B summarizes the investigation made in order to determine the cause of nickel contamination of the titanium oxide collector. The etch treatment (which consisted of cotton swabbing each sample with a volumetric mixture of $HF:HNO_3:H_2O::50:100:850$), was employed in

TABLE XI

CHEMICAL COMPOSITION OF ELECTRODE SURFACES OF
CONVERTER NO. 121

7612-11

Chemical Specie	W Emitter %	LaB_6 Collector %
B		4 - 12
C	10 - 36	28 - 50
N	1 - 2	0. 3
O	11	4 - 8
Al		1 - 3
Si		1. 9
S	1 - 2	1. 1 - 1. 6
Ca		0. 5
Ni		2
Cs	36 - 60	23 - 32
W	12 - 20	8 - 20

TABLE XII-A

CHEMICAL COMPOSITION OF ELECTRODE SURFACES OF CONVERTER NO. 123

7612-12a

Chemical Specie	Emitter %	Collector %
C	50	38
O	2	5 - 16
Na	7	
Al		0 - 7
S		0.5
Ti	2	3 - 20
Ni		1 - 2.5
Cs	16	23 - 42
W	18	

TABLE XII-B

CHEMICAL COMPOSITION OF THE Ti/Ni/Mo CONFIGURATION

7612-12b

Chemical Specie	Collector of No. 123 %	Etched Collector of No. 123 %	0.010"Ti/ Ni/Mo %	Etched 0.010"Ti/ Ni/Mo %	0.050"Ti/ Ni/Mo %	Etched 0.050" Ti/ Ni/Mo %
C	38	62 - 67	65	59	52 - 59	55
O	5 - 16	10	9	11	17	
Na		5	7	1.2 - 2.6	2.4	1.2 - 2.3
Mo						2.5
Al	0 - 7					
Si						0.9 - 2.2
S	0.5		0.9	0.6	0.2	0.2
Cl			1.5	1.1 - 1.8	0.5	0.7 - 2.0
Ti	3 - 20	16	16	16	22 - 26	18
Fe		1.2	0.5	2	0.4 - 1.8	2.3
Ni	1 - 2.5	0.7 - 1.2	0.3	7		1.6 - 1.9
Cu		0.6		0.2		
Cs	23 - 42					

39

order to remove surface contaminants introduced by vapor deposition. A 0.010-inch titanium sheet was nickel-brazed to a molybdenum cap in the same manner as the collector of Converter No. 123. This collector structure was analyzed before and after etching. A similar configuration, but made from a 0.050-inch-thick sheet of titanium, was given the identical treatment. Chlorine, sodium, and carbon could have been introduced by handling. The sources of magnesium, aluminum, and silicon are uncertain. Iron could have been introduced when the titanium was machined on a lathe using a carbon-steel tool. Since nickel is present on the surface of all of the samples, the converter atmosphere was not the source of contamination. Since the nickel concentrations for the two control samples increased with the material removed, it was concluded that the source of surface nickel contamination was diffusion through titanium from the braze joint.

Grain boundary delineation by etching showed that the grain size was of the order of 1 mm for all three samples. Since the path from the titanium/nickel interface to the surface is direct, grain boundary diffusion is most likely the source of nickel contamination. This is supported by the observation that the surface concentration of nickel is less than for the thicker sample. To avoid recrystallization/grain growth at the brazing temperature, a titanium alloy having a higher recrystallization temperature could be used.

Converter No. 130 utilized a tungsten emitter and a strontium oxide collector. The collector material had been sprayed onto a standard nickel collector assembly. After testing, the emitter appeared to have an etched area and the collector had a gray-black deposit. These two regions were opposite one another in the sealed converter. The Auger analyses of these electrodes are summarized in Table XIII. It is evident that transfer of the spray coating to the emitter took place at the "etched area," probably by physical contact during diode operation. Tungsten may have reached the collector surface by vapor transport tungsten oxide. If such is the case, then the lower concentration of tungsten on the gray-black area of the collector indicates that interelectrode contact was made late in the converter test period.

Converter No. 140 incorporated a standard tungsten emitter assembly painted with Aquadag and a nickel collector. The surface compositions of the post-test electrodes are summarized in Table XIV. The graphite-coating emitter remained intact throughout converter operation. Chemical composition of the emitter was uniform. No traces were found of the characteristic carbide Auger spectrum which would have indicated a chemical reaction between the graphite and its converter environment.

40

TABLE XIII

CHEMICAL COMPOSITION OF ELECTRODE SURFACES OF CONVERTER NO. 130

7612-13

Chemical Specie	Collector White Area %	Collector White Area %	Collector Gray-Black Deposit %	Emitter Etched Area %	Emitter Etched* Area %	Emitter Shiny Area %
C	49	40	57	62	66	57
N	0.1		0.2	1.0	1.0	1.3
O	9.5	13	8.0	14	11	6.5
Na			2.0	3.5	2.1	4.0
Mg	1.1				0.6	1.2
S	0.2	0.3	0.3	2.1	1.8	?
Ca			0.1			
Ni	1.4	3.1	2.1			
Sr	31	34	26	2.2	5.7	3.5
Cs	4.5	6.2	4.6	3.5	1.8	5.8
W	3.8	3.4	0.8	11	9.7	21

*This region incandesced under bombardment from electron beam.

TABLE XIV

CHEMICAL COMPOSITION OF ELECTRODE SURFACES OF
CONVERTER NO. 140

7612-14

Chemical Specie	Emitter Surface %	Collector Surface %
C	99	11
N	0.1	
O	0.1	11
Na		2.0
Si		4.7
S		2.0
Ca		4.9
Ni		8.1
Cs	0.9	4.6

The chemical composition of the collector surface was also quite uniform. The high levels of calcium and silicon are atypical compared to previously studied nickel collectors. These contaminants probably were introduced by the Aquadag suspension used to bind the graphite coating on the emitter.

3. Surface Activation Chamber Analyses

This section summarizes the results of Auger analyses performed on sample materials that had been studied previously in the Surface Activation Chamber. Analyses of some of the rare earth compounds investigated are given in Table XV. All composites were prepared by spraying amyl acetate-nitrocellulose suspensions of powders. In the case of lanthanum oxide, the carbonate was used as a precursor. The considerably higher carbon levels on the europium hexaboride and ytterbium oxide surfaces were most likely incurred in handling between studies in the Surface Activation and Surface Characterization Chambers. Since the concentration of surface carbon on the lanthanum oxide is so low (indicative of less contamination in handling), it is most likely that the sodium detected originated from the material itself. Aluminum, silicon, iron, nickel, and copper are most likely bulk impurities that segregated out at the surface. In the case of europium hexaboride on tungsten, the fact that the concentration ratios of boron to europium are very close to stoichiometric indicated that the compound remained intact. The substantial amount of rhenium present agrees with visual observation (i.e., the sprayed coating did not completely cover the support). The high degree of silicon present on the ytterbium oxide samples indicates a preferential surface segregation of the element, not a high degree of bulk contamination.

Table XVI gives analyses of selected zinc oxide samples studied in the Surface Activation Chamber. All five of these samples were fabricated by evaporation of zinc oxide onto a nickel Vidicon assembly from a spray-coated platinum strip. Samples 111, 112 and 113 could not be activated. The reason is obvious for Sample 111, since no zinc was present. This thin film coating was vacuum deposited and exposed to laboratory atmosphere before testing. The failure in obtaining a coating in this case was attributed to the poor vacuum under which the evaporation was made. Evaporations for Samples 112 through 115 were performed inside the Surface Activation Chamber just prior to activation. As indicated by the substantial amount of nickel detected on Samples 112 and 113, these coatings were incomplete and, most likely, patchy. For Samples 114 and 115, all associated components were cleaned thoroughly prior to insertion of the evaporation-test assembly into the Surface Activation Chamber. These two samples gave the best performance and had the highest surface concentrations of zinc and oxygen. Samples 114

43

TABLE XV

SURFACE CHEMICAL COMPOSITION OF POST
ACTIVATED RARE EARTH COMPOUNDS

Concentrations (%)

7612-15

Chemical Specie	L_2O_3/W	EuB$_6$/Re		Yb$_2$O$_3$	
		Spot #1	Spot #2	Sample #1	Sample #2
B		2.9	5.0		
C	1.3	46	43	39	22
N		2.5	2.5		
O	16	6.4	6.6	19	35
Na	2.6				
Al	4.6	9.6	11		
Si	2.5				
Fe	11			34	17
Ni	1.6				
Cu	1.2				
Cs	36				
La	19				
Eu		0.4	0.5		
Yb				8.9	26
W	5.2				
Re		32	32		

TABLE XVI

SURFACE CHEMICAL COMPOSITION OF POST ACTIVATED ZnO SAMPLES

7612-16

Chemical Specie	Concentrations (%)					
	#111	#112	#113	#114	#115	#122
C	30	7.1	15	0.5	0.3	
N	0.3	0.1	0.9			
O	12	8.3	8.0	12	12	13
Na	1.1					
Mg	2.0	0.6	0.8	0.5	1.6	
Al						1.5
S	1.4	1.1	2.9	1.0	0.3	1.4
Cl	1.0					
K						1.2
Ni	37	16	16			
Zn		38	26	51	50	14
Cs	16	29	31	36	36	69

and 115 also had no nitrogen and were almost carbon free. As mentioned elsewhere in this report, removal of surface carbon from zinc oxide by heating is easily accomplished. Magnesium, detected in practically all Auger analyses of zinc oxide performed to date, is apparently a material impurity. Sulfur may have been introduced into zinc oxide from the nickel substrate. Potassium had been deliberately introduced into Sample 122. It apparently has little, if any, tendency to segregate out at the surface. It is interesting that the surface concentration of cesium for this sample is at least twice that found on the other samples. There is no apparent explanation for aluminum contamination.

4. Simulated Converter Analyses

Special holders were designed and fabricated to permit Auger analyses of Simulated Converter samples. Table XVII summarizes those samples tested this year. The three test surfaces studied were ZnO. It is difficult to say whether the high degree of carbon contamination on test surface ZnO No. 3 was due to incomplete activation or to atmospheric handling subsequent to the original testing. The sodium contamination which is peculiar to the test and reference electrodes of Simulated Converter No. 3, however, suggests that it was the latter cause. Aluminum, silicon, calcium and copper were most likely introduced by the converter's atmosphere. As mentioned previously, the copper tube cesium reservoir is a strongly suspected source for copper contamination.

5. Fundamental Materials Studies

Surface characterization studies were conducted on materials which have been used in the fabrication of thermionic converters as well as on new materials which show promise as collectors and emitters for high efficiency thermionic energy conversion.

A study of the effects of processing on the surface chemistry of converter tungsten was conducted. Slices of arc cast tungsten were cut to 0.015-inch thickness by electron discharge machining (EDM). All samples were initially vapor degreased in 1, 1, 1 - trichloroethane, ultrasonically agitated in acetone, rinsed in methanol, and hydrogen fired for thirty minutes at 1030 C. Each sample was subjected to a different preparation treatment, as summarized in Table XVIII. Carbon, oxygen, and nitrogen can be expected to be present on specimens exposed to air. Carbon, sodium, and silicon are bulk impurities naturally

Thermo
Electron
CORPORATION

TABLE XVII

SURFACE CHEMICAL COMPOSITION OF
SIMULATED CONVERTER SAMPLES

Concentrations (%)

7612-17

Chemical Specie	ZnO/Ta		Test Surface ZnO #3	Ref. Surface ZnO #3	Test Surface #4
	Gray Spot	3 mm to Left			
C	9	9.2	50	19	1.2
N			0.5		
O	10	8.3	5.9	15	5.6
Na			4.3	2.4	
Mg	0.7		1.2		
Al					3.6
Si				5.6	
S			0.3		0.1
Cl	3.5	1.2	1.0	14	
Ca					0.3
Cu		22			
Zn	37	25			2
Mo				9.2	1
Cs	40	35	29	34	86
W			8.1		

TABLE XVIII

EFFECTS OF PREPARATION TREATMENT UPON TUNGSTEN SURFACE CHEMISTRY

Sample	W1	W2	W3	W4	W5	W8	W10
Preparation Treatment	Degreased	Vacuum Fired at 1130 C for 2 minutes	Vacuum Fired Dipped in Machine Oil Degreased	Sandblasted and Degreased	Vacuum Fired and Electropolished	Etched for 30 Seconds in 10% KOH	Lapped on Wet SIC Paper
Chemical Specie (%)							
C	60	61	60	67	80	51	59
N	1.6	1.3	0.9	0.4	2.5	2.2	2.1
O	7.7	9.1	8.8	4.2	9.4	8.2	9.2
Na	3.1	1.0	1.5	11		6.3	
Mg	1.1	2.3	2.8	0.7			1.2
Al	2.0	3.6	5.1				
Si	3.3	15	14	4.3		1.1	
K						1.4	
Ca	1.6	4.0	4.3	1.1	1.0	0.7	1.1
Fe	2.9			1.5	0.4	0.7	
Ni	1.1					0.2	1.5
Cu	0.8					0.4	
W	15	3.4	2.9	9.7	8.4	28	35

7612-18

occurring in tungsten, iron, calcium, magnesium, aluminum, nickel and copper and could have been picked up during the machining process. Chemical removal of surface material produced the cleanest surfaces. The iron and potassium on Sample W10 most likely were introduced by the etching process. If calcium was removed by etching, it may have been reintroduced by the subsequent washing of the etched sample with tap water. Lapping of the sample removed several impurities but, as demonstrated by subsequent Auger analyses (see Table XII) of the heat treated sample, silicon was apparently added to the sample from the silicon carbide abrasive.

The effects of heat treatment upon samples W1, W2, W5, W8, and W10 are outlined in Tables XIX through XXIII. The heat treatment activated diffusion to the surface of impurities which had been super-ficially removed by etching or abrasion. The pronounced rise in silicon concentration on the surface of W10 was most likely caused by imbedding of the silicon carbide abrasive during lapping. Calcium, magnesium, aluminum and titanium could have been introduced by the EDM slicing of the tungsten wafers. Sulfur and phosphorous are most likely bulk impurities which segregate at the surface at the medium range temperatures (600 C< T< 1200 C). Practically all impurities, except for oxygen and carbon, are removed by heat treatment to 1600 C. Above 1000 C the surface carbon changes from graphite to tungsten carbide, as evidenced by the characteristic change in the shape of carbon Auger spectrum (private communication with Dr. Lawrence Davis of Physical Electronics Industries, Inc.). Carbide surface concentration increases up to 1600 C and decreases thereafter. Samples W2 and W3 both had a higher surface concentration of silicon and also were the only samples tested which had undergone the previous treatment of firing in a vacuum system pumped by silicon diffusion pump oil. As evidenced by Table XX, the silicon contaminant, apparently introduced by the initial vacuum firing process, is fairly tenacious. The presence of molybdenum on W2 can be attributed to the fact that the sample was inside of a molybdenum bucket during the initial heat treatment.

The goal of this study is to determine an optimum surface preparation procedure applicable to the fabrication of low work function tungsten con-verter electrodes. The effect of carbon upon the work functions of cesiated and cesiated-oxygenated tungsten surfaces will eventually be studied.

Samples of Marz-grade molybdenum and of the low-carbon molybdenum used in converter electrode fabrication were fired in the Surface Characterization Chamber. Both types of samples were vacuum fired in excess of 1480 K to remove the surface oxide layer.

Thermo Electron CORPORATION

TABLE XIX

EFFECTS OF HEAT TREATMENT UPON THE SURFACE CHEMISTRY OF SAMPLE W1

7612-19

Treatment	Chemical Specie (%)														
	C	N	O	Na	Mg	Al	Si	P	S	Ca	Ti	Fe	Ni	Cu	W
As Admitted	60	1.6	7.7	3.1	1.1	2.0	3.3			1.6		2.9	1.1	0.8	15
400 C	57		6.6	2.6	1.1	1.3	2.3	2.2	0.4	1.6		2.4	0.3	0.5	21
600 C	44		3.5	1.4		1.1	2.5	9.6	1.1	3.4		3.8	0.8	1.0	27
700 C	17		1.6			2.0	3.5	25	2.3	1.9		3.1	1.1		41
750 C	19		2.2			1.4	2.9	26	2.1	2.9		3.5	0.8		38
800 C	21		1.8			1.7		24	1.8	2.9	2.8	1.1	0.4		39
900 C	8.4		3.8			2.8	1.7	20	1.4	5.1	5.5	0.3			48
1000 C	2.6		12			4.8	2.8	0.2	0.2	20	3.0				51
1100 C			13			5.3	1.8			14	3.0				52
1200 C	8.8		6.9			1.0	1.3	2.7	0.5		1.5				76
1300 C	15		3.4			1.8		0.9	0.5						76
1400 C	22		2.8												73
1700 C	9.7		3.1												87

Thermo Electron CORPORATION

TABLE XX

EFFECTS OF HEAT TREATMENT UPON THE
SURFACE CHEMISTRY OF SAMPLE W2

7612-20

Treatment	Chemical Specie (%)										
	C	N	O	Na	Mg	Al	Si	Ca	Ti	Mo	W
As Admitted	61	1.3	9.1	1.0	2.3	3.6	15	4.0			3.4
400 C	53	0.6	9.8	1.3	2.9	4.8	16	4.9	0.7	2.8	3.3
600 C	54	0.6	9.4	1.0	2.6	4.2	16	4.4	0.8	3.6	3.5
700 C	52	0.6	10		2.6	3.7	18	4.4	0.9	4.2	3.3
800 C	38	0.4	12		2.1	5.7	20	5.2	1.5	11	4.7
900 C	4.4	0.7	16		1.7	6.6	22	5.6	6.5	26	11

TABLE XXI

EFFECTS OF HEAT TREATMENT UPON THE SURFACE CHEMISTRY OF SAMPLE W5

Treatment	Chemical Specie (%)											
	C	N	O	Na	Al	Si	P	S	Ca	Fe	Cu	W
As Admitted	80	2.5	9.4						1.0	0.4		8.4
200 C	58	1.4	6.5	3.0		1.4			0.7	0.2	0.2	28
400 C	56	1.2	5.6	4.8		1.0			0.8	0.4	0.4	30
600 C	55		4.8	8.8	1.0	1.1			0.3	0.4		22
800 C	22		1.5			2.8		0.3	2.5	1.0		71
900 C	14		0.4			7.2	2.8	2.2		7.4		66
1000 C	12		0.4			9.0	5.0	1.1				73
1100 C	10		0.5			6.1	8.3	1.3				74
1200 C	4.7		0.3			2.2	12	4.0				77
1300 C	8.7		0.7			1.5	9.2					80
1400 C	12		1.0			4.9	5.1	0.5				76
1500 C	13		1.0			1.0	4.3					81
1600 C	3.8		1.1			0.5	6.7					88
2000 C	9.3		1.2									89

7612-22

TABLE XXII

EFFECTS OF HEAT TREATMENT UPON THE
SURFACE CHEMISTRY OF SAMPLE W8

Treatment	Chemical Specie (%)													
	C	N	O	Na	Si	P	S	K	Ca	Ti	Fe	Ni	Cu	W
As Admitted	51	2.2	8.2	6.3	1.1			1.4	0.7		0.7	0.2	0.4	28
400 C	44	1.3	7.7	7.3	1.8			3.1	0.7		1.7	0.3		33
600 C	8.2	1.9	8.0		2.5	2.1	0.3	0.2	3.2		7.0			67
700 C	2.7	3.2	2.0		1.9	6.5	4.6		1.6	1.8	8.7			67
800 C	2.5	4.1	5.9			4.6	2.8		5.5	2.7				70
900 C	4.2	4.5	3.6			8.6	2.2		1.7	4.1				71
1000 C	4.7	2.8	1.2		1.3	16	1.5			1.8				70
1100 C	12		1.5		1.8	7.1								77
1200 C	18		5.7											76
1300 C	23		0.7											77

53

Thermo Electron CORPORATION

TABLE XXIII

EFFECTS OF HEAT TREATMENT UPON THE
SURFACE CHEMISTRY OF SAMPLE W10

7612-23

Treatment	Chemical Specie (%)											
	C	N	O	Na	Mg	Si	P	S	Ca	Ni	Cu	W
As Admitted	59	2.1	9.2		1.2				1.1	1.5		35
400 C	52	0.7	7.2	1.7		1.4		0.2	0.6		0.6	35
600 C	40	0.6	5.1	2.6		1.2		0.5	1.1		3.9	46
700 C	4.3	0.6	0.8			5.0		6.2	2.8		8.6	72
800 C	6.7		0.4			15		5.4	0.6			72
900 C	1.7		0.1			37		0.1	0.2			59
1000 C	1.7		0.1			41		0.1	0.3			57
1100 C			0.5			10						89
1200 C	6.4		0.5			6.1			0.2			87
1300 C	11		0.6			5.2						83
1400 C	19		1.1			1.0						79
1500 C	22		0.9									78
1700 C	22		0.8									77

The firing resulted in a substantial surface buildup of carbon in the form of molybdenum carbide. The surface segregation of carbon on refractory metals has been discussed in the literature (refs. 5 and 6). The effect of surface carbon upon collector work function and collection efficiency is not clear. Since its presence was measured to be greater than 20 percent, the further study of this subject is warranted.

An experimental study was made of the W(110) surface composite. A Marz-grade (110)-oriented single crystal was cleaned by heating to an excess of 2000 K in a 10^{-6} torr atmosphere of oxygen and then flashing to 2300 K after the chamber had been evacuated. Room temperature exposure of the clean surface to 300 Langmuir (10^{-6} torr sec) of oxygen had no noticeable effect. As shown in Figure 6, a high order (greater than 5 x 1) LEED pattern was obtained from a 300 Langmuir oxygen exposure at either 1275 K or 575 K. The order of a LEED pattern describes how it differs from the pattern one can expect for a surface having the same periodicity as the underlying bulk. A bare tungsten (110) surface would give a simple six point array, which here forms the basis of each of the rows seen in LEED photographs. Because of the inverse relationship between spacing and diffraction, a surface layer having a repeat distance which is an integer factor of the bulk repeat distance would give a diffraction pattern having this same factor, but with more dots. For these patterns the number of dots is enhanced in one direction by at least a factor of five — hence an order of higher than 5 x 1. The first pattern is a composite of two patterns, produced by two sets of surface domain structures oriented at about 60 degrees to one another. This particular crystal was not perfectly aligned parallel to the (110) plane, which may have resulted in a preference for a particular domain. The greater degree of agitation produced by higher temperature also may have permitted the formation of the second domain seen in the first LEED photograph. For both of these cases, Auger measurements indicated that oxygen coverage was of the order of 10 percent.

As shown by the third pattern, exposure of the sample to cesium results in diffuse scattering and a reduction of pattern order. It may be that the adsorbed surface layer becomes amorphous, and all that remains is a diffuse diffraction pattern from the underlying bulk. Three doses each of cesium and oxygen were sufficient to obliterate the LEED pattern and the lower energy peaks of the tungsten Auger spectrum. On the basis of published values for electron escape depth (refs. 7 and 8), these data imply that an amorphous layer of between 30 to 100 Å thick was formed. It is this amorphous layer which has given the lowest threshold FERP spectrum, shown in Figure 7, observed for the W/Cs/O surface composite.
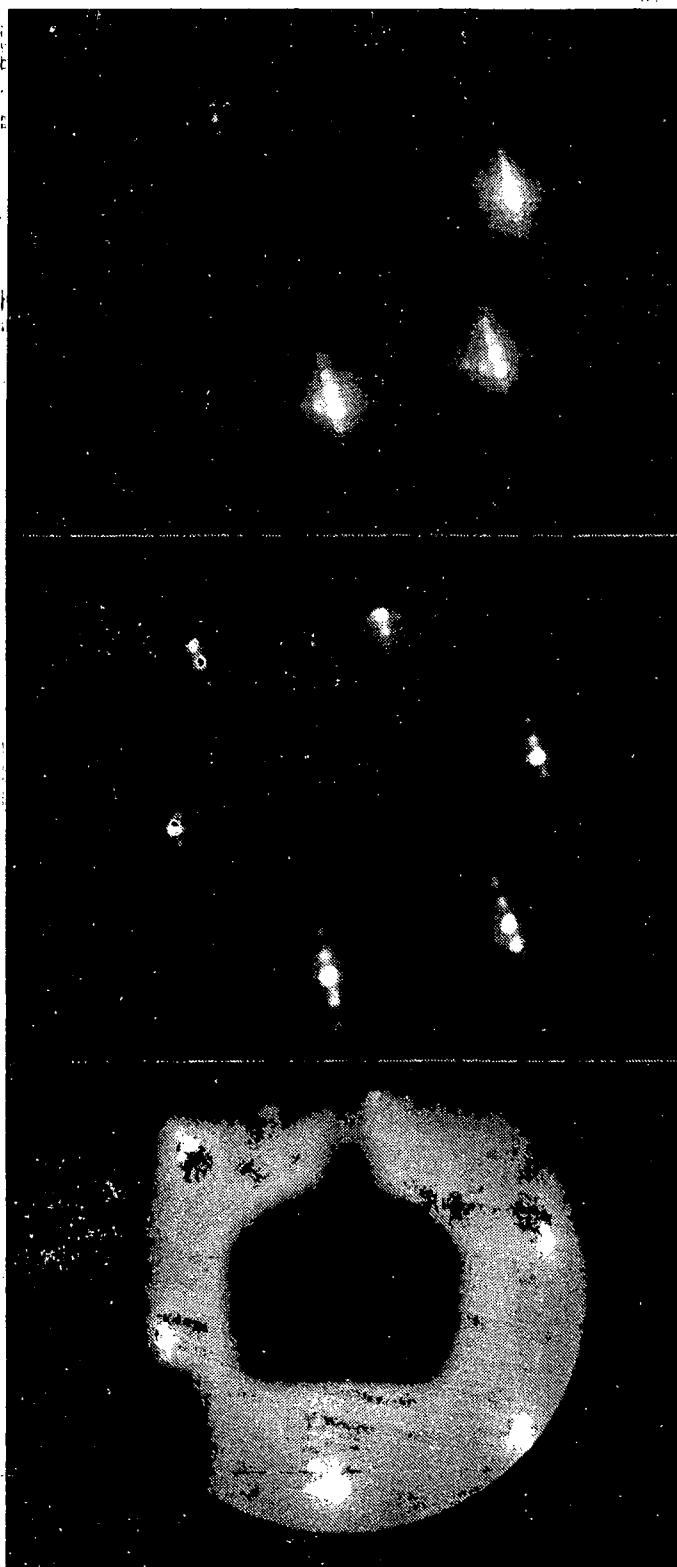
63 V LEED Pattern of
W(110)/O surface formed
by 300 Langmuir exposure
at 1275 K.

63 V LEED Pattern of
W(110)/O surface composite
formed by 300 Langmuir
exposure at 575 K.

63 V LEED Pattern of
W(110)/O/Cs surface
composite

Figure 6. LEED Patterns
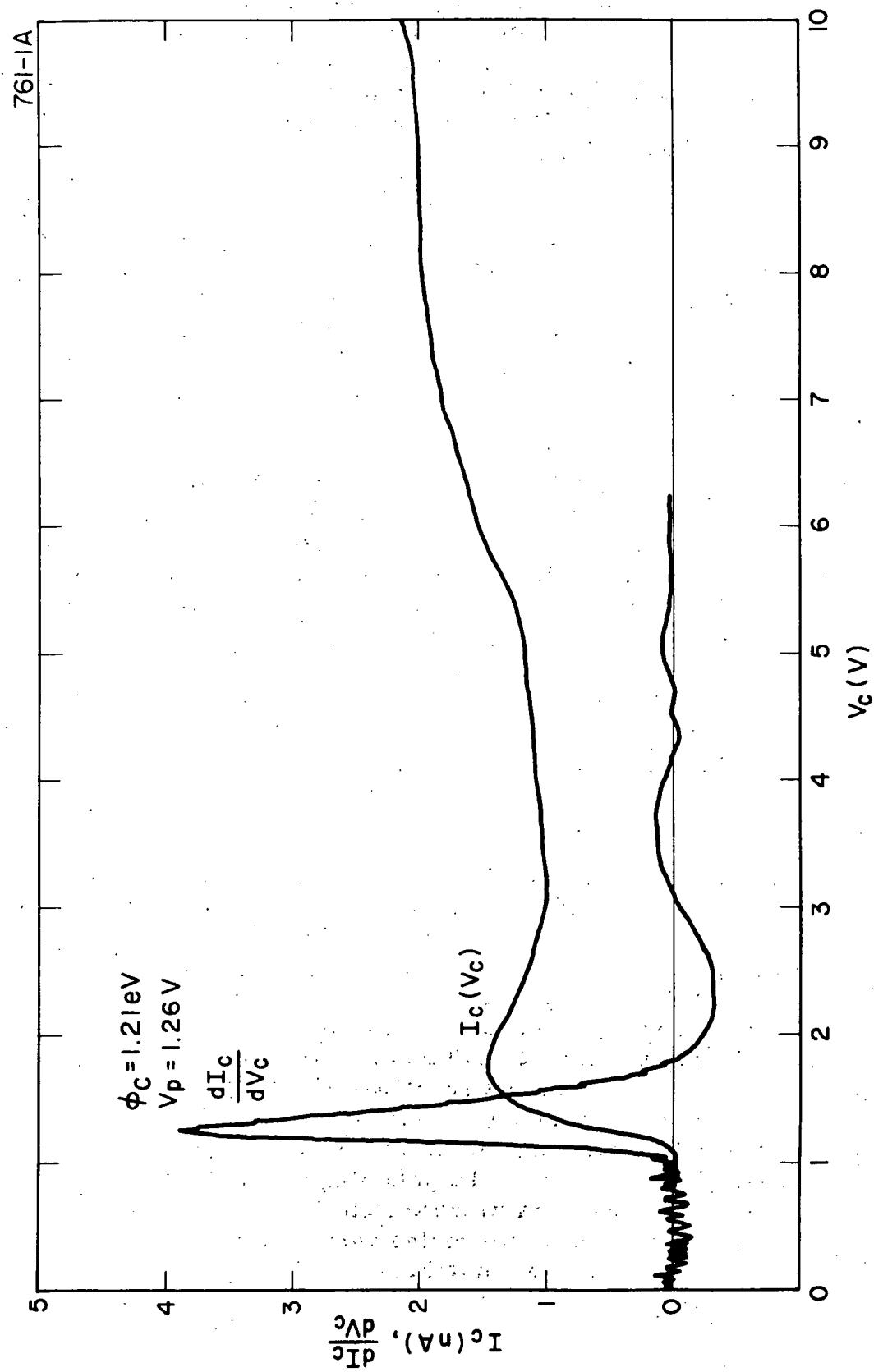
Figure 7. Electron Collection Spectrum of $W/C_s/O$ Surface Composite on a (110) Tungsten Surface.

761-1A

$\phi_C = 1.21\,eV$

$V_p = 1.26\,V$

$\frac{dI_c}{dV_c}$

$I_c(V_c)$

$V_c(V)$

$I_c(nA)$, $\frac{dI_c}{dV_c}$

Zinc oxide spray coatings were studied in the Surface Characterization Chamber. Heating these coatings at 973 K for two minutes is sufficient to remove all detectable impurities except for traces of magnesium and sulfur. Zinc oxide powder is the easiest substance to clean of any tested in the chamber. Preliminary activation experiments with cesiated zinc oxide did not show a significant reflectivity spectrum. Auger determinations showed that a substantial amount of cesium remains on the zinc oxide surface after heating to 1065 K.

When deposited upon a metal surface by means of sputtering, zinc oxide is equiaxed with the desired oxygen surface orientated toward vacuum (ref. 9). This empirical observation is of special interest to the incorporation of zinc oxide into a thermionic converter, since it is the oxygen surface of this material which exhibits such a great tenacity for adsorbed cesium (ref. 2) and also it is on this surface that cesium adsorption would be expected to result in the greatest reduction in work function.

An activation study was conducted on silicon carbide. This very stable material is of interest as a hot shell for fossil fuel topping. Like zinc oxide, silicon carbide has a polar structure. So far, the carbon surface has been studied. Firing of a silicon carbide sample to about 1100 K in vacuum resulted in a carbon surface which was predominantly amorphous graphite. Auger analysis showed the surface to be over 90 percent graphite and no LEED pattern could be obtained from this surface. A FERP work function of less than 2.25 eV was obtained when the sample was exposed to cesium. No reflection structure was observed for this surface.

6. New Support Facilities

Equipment was obtained and developed to support experimental work done in the Surface Characterization Chamber. Tests were run on the DS-9 cleaning agent, a proprietary chemically active solution sold by the Diversey Chemical Corporation. This agent, as advertised, works best on the austenitic stainless steels, which are widely used in the fabrication of ultrahigh vacuum components. It may also be used to clean nickel, Kovar and Inconel. Although DS-9 reacts violently with molybdenum, there is no apparent reaction with tungsten, titanium or tantalum. The chemical polishing of stainless steel with DS-9 falls just short of what can be obtained by electropolishing. The DS-9 process, however, is simpler and permits the polishing of large areas, limited only by the size of the vessel in which the etching takes place. For stainless steel the DS-9 process obviates vacuum firing, which can result in annealing if the temperature is too high.

Figure 8 shows a high gain — low noise signal processor for work function measurements. Op amp A1 and its immediately associated components constitute a floating dc voltage supply for sample bias with respect to ground. With the triple pole/double throw switch in the up position, A1, R1 through R4, and C1 provide a voltage ramp for a linear sweep of the bias. Ramp rate and polarity are determined by R2. Bias voltage can be manually determined with R2 when the switch is in the down position. Bias voltage is reproduced by unity gain isolation amplifier A2. In addition to providing an external sweep signal, A2 also provides a guard voltage for the input signal. A1 is tied to ground through A3, which amplifies the signal input current. The output of the latter provides for separation of the dc and ac portions of the signal to be analyzed.

A 1:1 conjugates lens system was designed and fabricated to permit photographs of LEED patterns. The camera consists of an 8-1/4-inch focal length f/4.5 copy lens, an appropriate lens extender, and a 3 x 5 camera housing.
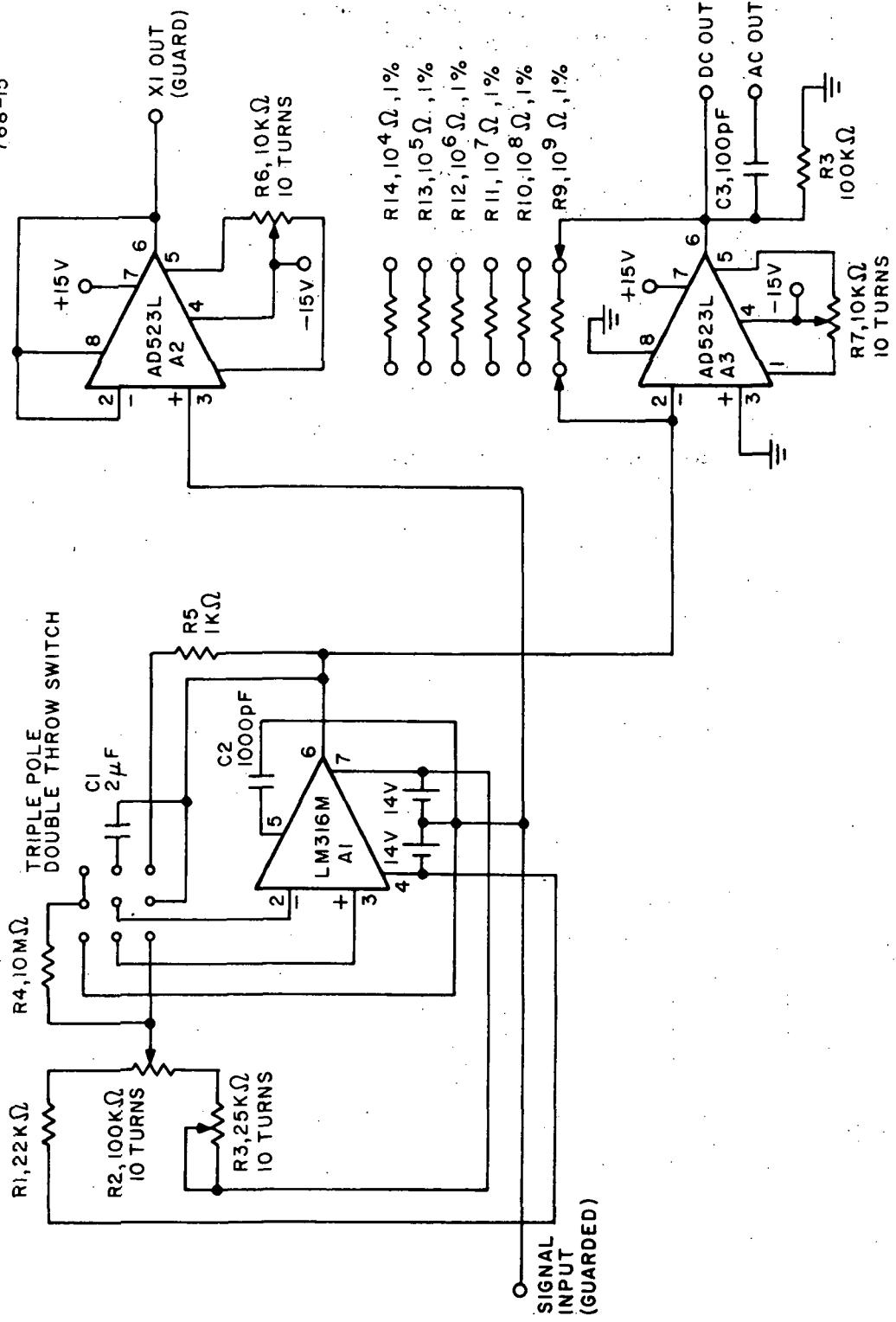
Figure 8. Surface Characterization Instrumentation Amplifier

60

III. HIGH EFFICIENCY DIODE EXPERIMENTS

A. INTRODUCTION

High efficiency converters utilize specially constructed collector electrodes opposite electropolished arc-cast tungsten emitters. The primary emphasis is on obtaining low work function collector surfaces in the presence of oxygen.

Two types of oxygen sources were studied: (1) the decomposition of a metal oxide collector electrode, and (2) the introduction of oxygen through a silver tube on the collector body.

The thermionic diode used in the silver tube experiments is shown in Figure 9. For metal oxide experiments, the collector tubulation was omitted. This diode is well suited for collector studies since the collector may be fabricated separately and then electron beam welded to the emitter subassembly. Thus the prepared electrode surface is subjected to minimal heating and handling.

Because of the simple converter construction and assembly, a number of different surfaces and configurations can be examined inexpensively. All heating, cooling and spacing components are contained on a test stand as shown in Figure 10. This stand is reused for many converters and allows the devices to be readily changed.

All converters are processed through a "predegas" step in which the emitter and collector subassemblies are preheated in an ultrahigh vacuum chamber. Figure 11 shows this predegas flange. This structure allows the electrodes to be heated to temperatures above their operating range while maintaining low pressures at the surfaces. Subassemblies are degassed to a maximum pressure of 10^{-7} torr.

B. TEST PROCEDURES

After outgassing and cesiation, converter performance and electrode work functions are evaluated. Collector work functions are measured by back emission and/or retarding plot techniques. The performance is measured by obtaining cesium families for several spacings over the applicable emitter temperature range. For each family, the minimum potential difference from the J-V curve envelope to the Boltzmann line (i. e., the curve corresponding to zero collector work function and zero collector temperature) is determined. This potential difference is defined as the "barrier index" and is nearly independent of converter conditions at the optimum cesium pressure. J-V curves are traced by sweeping the load voltage at a 60 Hz rate and measuring converter current and voltage.

7510-30

SILVER TUBE

COLLECTOR

CERAMIC SEAL

FLEXIBLE BELLOWS

EMITTER FLANGE

EMITTER SLEEVE

EMITTER WITH PYROMETER AND THERMOCOUPLE HOLES

OUTGASSING TUBE

TO CESIUM RESERVOIR
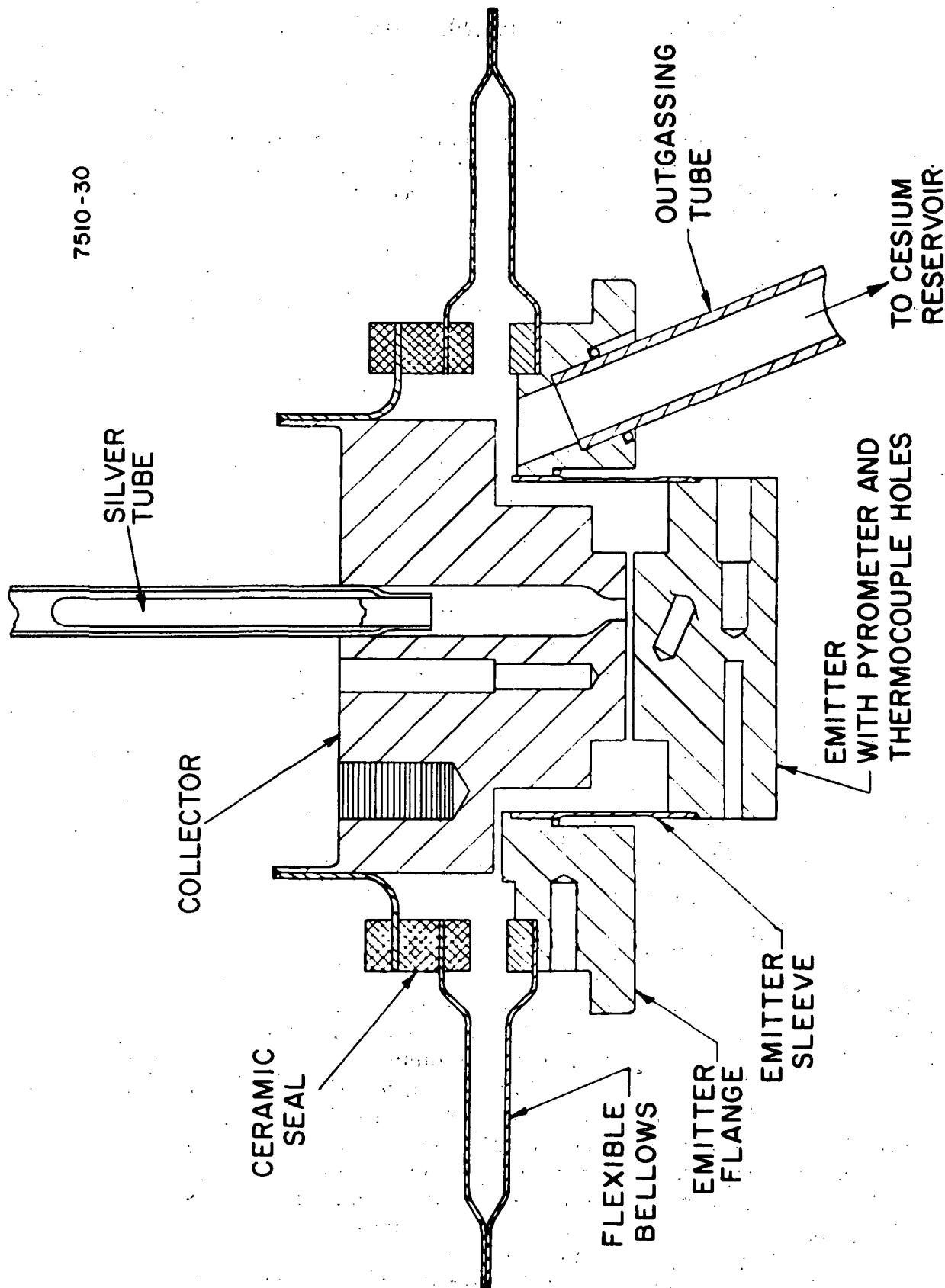
Figure 9. Cross Section of the Standard Variable Spacing Converter with Silver Tube for Oxygen Addition

COLLECTOR
COOLING

BELLOWS

MICROMETER
SCREW

SPACING
ADJUSTER

COLLECTOR
HEATER

COLLECTOR

EMITTER

EB GUN
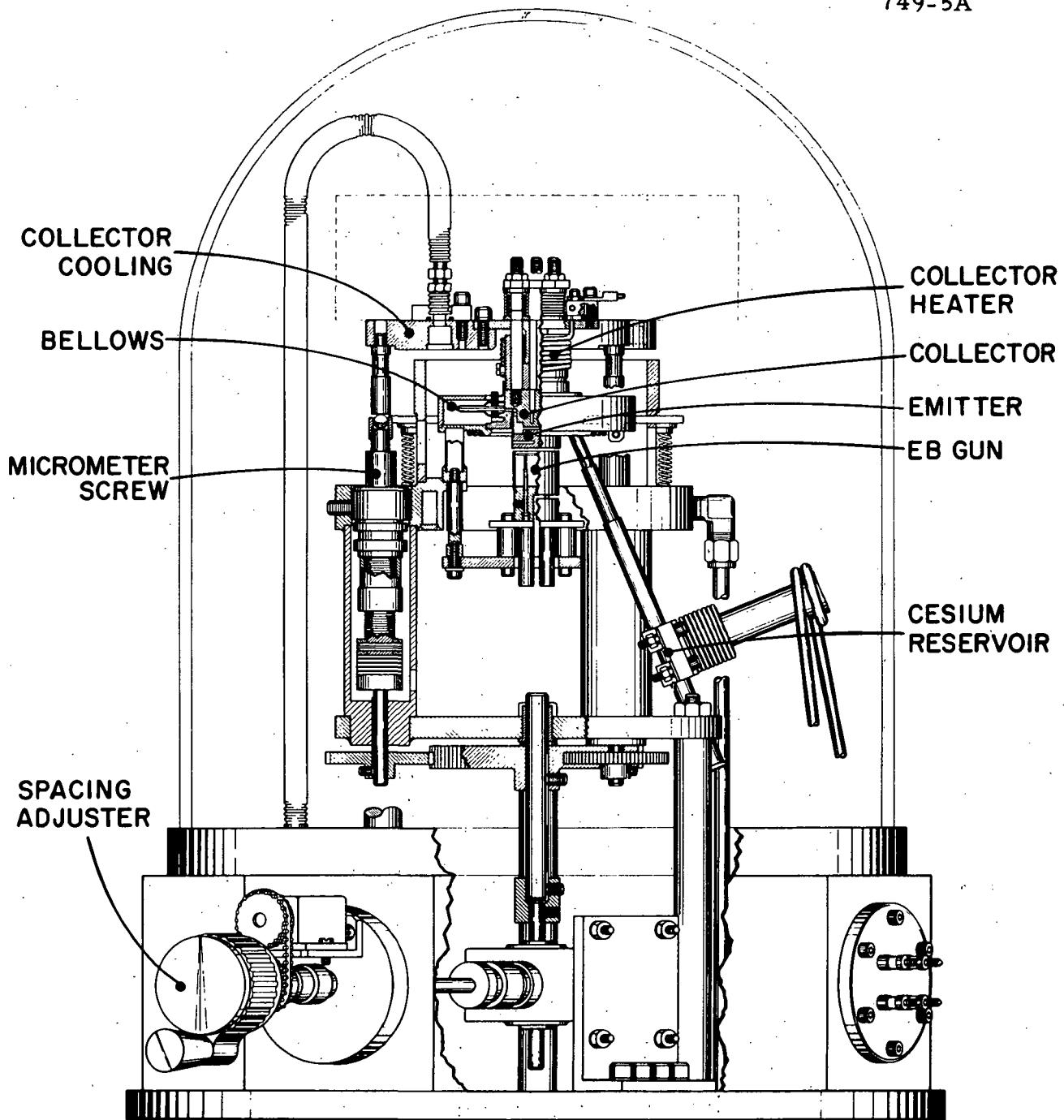
CESIUM
RESERVOIR

Figure 10.   Thermionic Converter Test Stand
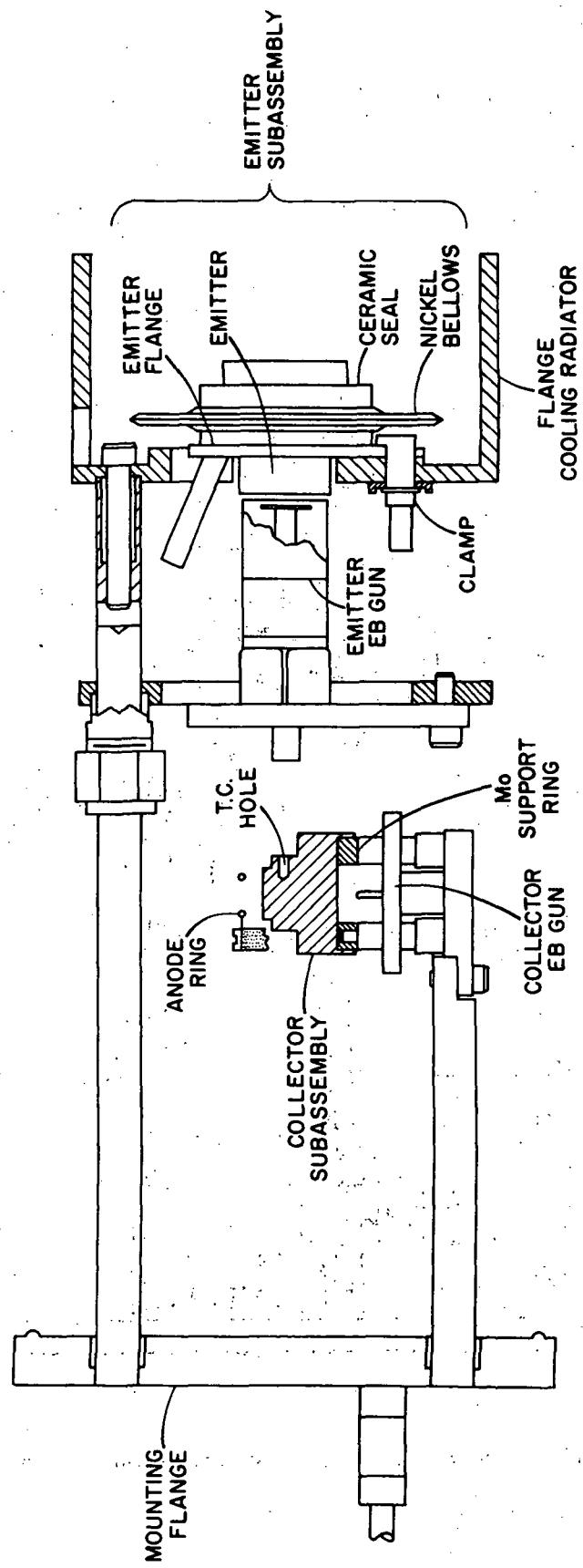
Figure 11. Cross Section of the Predegas Flange

7510-4

64

1. Lanthanum Hexaboride Converter No. 121

Lanthanum boride has been shown to have a low collector work function when activated with cesium and oxygen in the Activation Chamber. A converter was constructed with an LaB_6 collector electrode and included provisions for admitting oxygen during operation. A collector consisting of a 10 mil thick disk of LaB_6 was brazed with nickel to a molybdenum substrate. The substrate, in turn, is copper brazed to the nickel collector body. An 80 mil hole near the center of the disk provides a passage for oxygen into the interelectrode space.

Admission of oxygen into the converter is accomplished through a silver tube arrangement similar to that used in the Activation Chamber. This tube assembly is attached to the rear of the collector as shown in Figure 9. The tube assembly passes through the collector heater and is provided with a separate heater for oxygen pressure control. The outer tube connects through the base plate to the ambient laboratory atmosphere which provides an oxygen supply outside the silver tube. A thermocouple monitors the silver temperature.

Tests of oxygen admission during outgassing indicated that a pressure of 10^{-7} torr was achieved at a thermocouple temperature of about 970 K. Since the thermocouple was in contact with both the stainless-steel outer shell and the silver tube, the indicated temperature may have been somewhat high.

Initial retarding mode work function measurements for cesium gave a work function of about 1.60 eV. The T_C/T_R ratios ranged from 1.30 to 1.17 for the collector temperature of 550 K. At $T_C = 600$ K, the work function increased slightly to 1.62 eV. The performance data showed no evidence of oxygen on the emitter with a 600 K collector and a 1400 K emitter.

When the silver tube was heated to admit oxygen (875 to 1000 K), there was an improvement in both performance and collector work function (1.55 eV). At this point the characteristics appeared to be similar to those of tungsten oxide collectors. Changes in silver tube temperature did not produce an oxygen effect on the emitter. At low silver tube temperatures, the tubulation would condense cesium and then evaporate it when the temperature was increased to add oxygen, resulting in a transient increase in current.

After the initial experiments, which showed an oxygen admission capability, prolonged heating to 775 K could not restore the oxygenated characteristics. In fact, there was no further indication that oxygen came through the silver tube. The minimum barrier index measured

was about 2.1 eV. Retarding collector work function measurements gave values around 1.6 eV. Lower mode data looked somewhat similar to that for a tungsten oxide collector. It is possible that oxygen admitted through the silver tube into the diode formed tungsten oxide at the emitter which was then transported to the collector surface.

Upon opening the diode, microscopic inspection showed pitting of the tungsten emitter around the tubulation hole in the lanthanum hexaboride collector. The surface was silvery with slight tinges of blue. There was no indication of cesium oxide or any obstructions in the silver tube or in the collector orifice. Auger analyses of both emitter and collector detected nothing unusual on the surfaces.

2. AuCs Converter No. 131

Since gold and cesium are known to combine to form a semiconductor, and tests in the surface chamber have shown low work functions when combined with oxygen, a second silver tube converter was constructed utilizing a gold foil collector electrode. This converter had a standard electropolished tungsten emitter and a gold collector. The 10 mil thick gold collector surface was bonded to a molybdenum substrate at 1000 C and then copper-nickel brazed to a nickel collector structure. A silver tube was brazed onto an opening in this structure to provide a controllable source of oxygen for high efficiency experiments.

After outgassing, dc back emission measurements were taken to determine collector work function. During this time the silver tube was heated to admit oxygen. After several alternate exposures of cesium and oxygen, a work function of 1.35 eV was measured. Next, retarding plots taken at similar conditions gave work functions in the 1.7 eV range and subsequent back emission measurements confirmed the results. Power data indicated that oxygen could be admitted into the diode through the silver tube but not during the periods of high cesium pressure. Instead of elemental oxygen, it is possible that the emitter may be oxygenated from the formation of cesium oxide which is decomposed by the emitter to release oxygen. After the above tests, testing was terminated because the gold foil began to lift from its bond causing the converter to short.

3. Titanium Oxide Converter No. 123

As part of Thermo Electron's studies of metal oxide collectors, a standard variable spacing converter was constructed with an oxidized titanium collector. The purpose of this converter was to reproduce the results of Professor J. P. David (University of Marseille, France), presented at the Eindhoven Conference.

The collector was fabricated by nickel brazing a titanium disk to a molybdenum cap which, in turn, was Cu-Ni brazed to the usual nickel collector body. The complete assembly was then oxidized at 725 K for four hours in one atmosphere of oxygen. The assembly was then final machined except for the electrode surface. The emitter was electropolished tungsten. Predegassing was carried out with 525 K as a maximum collector temperature. Outgassing was completed with the same temperature restriction.

Initial testing in the lower mode gave collector work functions of about 1.5 to 1.6 eV at 500 to 600 K. The performance of the converter was relatively poor ($V_B = 2.3$ eV) with no evidence of an oxygen supply for the emitter. At 650 K the collector work function improved to 1.45 eV. At higher collector temperatures (850 K) and higher emitter temperatures (1800 – 1900 K), the barrier index improved to 2.15 eV. Since there was no evidence of an oxygen supply for the emitter, spacings of 10 mils or less were required. The performance was comparable to that of tungsten collector converters. The optimum collector temperature was in the range from 850 to 900 K with the barrier index in the range from 2.1 to 2.2 eV. The performance was measured from 1400 to 1900 K emitter temperature at spacings from 10 to 20 mils.

4. Tungsten Oxide Converter No. 122

Tungsten oxide collectors have produced improved converter performance both by providing a source of oxygen for the emitter and by acting as low work function collector electrodes. However, the chemical reactions occurring on the surface during converter operation are not well understood. Several converters using tungsten oxide as a collector are being constructed and will be used for a study of the surfaces at various stages of converter operation. After a period of testing, the converter will be shut down and the surfaces examined.

During operation of these collectors, three types of performance are typically observed. Initially the characteristics are relatively poor with series resistance apparent. After about 5 to 10 hours of testing, the barrier index improves to 2.1 – 2.2 eV. If the collector temperature is cycled to about 850 K at this time, a further improvement of the barrier index to 1.85 – 1.95 eV can be obtained. This level may be stable for about 100 hours after which the barrier index will return to 2.1 eV where it remains and cannot be subsequently reduced.

Converter No. 122 is one of a series used to study these changes. This standard variable spacing converter used a deposited tungsten oxide on a sandblasted tungsten substrate collector. The emitter was electropolished tungsten. After cesiation, the cesium tubulation

appeared to be plugged, trapping the cesium in the converter. The emitter flange was heated to 1020 K and the collector to 530 K which finally cleared the plug and allowed the cesium to condense in the reservoir.

The lower temperature performance of the converter was relatively poor (V_B = 2.3 to 2.4 eV, with collector temperatures of about 650 K). There was only a small amount of oxygen supplied to the emitter. At higher emitter temperatures (1800 and 1900 K) and a collector temperature of 750 K, there was still evidence of oxygen for the emitter, and the barrier index had improved to 2.2 eV. It is possible that the treatment used to unplug the cesium tubulation depleted the oxygen concentration on the collector. Testing was concluded on this converter without raising the collector temperature to over 750 K.

The collector showed a life history usually observed with the tungsten oxide converters. From the initial barrier index of 2.3 – 2.4 eV, the performance improved to 2.1 – 2.2 eV as testing continued. At this time the collector supplied ample oxygen for the emitter over the temperature range from 1400 – 1900 K. The collector was not heated to over 750 K so that this initial "pre-activation" state could be preserved for chemical and physical analyses of the electrode surface.

Figure 12 shows a cesium family at 1900 K emitter temperature. Figure 13 shows a similar family at 1600 K. These curves are representative of the converter at the later stages of the initial performance and give a barrier index of about 2.2 eV. By the time the curves of Figure 14 were obtained, the performance had improved to a barrier index of 2.1 eV. Notice that by comparing the curves of Figures 13 and 14 (1600 K), the presence of oxygen on the emitter is apparent. In Figure 13 the spacing is 0.5 mm while in Figure 14 it is 1 mm. Further, the cesium temperature required for the knee of the J-V curve at 5 amps has decreased from 528 K to 487 K. Collector work function was not measured on this device because the measurement might have modified the preactivated state which was to be preserved for analysis.

C. CONCLUSIONS

The silver tube experiments, combined with the results of the tungsten oxides and with experiments utilizing oxides deposited outside the interelectrode space, indicate that oxygen cannot be transported through cesium vapor to the emitter. Both diffusion through the cesium and the gettering of oxygen on the cesium covered walls of the device preclude the admission of oxygen from outside the interelectrode space. However, if the oxygen is in combined state (such as might be the case with a cesium oxygen reservoir) with the oxygen appearing only after contact with the hot emitter surface, external control and supply are feasible. Additional studies in this area are required to define the

68
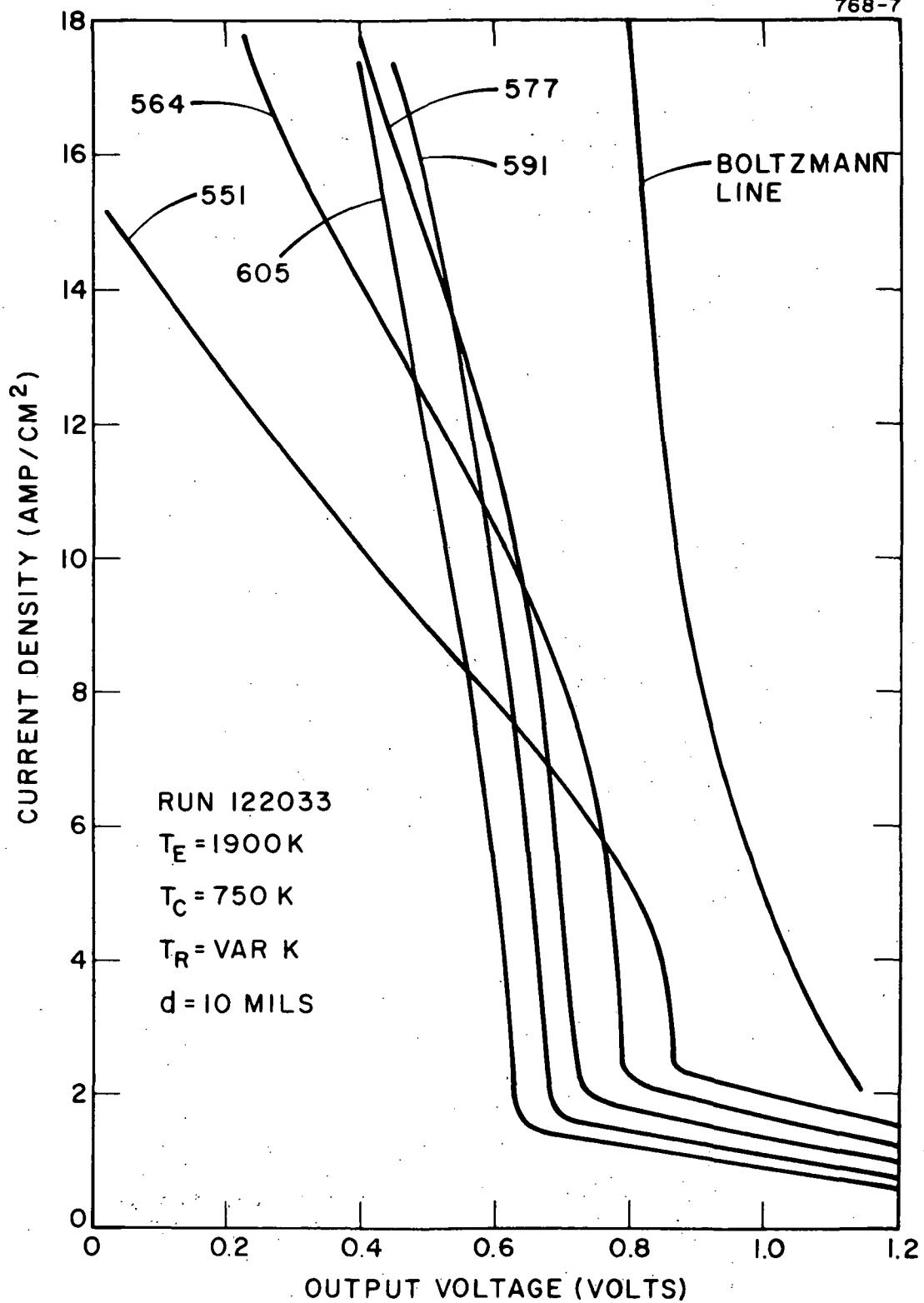
Figure 12. Cesium Family Tungsten Oxide Collector
(Early Data)
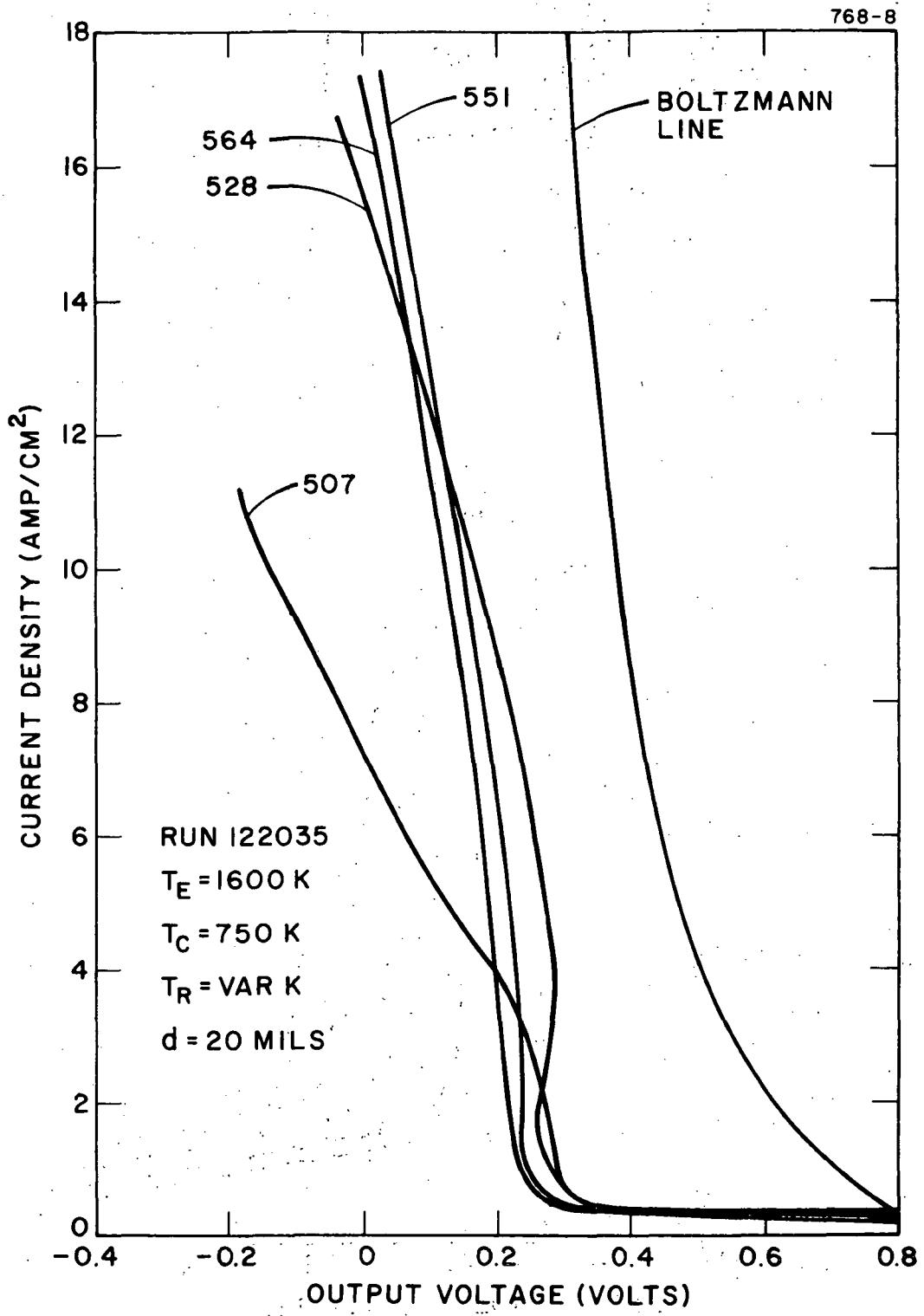
Figure 13. Cesium Family Tungsten Oxide Collector
(Early Data)
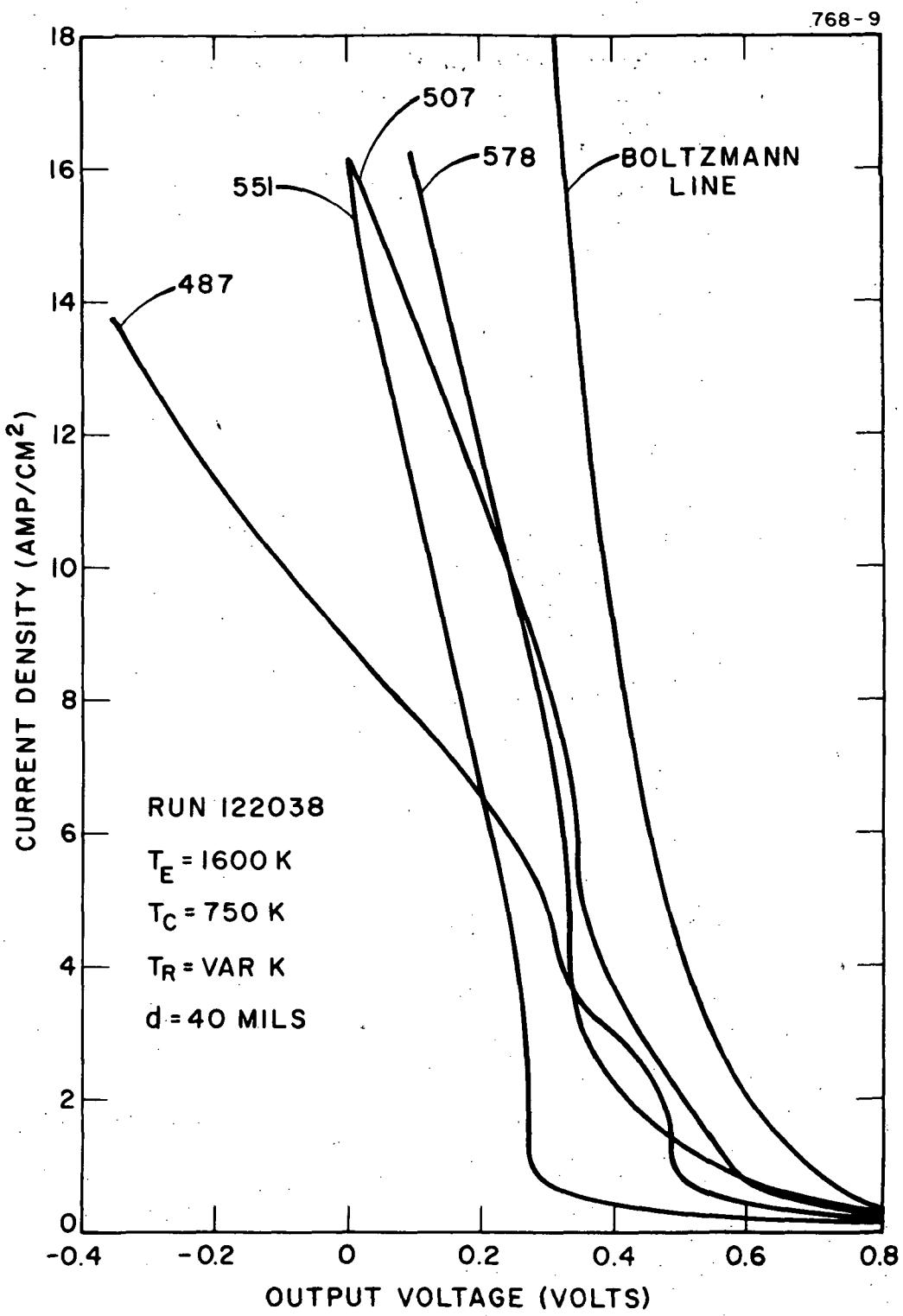
Figure 14. Cesium Family Tungsten Oxide Collector
(Later Data)

combined cesium oxygen reservoir operation. At low cesium pressures ($\sim 10^{-4}$ torr) batch additions of oxygen are possible. A converter may be temporarily oxygenated by heating the silver tube with the cesium reservoir at room temperature.

Selected metal oxides (e. g., tungsten oxides) are capable of both supplying oxygen for the emitter and acting as a low work function collector. The titanium-oxygen collector did effectively supply oxygen to the emitter and reduced the collector work function. More intense oxygen treatments will be required if this material is to be studied further. At present, the oxygenated tungsten is a more attractive material because of the low barrier indices generated and because of the compatibility with the emitter. Additional investigations are required to determine the chemical reactions in the oxidized tungsten converter.

IV. TRIODE CONVERTER EXPERIMENTS

A. INTRODUCTION

During the past twelve months Thermo Electron Corporation initiated an experimental program aimed at lowering voltage losses associated with the interelectrode plasmas in thermionic converters. Reduction of the plasma voltage drop is especially important for space system applications where high collector temperatures (desirable to minimize radiator size and system weight) preclude the use of collectors with work functions low enough to give appreciable back emission. The investigations focused on triode configurations in which an auxiliary electrode furnished (either by surface contact ionization or pulsed volume discharge ionization) the ions for space charge neutralization. By tailoring such techniques to optimize the supply of ions for a given auxiliary input energy, it should be possible to enhance operation of the converter with respect to that obtained from the usual ignited-mode diode.

A second approach to reducing interelectrode losses is to decrease the spacing between the emitter and the collector to extremely low values, thereby preventing the formation of a substantial space charge in the interelectrode region. The following pages describe the status of both approaches.

B. TRIODE EXPERIMENTS

The triode configuration tested is shown in Figure 15. The grid is constructed of either four or five 0.125 mm diameter tungsten – or 0.125 mm diameter molybdenum – wires spaced 2 mm apart. The grid is located in a fixed position approximately 1 mm from the collector. Emitter-to-collector spacing is variable from 2 to 6 mm. Initially the grid was dc heated to 2000 K with the converter operating in the surface-ionization diffusion mode. Enhanced output was observed at low cesium pressures ($\sim 8 \times 10^{-3}$ torr), in reasonable agreement with theoretical analyses. Lower output was obtained at higher cesium pressures (~ 0.1 torr) than analytically predicted. An increase in thermionic current was observed upon pulsing the ionizer heating current. This increase was probably due to elimination, during the off-portion of the pulse, of the voltage gradient existing along the ionizer wires during heating which prevents effective space charge neutralization (ref. 10). In the course of these experiments, a discharge developed between the emitter and emitter sleeve which seemingly enhanced the output current over that obtained from surface ionization at the grid. Subsequently, the triode was operated in a discharge mode similar to that reported by Knechtli and Fox (ref. 11), albeit in a cesium environment. Enhanced output over surface ionization was observed but secondary discharges within

CESIUM
INLET

IONIZER
GRID
WIRE
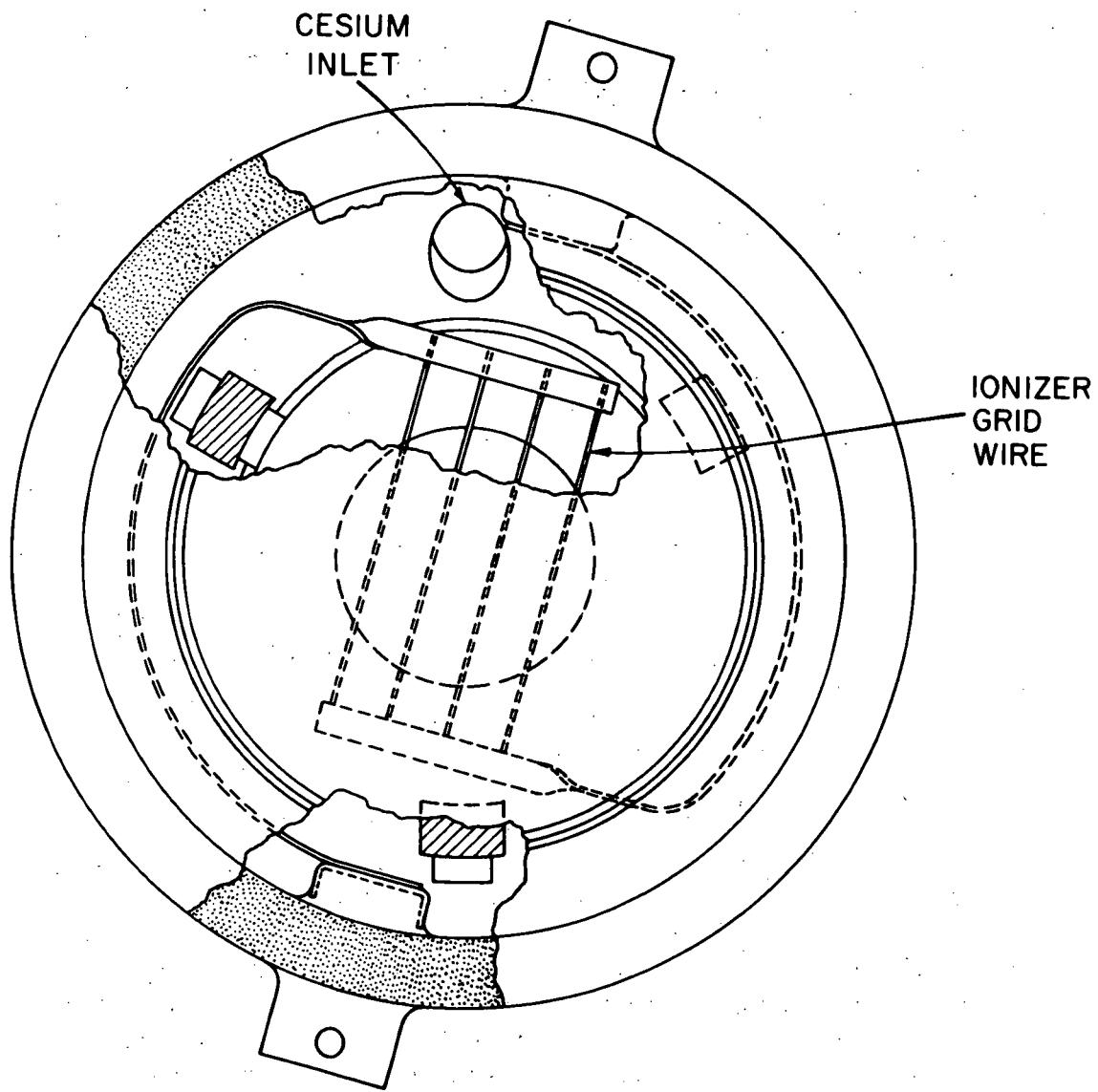
Figure 15. Grid Triode (Top View)

the converter precluded quantitative evaluation of the measurements. The improved performance suggested that future experiments be conducted with this discharge mode.

In order to optimize ion production in a discharge for a given amount of auxiliary power, one should maximize the ratio of ionization-to-elastic electron-atom scattering cross sections (see Figure 16). For plasma elements of interest to thermionics, such maximization occurs at relatively high voltages (around 100 V). Even if such high potentials could be sustained in a continuous dc discharge within a thermionic converter plasma (which they cannot, since breakdown voltages in low pressure cesium atmospheres are typically around 10 V), the auxiliary energy drain would be prohibitive. Consequently, attention was centered on high-voltage, high-frequency, short-pulsed systems with rapid pulse rise times to allow substantially higher than dc breakdown voltages with minimum time-averaged energy expenditure. The electronic pulsing circuit design is shown in Figure 17. By using a low-valued capacitor (C_D in the range of 10 - 20 nF) charged to voltages of 80 - 100 V, small amounts of energy are rapidly discharged into the interelectrode plasma to create ions collisionally. Inert gas atoms impede diffusion of these ions to the electrode surfaces where they are lost by recombination with electrons. Thus the inert gas pressure (typically around 2 torr) maximizes the ability of the ions to neutralize the converter current limiting electron space charge. If the plasma is composed of inert gas atoms then ion production is appreciable from the energetic discharge electrons while, due to the Ramsauer minimum in the elastic cross-section curves, the resistance effects of the atoms on the low-energy (~0.3 eV) thermionic electrons is minimal (see Figure 16).

Two configurations were considered for the pulsed-discharge triodes. The first incorporated the auxiliary grid electrode described previously. Although inert-gas, noncesium bell jar experiments showed that this configuration distributed the high-energy discharge evenly across the surface of the electrodes, the physical dimensions of the grid limited the minimum separation of emitter and collector to about 2 mm. Consequently, a second configuration was formulated wherein a thin tantalum auxiliary ring electrode surrounds the emitter and collector so that (Figure 18) the discharge occurs almost tangentially across their surfaces. Schematically, operation of the grid and ring-triodes are shown in Figures 19 and 20, respectively. In inert-gas bell jar simulation experiments of ring triodes containing no cesium, uniform distribution of the discharge across a room-temperature electrode surface was observed.
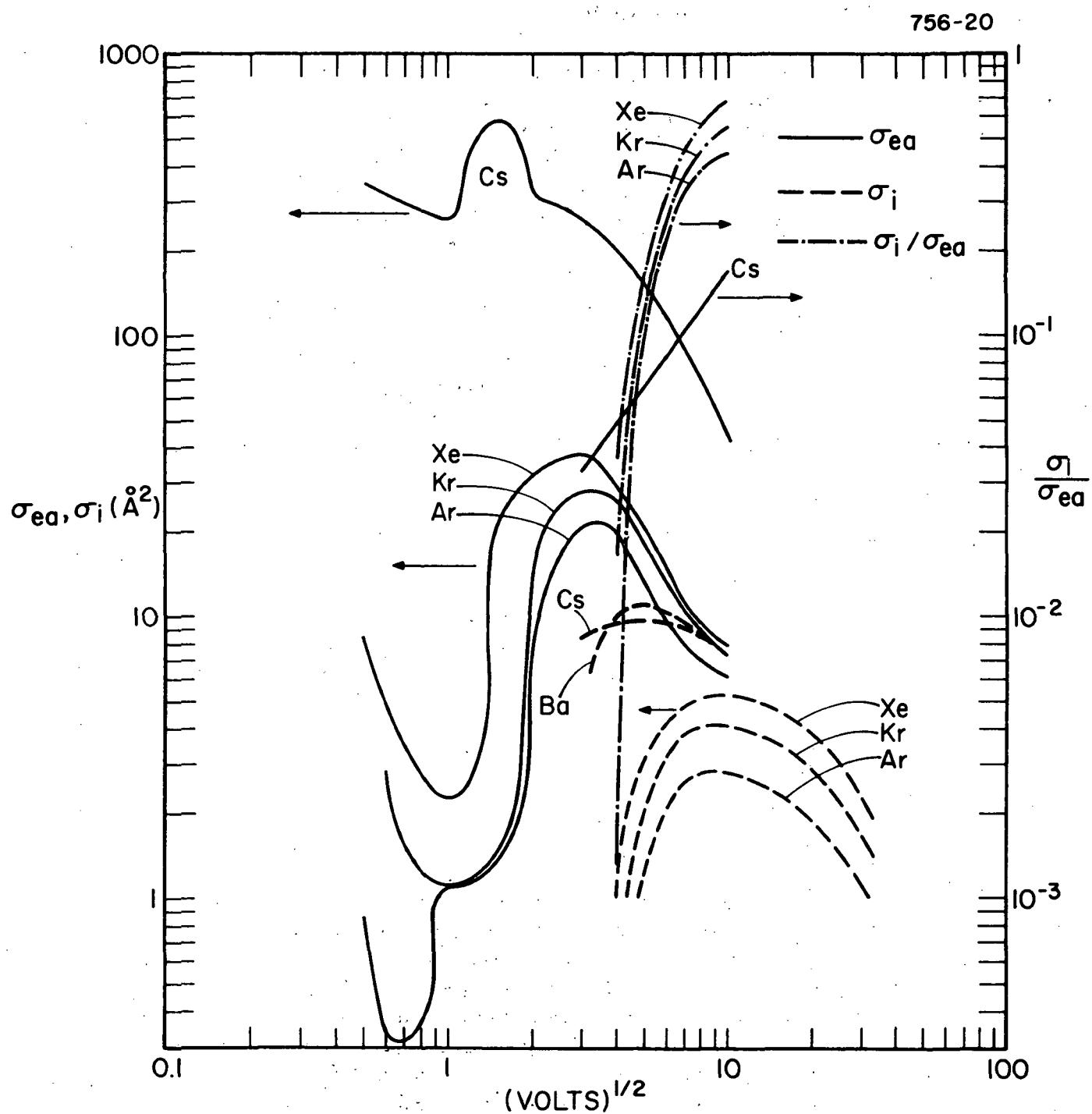
Figure 16.   Electron Collisional and Ionization Cross-Sections
for Cs, Ba, A, Xe and Kr

7510-14A
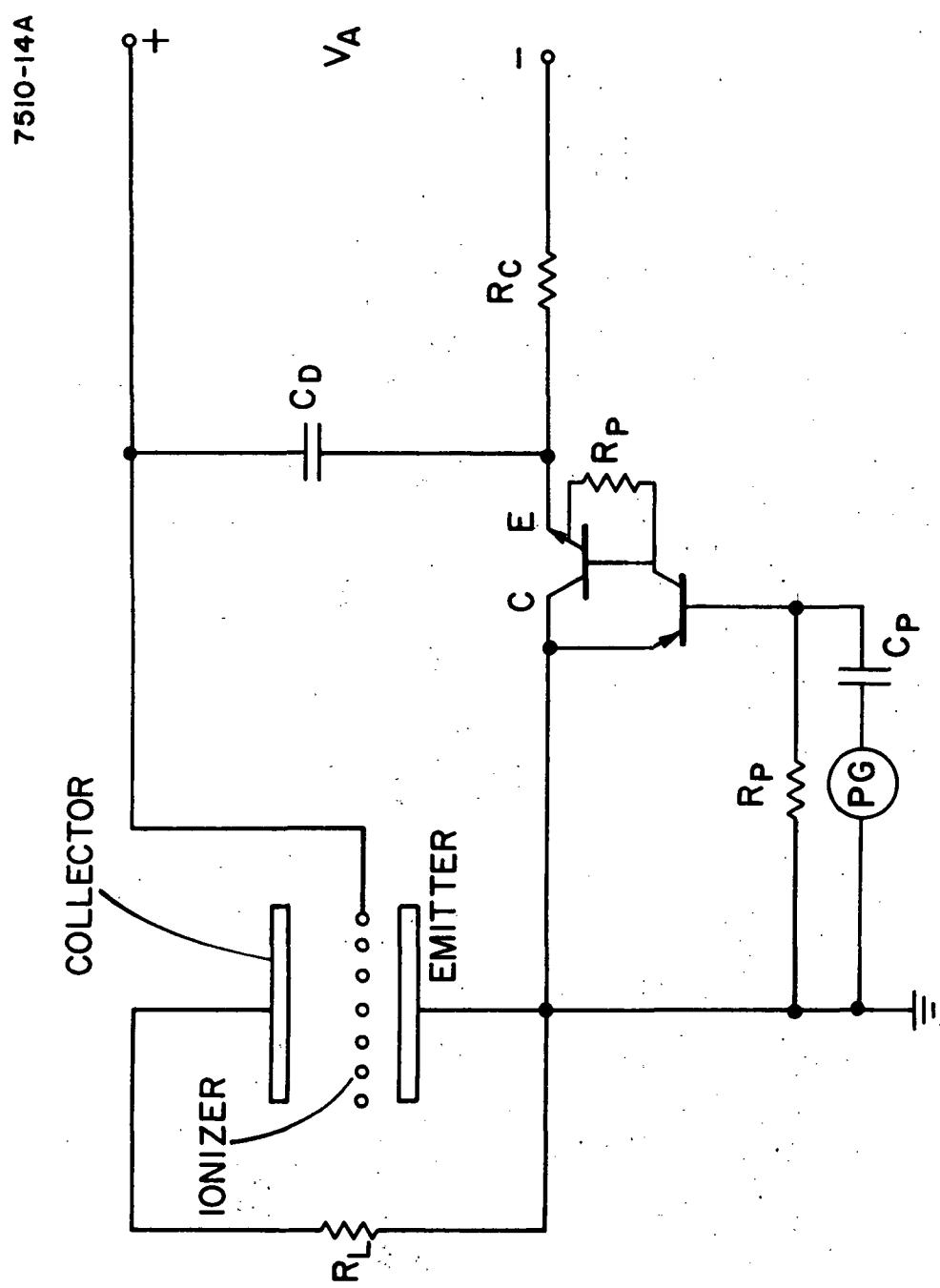
Figure 17. Electronic Pulsing Circuit for the Grid Triode Converter

7510-15

EMITTER

IONIZER
RING
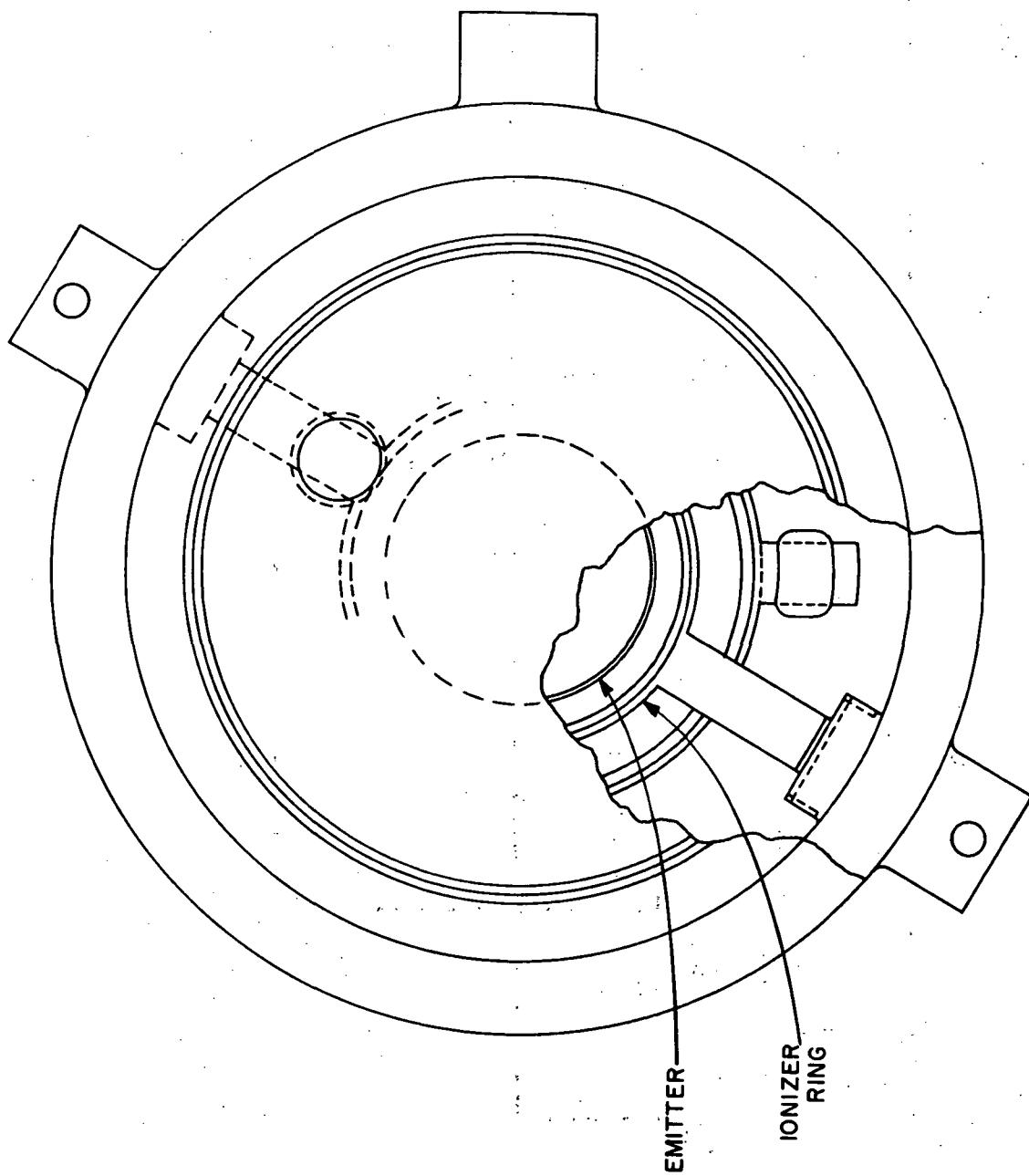
Figure 18. Ring Triode (Bottom View)
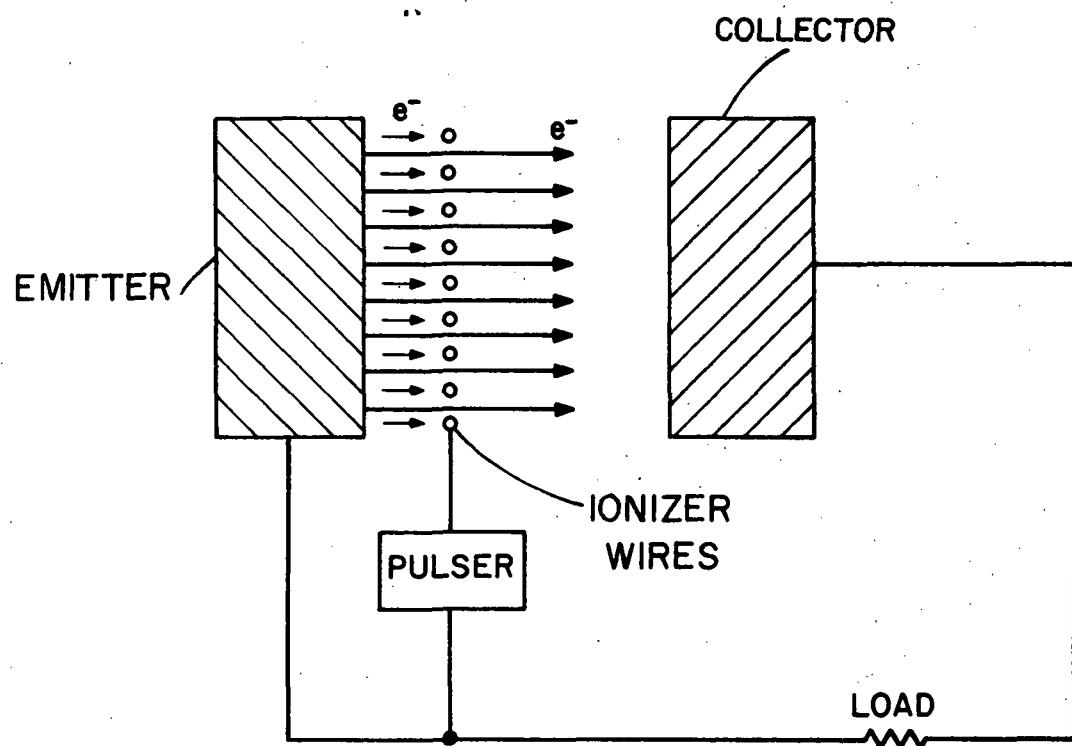
Figure 19. Schematic of the Operating Grid Triode Converter

IONIZER
RING
EMITTER   COLLECTOR

PULSER

LOAD
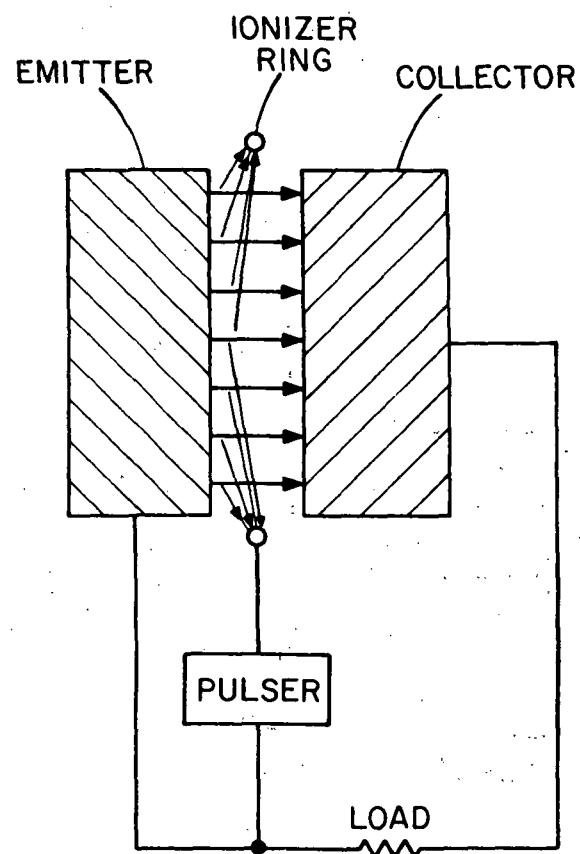
Figure 20.   Schematic of the Operating Ring
              Triode Converter

The bell jar simulation-experiments were also used to measure ion lifetimes. At 2 torr of argon, up to 100 V positive on the ring electrode, and pulse lengths of 5 µs, electron-ion recombination emission was spectrally resolved and observed to last over 100 µs after completion of the pulse. Thermionic converter measurements of thermionic current decay for currents up to one ampere, in a pulsed system, corroborated these findings.

The high resistance of cesium to the flow of thermionic electrons makes this element less than optimum as the plasma source. As noted earlier, the inert gases should be substantially better. Nonetheless, at present a significant amount of cesium is required to reduce electrode work functions for efficient thermionic emission and collection. In order to quantitatively determine the effects of mixtures of inert gases with cesium in a pulsed triode converter, a grid triode was constructed containing a Philips Type M dispenser emitter. This cathode operates with a work function of approximately 2.1 eV without cesium coverage. The collector was biased positively with respect to the emitter to simulate low collector work functions allowing this type of converter to be used to investigate the possibility of pulsed space charge neutralization in cesium-rare gas mixtures.

No cesium was introduced in the initial series of experiments and the converter was filled with either argon or xenon to pressures up to 25 torr. Positive potentials as high as 60 V were imposed across the plasma. Emitter-to-collector spacing varied from 1.85 to 5.85 mm, with a fixed grid-to-collector separation of 0.93 mm. Best results were obtained at 1 torr pressure and close to maximum electrode spacing. With the dispenser cathode at 1575 K, the mean auxiliary power expended to provide 370 mA of thermionic current was 0.016 W for a V_d^* (potential loss due to auxiliary power input) of 0.04 V. The experimental results are shown in Table XXIV. A high ratio (240) of triode current to time-averaged auxiliary current was measured for a pulse discharge period of approximately 0.2 µs. However, saturation currents from the dispenser emitter were only of the order of 1A. A leak was found to have developed in the converter during testing, thereby continually contaminating the emitter surface.

Replacing the pulsing auxiliary supply by a dc power source produced no current amplification. Voltages were limited to 13 V where gas breakdown occurred.

Although the triode currents did not exceed one-third of an ampere, the significance of these results was to show that fast-pulsing techniques can allow large voltages to be applied to the plasma for short periods of

TABLE XXIV

GRID TRIODE TESTS (NO CESIUM)

A	P_{aux} (mW)	V_d^* (V)	Gas	P (torr)	T_E (K)	T_C (K)	d_{EC} (mils)	V_A (V)	V_{pl} (V)	$I_{A(avg)}$ (mA)	$V_{EC(Biased)}$ (V)	I_{EC} (mA)	C_D (nF)	Freq. (kHz)	Pulse Length (μs)
			Ar	25	1423	-	132	90		1.1	1.5	75	20	3	
				16	1423	-	146	90		1.1	1.5	94	20	3	
				12	1423	-	188	90		1.1	1.5	135	20	3	
				8	1423	-	194	90		1.1	1.5	145	20	3	
				6	1423	-	234	90		1.1	1.5	150	20	3	
78	60	0.32		6	1423	-	234	90	45	w/o ammeter	1.5	190	20	3	1
99	70	0.21		14	1425	-	207	90	60	"	1.5	340	20	3	1
			Xe	12-20	1533	-	213	90	45	"	1.5	160	5	3	0.2-0.5
				18	1533	-	213	90		"	1.5	160	5	3	
				12	1533	-	213	90		"	1.5	250	5	3	
				10	1533	-	213	90		"	1.5	280	5	3	
				8	1533	-	213	90		"	1.5	300	5	3	
				6	1533	-	213	90		"	1.5	310	5	3	
213	25	0.077		4	1533	-	213	90	66	"	1.5	320	5	3	0.3
247	16	0.04		1.2	1580	-	217	90	58	"	1.5	370	5	3	0.2
167	2.8	0.14		0.8	1459	-	217	90	55	"	1.5	200	5	3	0.4

time to permit optimizing the ionization process by operating at the most advantageous ionization cross section. Furthermore, these large voltages do not constitute a substantial auxiliary input energy (as evidenced by the low values of V_d^* obtained in Table XXIV for low duty cycles of pulsing). In addition to providing ions by electron-atom collisions, the large atom-ion elastic cross sections impede ion diffusion out of the converter. This effect was substantiated by ac probe measurements of the triode thermionic current which reached a maximum during the pulse and then decayed at a rate inversely dependent on the inert gas pressure. At several torr pressures, current decay of only 10-20 percent was observed over the 333 μs time period between pulses (3 kHz pulse repetition rate).

In the next series of tests, the inert-gas plasma was augmented by cesium vapor in the interelectrode region of the grid triode. A cesium pressure of 0.033 torr increased the triode current dramatically to nearly 1A for an auxiliary voltage of 180 V (78 V across the plasma), 4 torr of xenon, 5 nF pulsing capacitance, an emitter-to-collector spacing of 5.85 mm, the collector biased at 2 V and an emitter temperature of about 1640 K. V_d^* continued to remain low for a 3 kHz pulse length of about 120 ns. Most of this increase in current is attributed to a reduction in collector work function by the cesium vapor. A list of these test results is shown in Table XXV. The significance of these experiments is that short pulses allow the use of higher grid potentials in substantially higher cesium vapor pressures than are possible with dc grid potentials (where breakdown at less than 10 V is typical).

The I-V characteristics of the grid triode were investigated by successive variation of each of the following parameters: emitter temperature (1423 - 1673 K), collector temperature (598 - 718 K), cesium reservoir temperature (353 - 503 K), emitter-to-collector spacing (83 - 234 mils), positively biased potential on the grid (50 - 150 V), capacitance of the pulsing circuit (3.3 - 20 nF), xenon or argon gas pressure (1 - 20 torr) and pulsing repetition rate (1 - 10 kHz).

The results indicate that, for the ranges analyzed, better performance was observed with increasing emitter temperature, higher cesium reservoir temperature (up to 440 K), larger electrode spacing, increasing grid voltage, larger pulse circuit capacitance and higher pulse repetition rates. Performance generally decreased with increasing collector temperature and increased with inert gas pressure up to 2 torr (with little additional change above this value). Argon gave slightly better results than xenon.

TABLE XXV

GRID TRIODE TESTS (WITH CESIUM)

A	P_{aux} (mW)	V_d^* (V)	Gas	P (torr)	T_E (K)	T_C (K)	T_R (K)	P_{cs} (torr)	d_{EC} (mils)	V_A (V)	V_{pl} (V)	V_{EC}(Biased) (V)	I_{EC} (mA)	C_D (nF)	Pulse Freq. (kHz)	Pulse Length (μs)
			Xe	2	1640	656	343	$8(10^{-5})$	234	180	55	2	670	5	3	0.20
			Xe	2	1642	770	339	$5(10^{-5})$	234	180	62	2	815	5	3	0.20
			Xe	2	1641	800	340	$6(10^{-5})$	234	180	60	2	800	5	3	0.16
			Xe	2	1639	815	340	$6(10^{-5})$	234	180	60	2	810	5	3	0.16
356	30	0.04	Xe	2	1641	817	340	$6(10^{-5})$	234	180	75	2	890	5	3	0.10
			Xe	4	1638	816	378	(10^{-4})	234	180	70	2	930	5	3	0.12
			Xe	4	1638	816	453	$3.3(10^{-2})$	234	180		2	960	5	3	
			Xe	4	1638	816	473	$7.4(10^{-2})$	234	180		2	950	5	3	
			Xe	4	1638	816	480	$9.7(10^{-2})$	234	180		2	940	5	3	
			Xe	4	1638	816	453	$3.3(10^{-2})$	234	180	78	2	975	5	3	0.12

The effect of cesium on the I-V characteristics in the pulsed grid triode is shown in Figure 21. Each curve is marked with the cesium reservoir temperature for which it was measured, both with pulsing (P) and nonpulsing (NP). At the low cesium pressures significant output enhancement is observed with pulsing, which, at constant auxiliary input energy progressively reduces as the cesium pressure is raised. Obviously, high density, high current ignited mode operation will require pulsing larger energies into unignited plasmas.

Unignited plasmas are possible for higher electron densities if the emitter-collector spacings are significantly small. In such configurations plasma resistance effects would be minimized. Ring triodes have the feature of a potentially long electron pathlength for ionization, yet a shorter length for thermionic electron passage from emitter to collector. Such a ring triode was constructed, but an unrepairable electrical short developed during activation of the Philips Type M emitter. A second triode is being constructed.
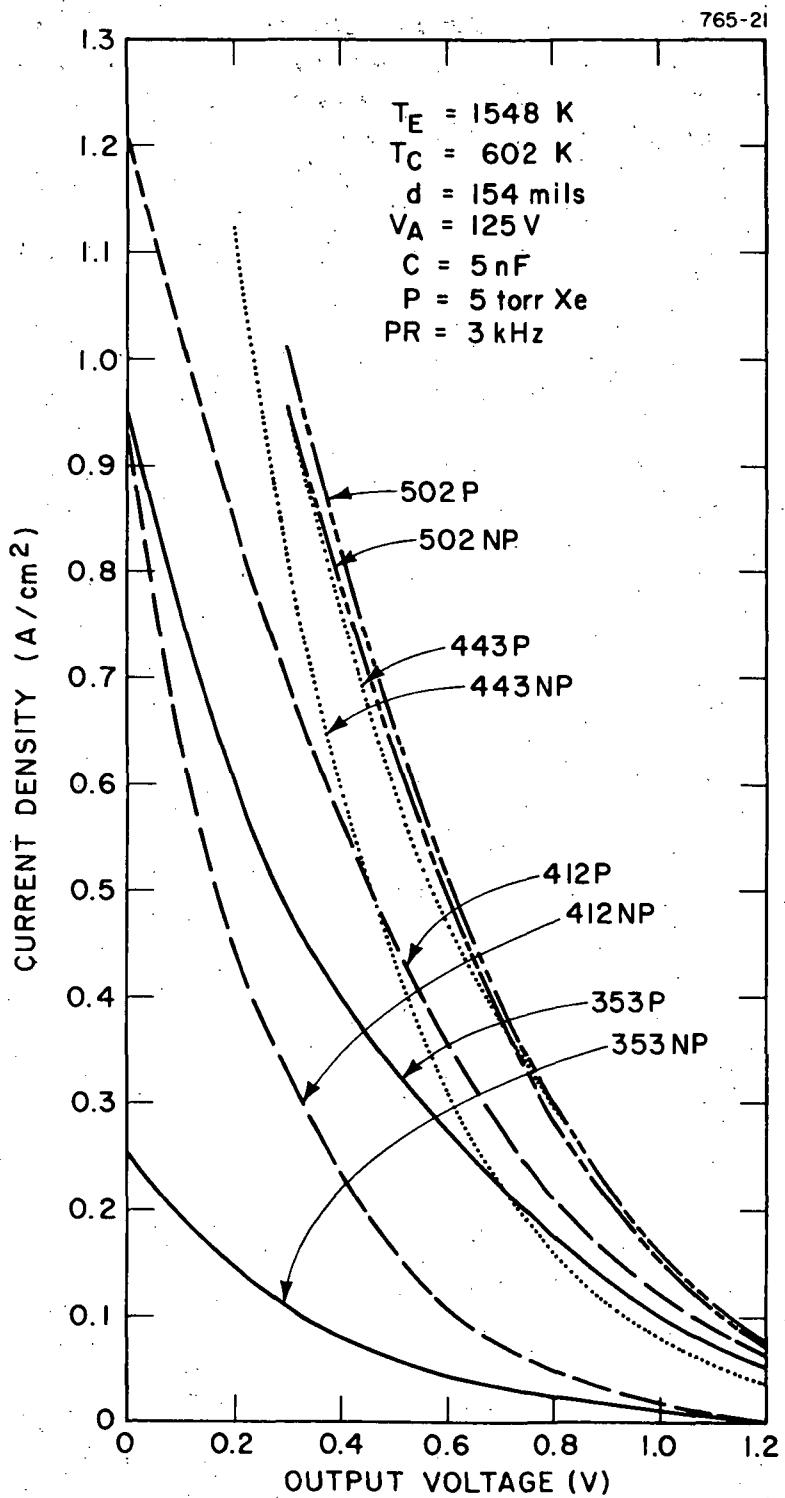
Figure 21. Effect of Cesium on I-V Characteristics in
the Pulsed Grid Triode

V. POWDER PUFF DIODE

A. INTRODUCTION

This section summarizes the design concept and development status of a novel thermionic converter termed the "Powder Puff Diode," or PPD. The principle object of the theoretically simple PPD is an improved thermionic converter which has the following advantages:

1. Zero arc drop (typically, an arc drop of about 0.5 eV is required to maintain ionization in the "ignited" mode)

2. Negligible scattering losses

3. No additional electrodes

4. No auxiliary power input

5. No rare or nitrogen gas fill

6. No external circuits required

7. Easy to analyze (relative to ignited mode or auxiliary discharge converters)

8. Oxygen additive for emitter not necessary (If oxygen is desired for the collector, its supply can be optimized for this purpose.)

9. Mechanically simple

10. Insensitive to mechanical and thermal shock

Basically, the PPD is a close-spaced thermionic diode in which design modifications offer the possibility of circumventing the mechanical and electrode problems which plagued earlier vacuum diodes. The elements of novelty are:

1. The use of an insulating powder spacer (such as zirconia, alumina, thoria, magnesia, etc.) in conjunction with

2. A compliant (or "pillow") collector which can yield to conform to the emitter distortions while the flexible powder spacer maintains the characteristic interelectrode gap without electrical shorting. In addition,

3. Cesium vapor is used to provide stable, low work function electrodes (in contrast to close-spaced vacuum converters with dispenser emitters which poisoned the collectors with barium).

With respect to Item 3, the PPD is similar to the Isomite miniature thermionic converter (ref. 12) built by McDonnell-Douglas which also operates in the space charge limited vacuum mode.

The use of a fine particulate powder (characteristic diameter of about 5 microns) coating for spacing the emitter and collector is an essential feature of the PPD. The critical question as to the PPD feasibility is: "Can the small interelectrode spacing be maintained by the powder spacing without electrical shorting and without excessive conductive heat transport?" Fortunately, there is considerable evidence that this question can be answered affirmatively since the PPD spacing technique is essentially that used in Thermo Electron's Multi-Foil thermal insulation (ref. 13). Multi-Foil insulation is described in Section E. This description includes relevant heat flux data and a discussion of particle selection for the PPD.

Preliminary steps have been taken to reduce the PPD concept to practice. The test diode design, membrane bonding studies and collector conformation investigations are described in Section F.

In summary, the mechanically and electrically simple PPD eliminates both arc drop and scattering losses. No additional electrodes are required, no auxiliary power input is necessary and no additive rare gases are required. Multi-Foil and Isomite experience should be applicable to the PPD. If the difficult spacing problem can be solved, incorporation of collector surfaces under development at Thermo Electron (e.g., WO_3, ZnO and BaO) should result in "second generation" performance. From a development philosophy viewpoint, it is desirable to be able to focus on a single technical challenge (spacing – for the PPD) rather than on a multiplicity of problems (e.g., ionizer work function, ionizer temperature, additional seals, rare gas additives, power conditioning, etc. – for the surface ionization triode). Although the mechanical problems associated with extremely close spacings are quite difficult, these problems are not complex. If such spacings can be achieved, it is anticipated that the fabrication steps will be straightforward once the proper techniques are established.

B. STATEMENT OF THERMIONIC CONVERTER PROBLEM

The "barrier index," V_B is a convenient parameter for characterizing thermionic diode development. It incorporates the diode losses due to scattering, ionization, reflectivity, electrode patches and collector double valued sheath. The "converter barrier index," V_B^*, also factors in any auxiliary power input to provide ions (as in pulsed diodes or ignited or nonignited triodes) as well as the power processing efficiency from converter output to auxiliary power input. Both indices are defined in the Appendix.

In order for thermionic energy conversion to realize practically its theoretical promise, consideration of the component terms of the barrier index in the Appendix indicates that it is essential that progress be made in: (1) reduction of collector work function and, (2) reduction of interelectrode plasma transport losses associated with electron scattering and the energy required to provide ionization for space charge neutralization. The Powder Puff Diode (PPD) eliminates the problem of plasma losses by means of close emitter-to-collector spacing. Since an oxygen supply for the emitter is not essential in the PPD, it may be easier to incorporate low work function collectors into this converter.

Most of the thermionic converters that have been developed have operated in the "ignited" mode, in which thermal ionization in the plasma is maintained at the expense of an output potential loss required to heat the interelectrode electrons. Ignited diode performance is adequate for some high temperature solar and space applications. However, projected low temperature out-of-core space reactor and terrestrial applications (e.g., thermionic topping of steam powerplants) cannot tolerate the plasma losses associated with current ignited mode operation. Parametric converter tests at Thermo Electron, as well as analytical studies by Rasor (ref. 14), Lam (ref. 15), Keck and Wang indicate that there is little experimental or theoretical expectation that the arc drop required to maintain ionization can be significantly reduced in a diode operating in the ignited mode. However, pulsed diodes and auxiliary discharge triodes have the potential of greatly reducing the arc drop.

This effort on enhanced mode converters has been reviewed by Rasor (ref. 14). Recent experiments using triodes with dispenser emitters at Rasor Associates (ref. 16) and Thermo Electron (Section D) have yielded high current amplification ratios in rare gas atmospheres. However, dispenser emitters have two associated problems. First, barium dispensed from the emitter is deposited on the collector and

results in a high collector work function (typically, about 2.2 eV).
Second, for the emitter temperatures required to give practical
current densities, no long-lived dispenser cathode exists. Thermo
Electron's attempt to circumvent the emitter lifetime problem by
oxygen dispensation to a tungsten emitter from a tungsten oxide
collector was not successful. Even at cesium pressures as low as
10^{-3} torr, the low voltage breakdown characteristics of cesium and
cesium/rare gas atmospheres prevented operation of the grid at
potentials which would have taken advantage of the more favorable
rare gas cross sections at higher electron energies. It should be
possible to operate the collector at low enough temperatures so that
extremely low cesium pressures will be adequate to provide low
collector work functions. However, the problems of barium dis-
pensation to the collector and dispenser cathode lifetime would still
remain. The foregoing problems with auxiliary discharge converters
may well be tractable. However, their difficulty stimulated a re-
consideration of the fundamental problems of thermionic energy
conversion.

An alternate means of eliminating the plasma losses (and, his-
torically, the first thermionic converters used this technique) is to
closely space the emitter and collector. Conceptually, this approach
is simple. However the extremely close spacings required (less than
0.001 cm) present many practical difficulties which will be reviewed in
the next section.

C. BACKGROUND ON VACUUM DIODES

Under subcontract to Martin, Thermo Electron evaluated four
techniques of establishing close emitter-collector spacings in vacuum
diodes. These techniques utilized: (1) cylindrical emitter on a thin
alumina tube, (2) wire suspension, (3) sapphire spheres, and (4) sapphire
rods.

The first support method was rejected because of several difficult
materials problems. Differential thermal expansion made it practically
impossible to mount the emitter on the alumina tube. In addition, the
thin wall alumina tubes were very fragile, cracked easily from machining
and were quite difficult to fabricate to close tolerances.

Wire suspension had the advantage that thin wires are strong in
tension and can be used as electrical leads. After many machining and
assembly difficulties, a prototype mock-up with the necessary close
spacing was built. However, this approach was abandoned because of
its size, complexity and nonsymmetrical thermal expansions of the wires.

Several test devices were built in which close spacing (approximately 0.5 mil) was achieved by means of sapphire spheres resting on an accurately machined ring in the collector. Sapphire spheres are suitable for support because of their high strength, low thermal conductivity and good electrical insulation. Tolerances on the spheres and wells in the collector were ±0.1 mil. The spheres were obtained without much difficulty, but much effort was required to develop machining techniques to work with such tolerances on collector surfaces. Experimental and analytical studies of sapphire sphere deflection (into the emitter) and heat transfer were performed. Both analysis and experiments indicated that the sapphire spheres may be used as spacers, but only at very small loads. For example, a 0.040 inch diameter sphere loaded with a 1.2 lb force deflects approximately 0.5 mil and conducts approximately 2 watts with a temperature differential of 600 K. The Isomite miniature thermionic converters built by McDonnell-Douglas have successfully used sapphire sphere spacing.

Analysis at Thermo Electron indicated that sapphire rod spacers would be superior to sapphire sphere spacers in both strength and heat conduction. However no experimental verification was obtained.

Beggs, of General Electric, constructed close spaced diodes (ref. 17) by refining conventional vacuum tube practice. These diodes were termed "Beggs' Buttons."

Experimental results on a close spaced diode (utilizing dispenser cathodes for both the emitter and collector) have been reported by Hatsopoulos and Kaye (ref. 18). Power densities of 1 watt/cm^2 and a thermal efficiency of 12 percent (based on measured power output and calculated heat input) were achieved.

With the foregoing techniques, and extreme difficulty, two rigid electrode areas of the order of 1 cm^2 can be held to spacings of approximately 0.5 mil. Since even closer spacings are desirable and much larger areas are necessary for most applications, these spacing methods offer little hope of utilization. Thus an improved approach to mechanically separating the emitter and collector must be formulated if close spaced diodes are to become practical. In the PPD, powder is used to separate the rigid emitter and compliant collector. This arrangement compensates for emitter distortions (due to nonuniform temperature distribution, differential thermal expansion and/or stress relief) which would either short the electrodes or increase the interelectrode spacing (resulting in unacceptably low output power densities).

In addition to the problem of mechanical spacing, which has just been discussed, vacuum diodes also exhibited poor collector work functions. Typically, the Type "B" and Type "S" impregnated cathodes (used for both the emitter and collector) gave a minimum work function of about 1.9 eV around 900 K. In order to obtain practical current densities in vacuum, such high temperatures were required that the emitter dispensed barium onto the collector. As a consequence, the collector work function would increase to about 2.2 eV and the diode performance would be correspondingly poor.

This problem can be eliminated simply by adding cesium vapor, as in the PPD. In this case the cesium vapor is used only to produce favorable and stable work functions on the emitter and collector. Because of the close spacing, electron-cesium interactions in the interelectrode space are negligible (even at cesium pressures up to 1 torr). In this respect, the PPD is similar to the Isomite.

D. DESCRIPTION OF POWDER PUFF DIODE

The design concept of the PPD (see Figures 22 and 23) uses an insulating powder spacer (e. g., metal oxides such as ZrO_2, Al_2O_3, ThO_2, MgO, etc.) in conjunction with a compliant (or "pillow") collector which can yield to conform to the emitter distortion while the flexible powder spacers maintain the close spaced interelectrode gap without electric shorting. Cesium vapor is used to provide favorable and stable emitter and collector work functions. The collector consists of a thin metal foil which is lightly pressurized by a liquid metal (which provides thermal and electrical conductivity as well as "puffing" the foil so that it can conform to emitter warping). The name, "powder puff diode," is obtained from the analogy of the powder-covered, puffed collector to that cosmetic article used to enhance female beauty. A more lengthy and descriptive term might be the "particulate-spaced, slaved-collector cesium thermionic diode." The emitter-collector sandwich with the powder spread can be reversibly cycled between severe distortions (relative to the characteristic interelectrode spacing) without "breaking" the spacer. The PPD should not be sensitive to mechanical shock since the primary effect would be to further pulverize the powder between the electrodes.

In contrast to the close spaced vacuum converters with dispenser emitters which poisoned the collectors with barium, the PPD utilizes a refractory metal emitter in a cesium atmosphere. Consequently, the desired emitter work function can be obtained by varying the cesium reservoir temperature without poisoning the collector. Thus a major
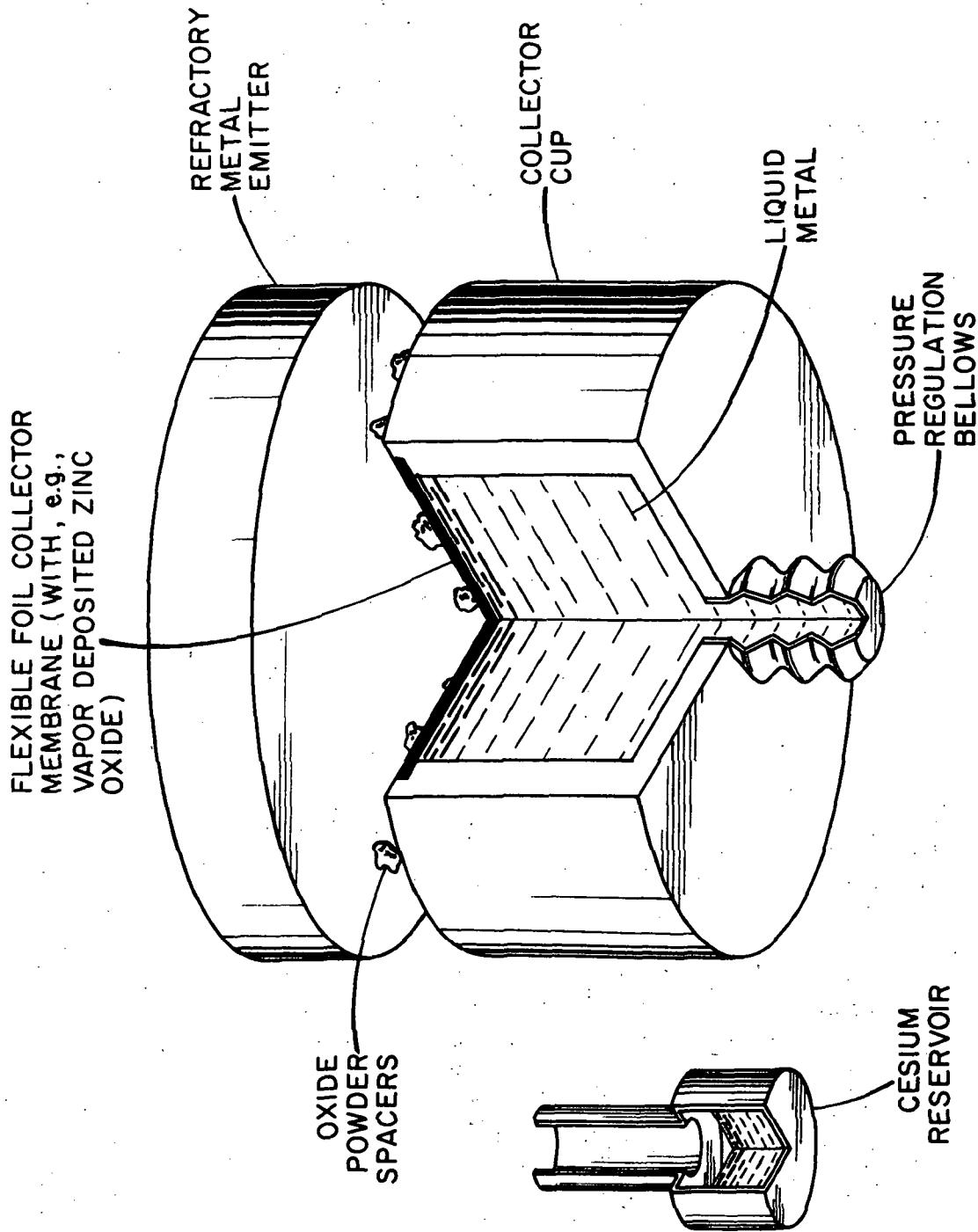
Figure 22.   Cut-a-way View of Powder Puff Diode

REFRACTORY METAL EMITTER

COLLECTOR CUP

LIQUID METAL

PRESSURE REGULATION BELLOWS

FLEXIBLE FOIL COLLECTOR MEMBRANE (WITH, e.g., VAPOR DEPOSITED ZINC OXIDE)

OXIDE POWDER SPACERS

CESIUM RESERVOIR
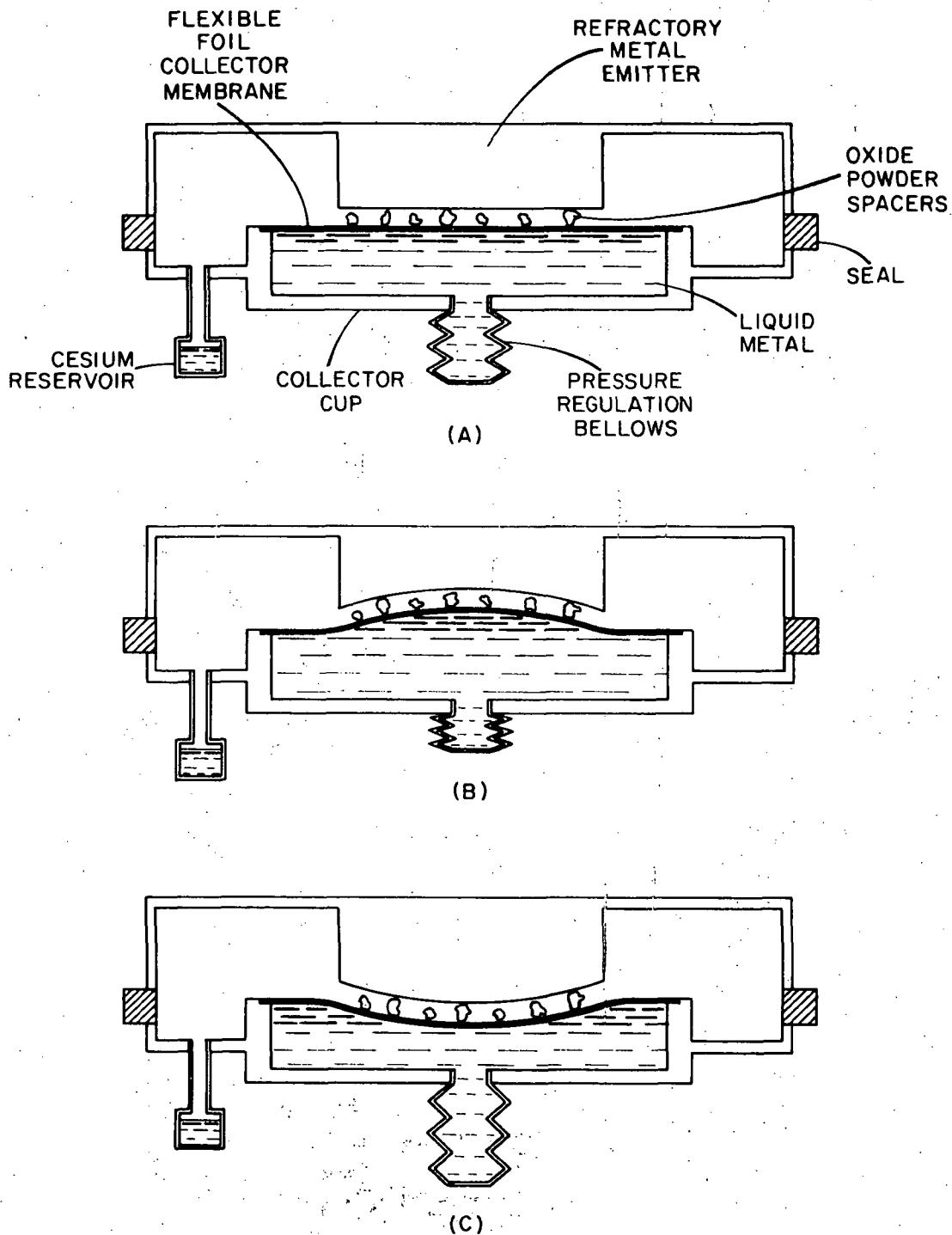
Figure 23. Powder Puff Diode (Illustrating Compliance of "Pillow" Collector)

limitation of the close spaced vacuum converters is overcome.
Because of the extremely close spacing, electron-cesium scatterings
in the interelectrode gap are negligible up to cesium pressures of
one torr.

1.   Multi-Foil Insulation

The use of a fine particulate powder (characteristic diameter of
about 5 microns) coating for spacing the emitter and collector is an
essential feature of the PPD. This spacing technique should be
applicable to large electrode areas since it is essentially that utilized
in Multi-Foil thermal insulation. Relevant Multi-Foil experience
is discussed in the next section. The spacer material is chosen for
compatibility with the electrodes and cesium vapor as well as for low
thermal conductivity. The particle size is chosen to provide the
requisite interelectrode spacing of about 10 microns. The area density
is the minimum which prevents electrical shorting. The liquid metal
pressure behind the foil is the minimum which will provide the desired
interelectrode spacing. If this pressure is more than a few psi the
thermal transport through the powder spacer will be unacceptably high.
This pressure can be provided in a variety of ways (e. g. – bellows
or the saturation pressure of an enclosed liquid). Thermal transport
through the powder spacer is minimized by: (1) choice of a low thermal
conductivity spacer material, (2) high thermal contact resistance to the
electrodes due to the small area, unbonded contact between the spacer
particles and electrodes, and (3) the small fraction of the powder
particles which bridge the emitter to the collector.

Compared to the wide spans between the spacer elements (sapphire
spheres or rods) in vacuum converters, the span between the powder
particles is quite small. Thus there is a reasonable expectation that
smaller interelectrode spacings can be achieved with powder spacers.
Minimization of the interelectrode spacing is essential since the current
density is inversely proportional to the square of the interelectrode
spacing. Since the thermal radiation losses are independent of spacing
and the thermal conduction loss is inversely proportional to the spacing,
while the output power is inversely proportional to the square of the
spacing, efficiency should increase as the spacing decreases (to the
limit at which electrical shorting occurs). –

The mechanical flexibility of the powder spacer is an important
consideration for the PPD since limited emitter distortions are anticipated.
The electrical and mechanical integrities are not dependent on a single
particle. The emitter-collector sandwich with the powder spread can be
repeatedly flexed without destroying the spacers. Based on experience
with Multi-Foil thermal insulation, such a structure should be rugged

and resistant to vibration as well as thermal and mechanical shocks (quite unlike the vacuum diodes with spacers of sapphire spheres and rods).

2. Electron Transport Losses

The nomenclature used in this section is defined in the Appendix. Since space charge neutralization is via close-spacing, positive ions are not necessary. Consequently, the arc drop, V_d is zero. However at the optimum operating point for the PPD (as in any close spaced converter), there will be a potential difference, $\Delta \Psi$, between the motive maximum and the surface potential of the collector. This potential difference will add to the collector work function to give an "effective collector work function," ϕ_c':

$$\phi_c' = \phi_c + \Delta \Psi$$

The size of $\Delta \Psi$ can be calculated from classical electromagnetic theory.

Unlike other enhanced mode converters (e.g., pulsed diodes, surface ionization triode, ignited triode, etc.), the PPD does not require an auxiliary power input. Therefore, V_d^* (the potential loss due to auxiliary power input required to provide ions for space charge neutralization) is zero. Performance loss due to conditioning the converter output power to that required for the auxiliary power input does not apply to the PPD.

Because the interelectrode spacing is a small fraction of the electron mean free path in cesium the scattering losses, S, are negligibly small – even for cesium pressures of several torr.

Lam (ref. 19) has recently pointed out that if positive ions are utilized in a thermionic converter for space charge neutralization, the arc drop in the plasma has a minimum value provided the emitter sheath has a motive peak – independent of how the positive ions are produced. Since the PPD does not use positive ions for space charge neutralization, this limitation does not apply.

The electron transport processes across the PPD are essentially identical to those in the vacuum diode. As a result, the theoretical analysis of the current-voltage characteristics has already been rigorously solved. Thus the electrical processes in the PPD should be well understood and experimental data interpretation should be free of ambiguity. Insulator leakage can be anticipated to be the major problem.

Because of the close spacing, additive oxygen is not essential to obtain practical emitter current densities without significant electron scattering. Thus if oxygen is desired to reduce the collector work function, its supply can be optimized for this purpose.

3. Parametric Power Density Data

The power density of close spaced converters such as the PPD can be calculated with confidence. Analytical formulations have been published by Hatsopoulos (ref. 20), Moss (ref. 21) and Webster (ref. 22). For calculations in this report, the equations and tables given in Hatsopoulos and Gyftopoulos (ref. 23) were used.

The output power density is given as a function of interelectrode spacing, parametric in collector work function, in Figures 24 through 28 for emitter temperatures ranging from 1200 to 1600 K. Back emission from the collector is neglected. Inspection of these figures demonstrates that spacings of around 0.25 mil are necessary for most applications.

E. MULTI-FOIL THERMAL INSULATION

The particulate metal oxide spacing technique in the Powder Puff Diode (PPD) is essentially that utilized in Thermo Electron's Multi-Foil thermal insulation. Thus a discussion of Multi-Foil characteristics should lend perspective to the question of PPD feasibility.

Multi-Foil denotes a thermal insulation system developed by Thermo Electron Corporation (initially under USAEC sponsorship) in which thin metal foils are spaced in a vacuum by oxide particles. Examples of cylindrical and planar Multi-Foil constructions are shown in Figure 29. The oxide material is selected on the basis of low thermal conductivity and foil compatibility, depending on the application temperature. The oxide particles are optimized with regard to particle size and areal density to minimize thermal transport. The multiple foils are effective thermal radiation shields. The vacuum environment eliminates convective heat transport. The oxide particles provide a high thermal impedance to conduction by: (a) selection of oxides with low thermal conductivity, (b) high thermal interface resistance between the foils and particles, and (c) the thermal resistance of the thin foil. An SEM photograph of 325 mesh zirconia particles sprayed onto a nickel foil is shown in Figure 30. Approximately 5 percent of the foil area is covered by the particles. For PPD application, it would be desirable to eliminate the small debris particles.

Multi-Foil has demonstrated low heat losses perpendicular to the foils. A thermal conductivity comparison of Multi-Foil and other insulations is shown in Figure 31. Thermo Electron has extensive experience in applying cylindrical-planar Multi-Foil insulation to such diverse applications as thermionic energy converters, vacuum furnaces, nuclear artificial hearts and radioisotope thermoelectric generators.
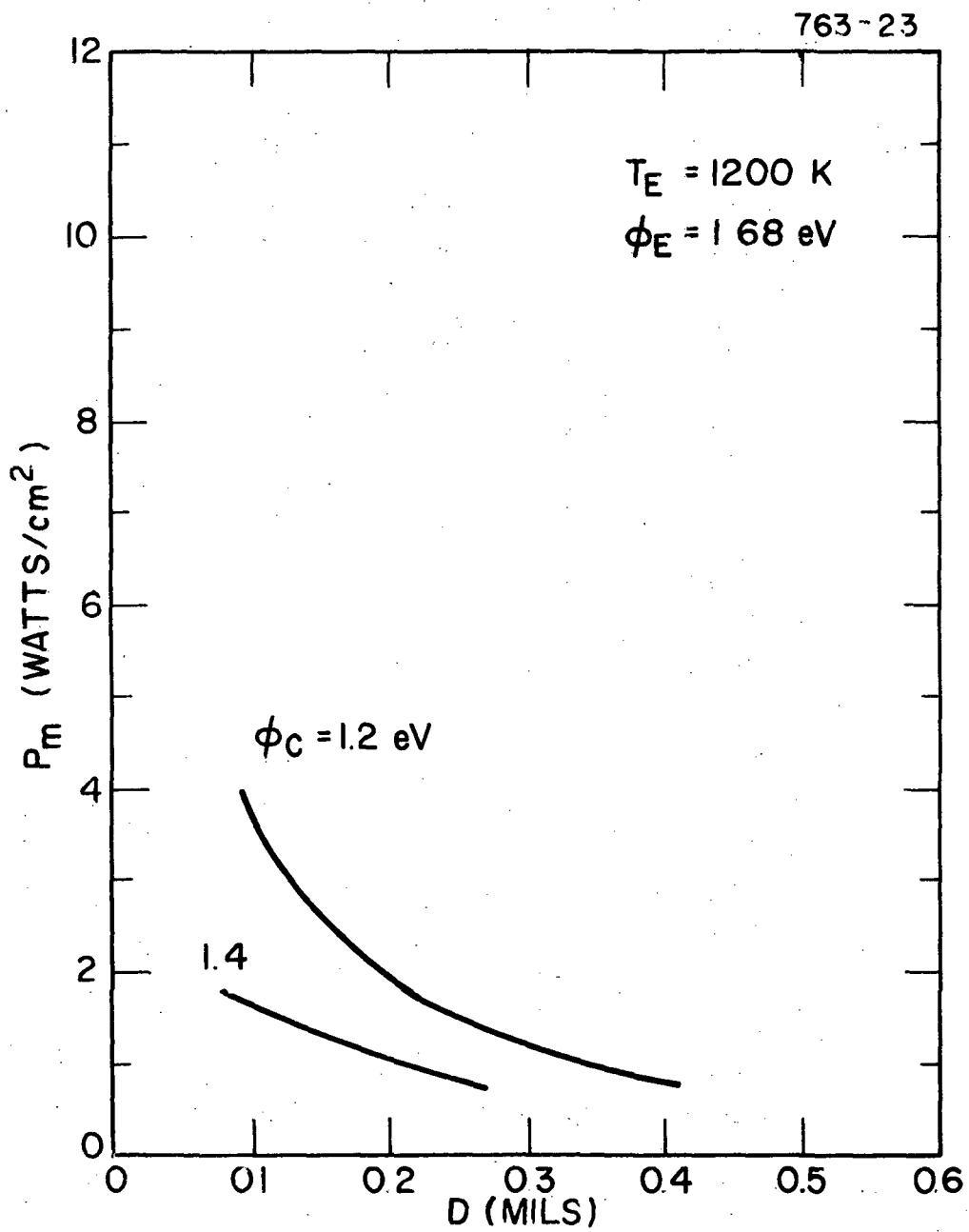
Figure 24. Close Spaced Diode Power Density as a
Function of Spacing for T_E = 1200 K and
ϕ_E = 1.68 eV
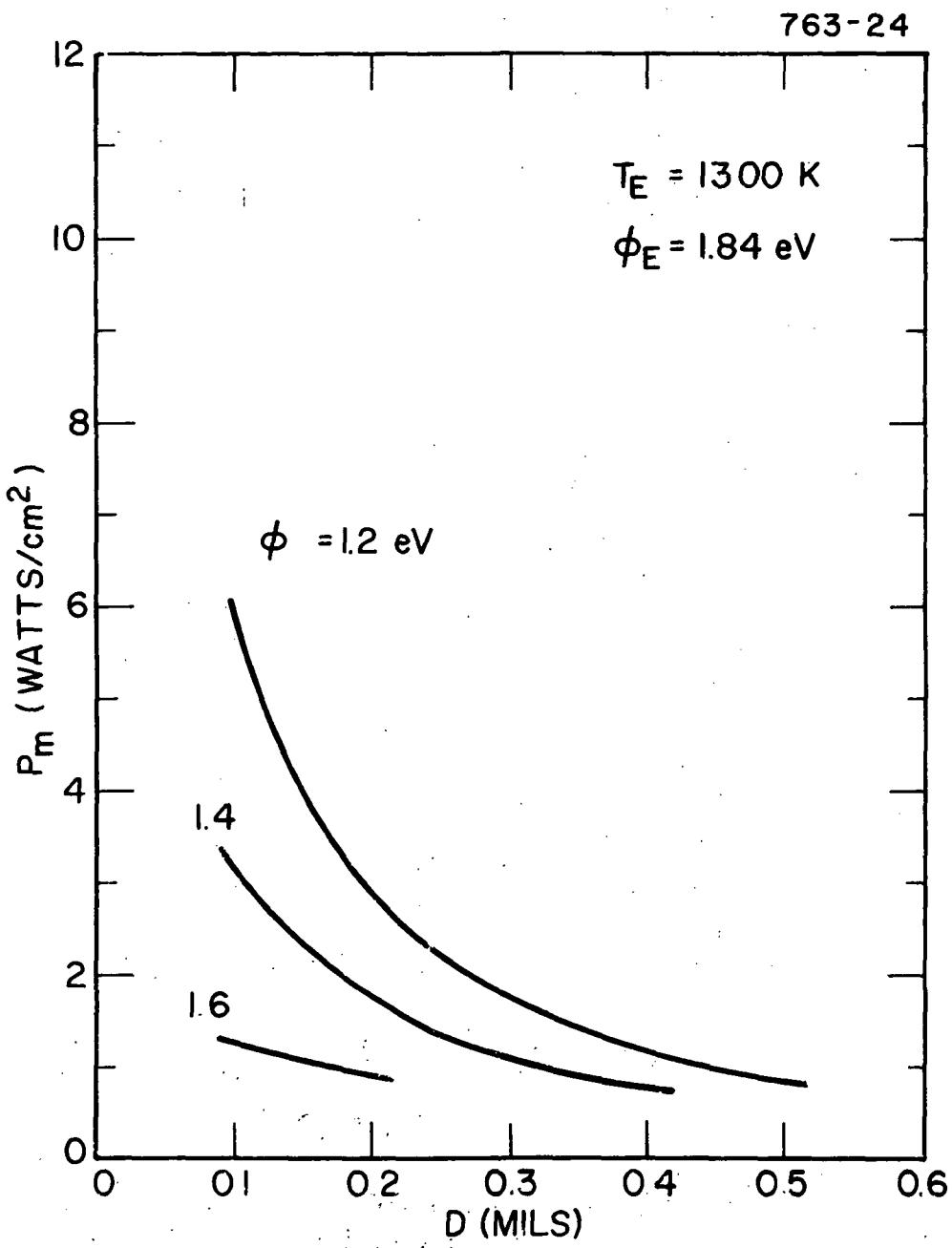
Figure 25. Close Spaced Diode Power Density as a
Function of Spacing for T_E = 1300 K and
ϕ_E = 1.84 eV
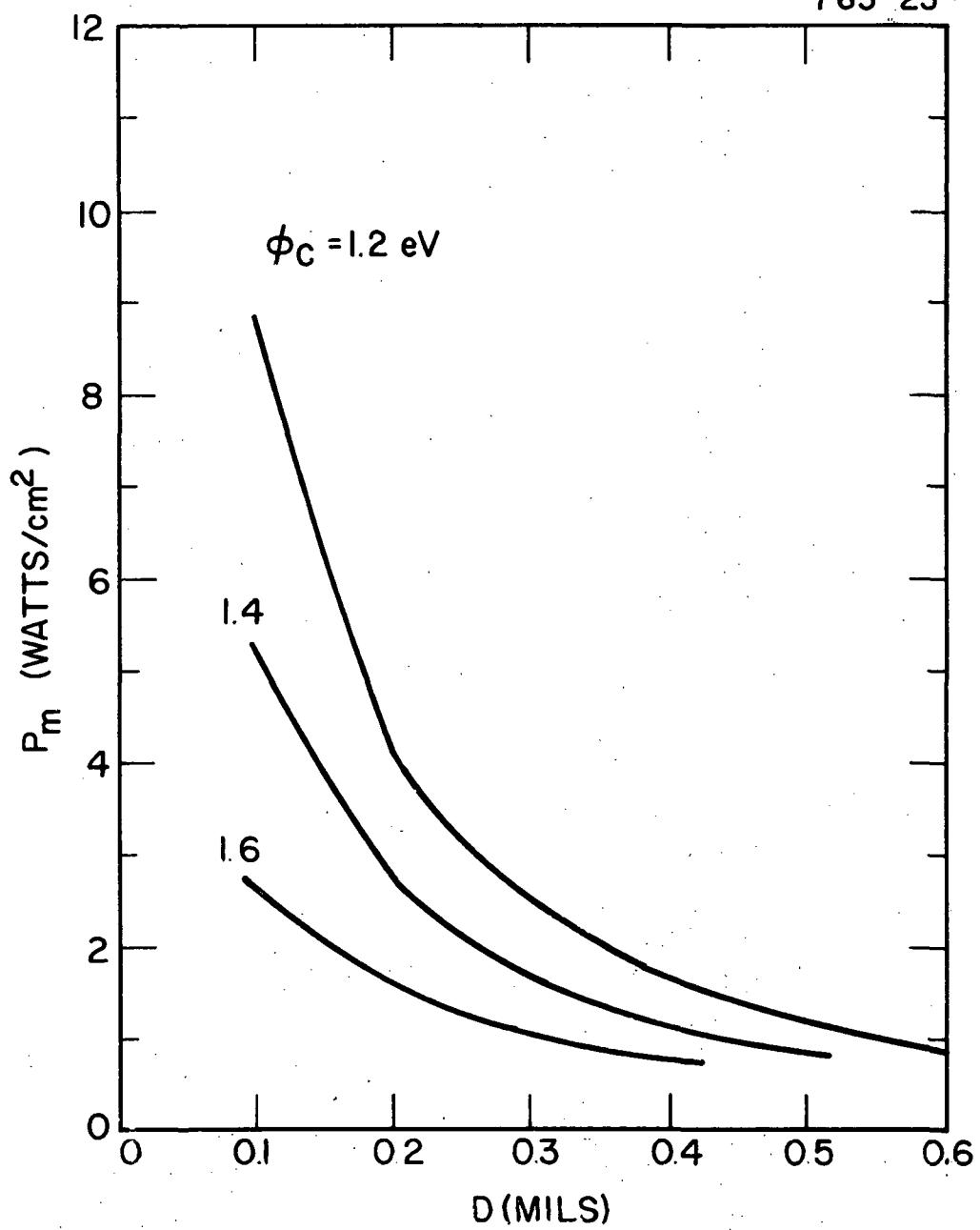
Figure 26. Close Spaced Diode Power Density as a
Function of Spacing for T_E = 1400 K and
ϕ_E = 2.00 eV
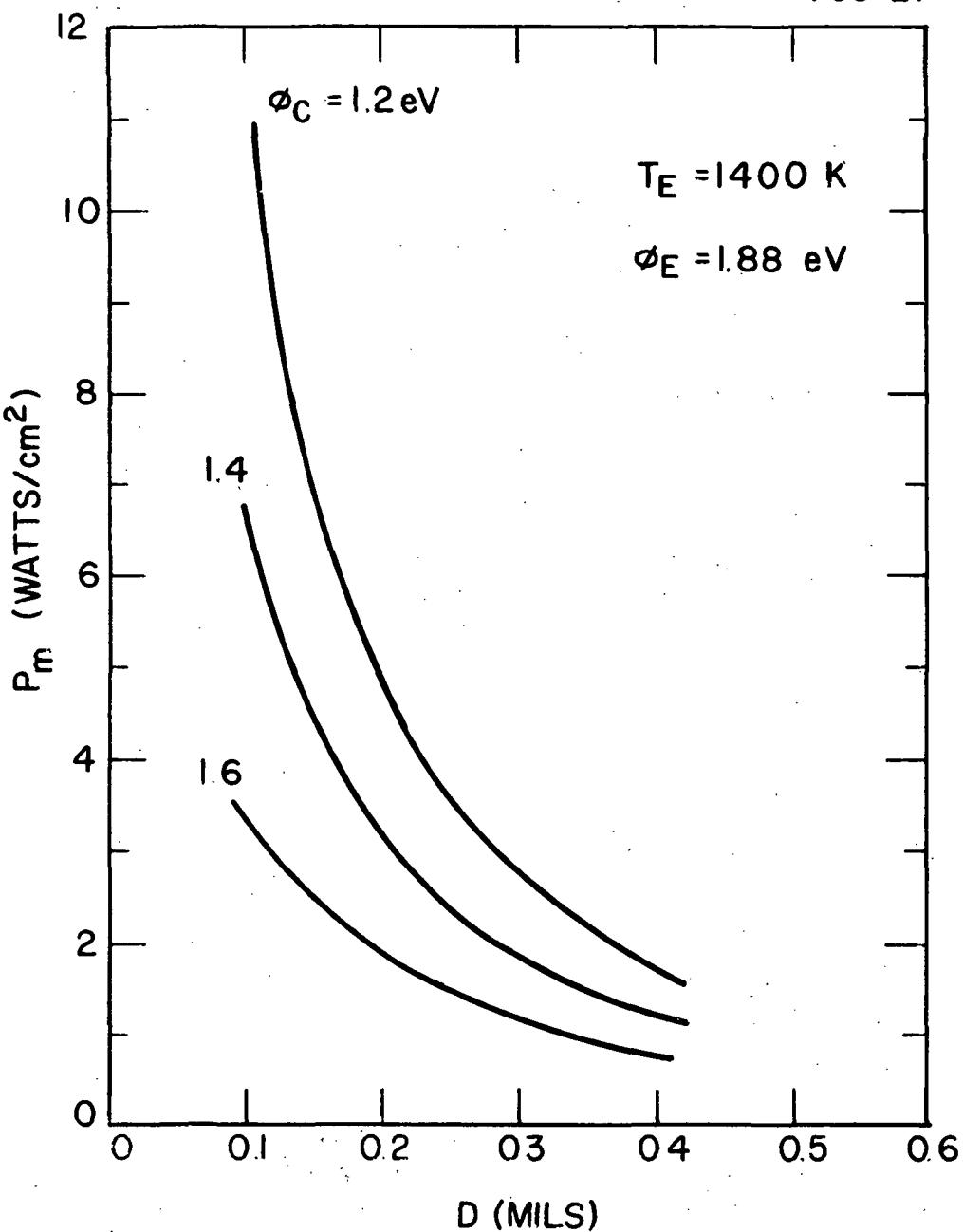
Figure 27. Close Spaced Diode Power Density as a
Function of Spacing for T_E = 1400 K and
ϕ_E = 1. 88 eV
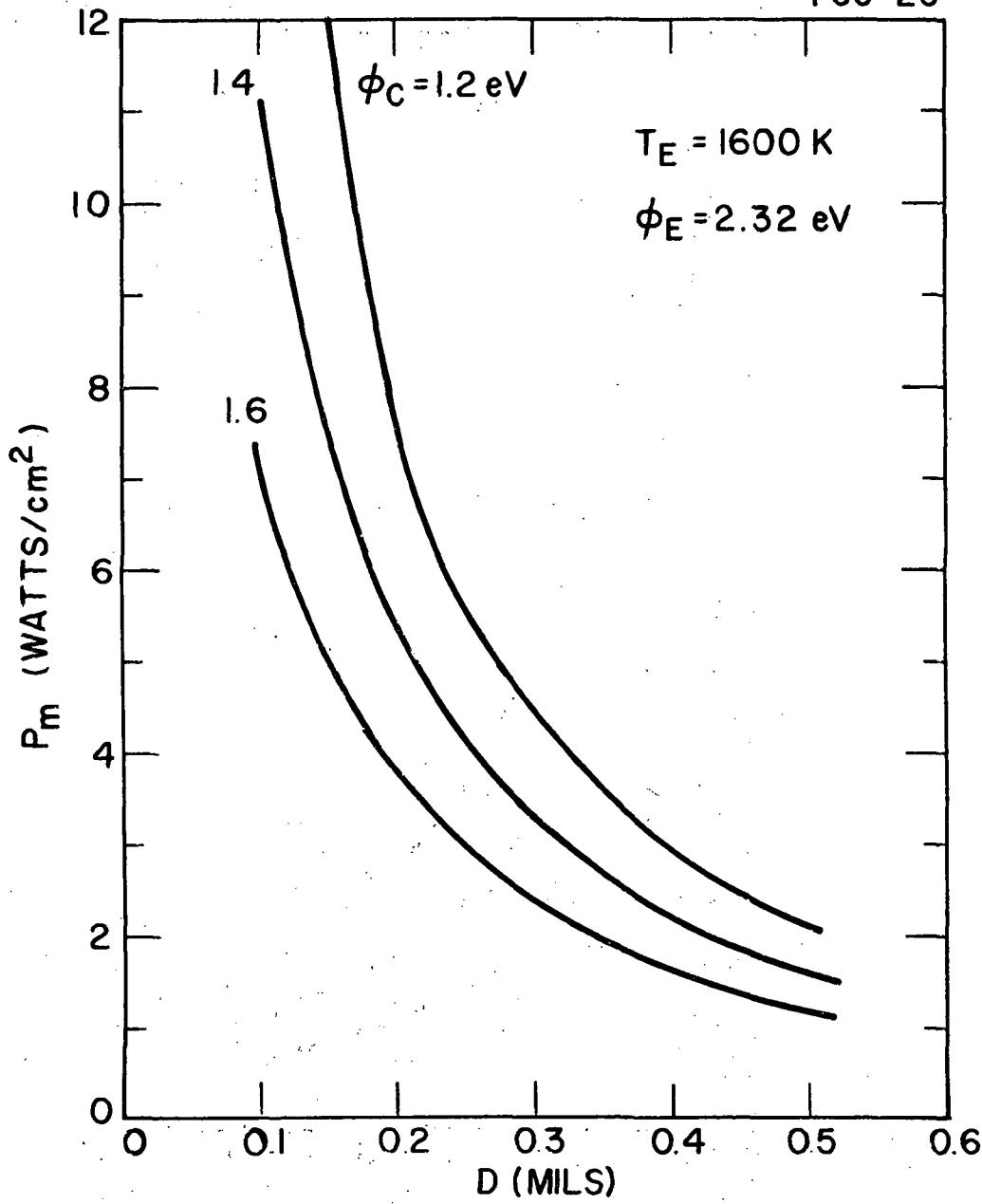
Figure 28. Close Spaced Diode Power Density as a
Function of Spacing for T_E = 1600 K and
ϕ_E = 2.32 eV

A Planar Insulation Sample

Cross-Sectional View
of a Planar Insulation
Sample

A Cylindrical Insulation Sample
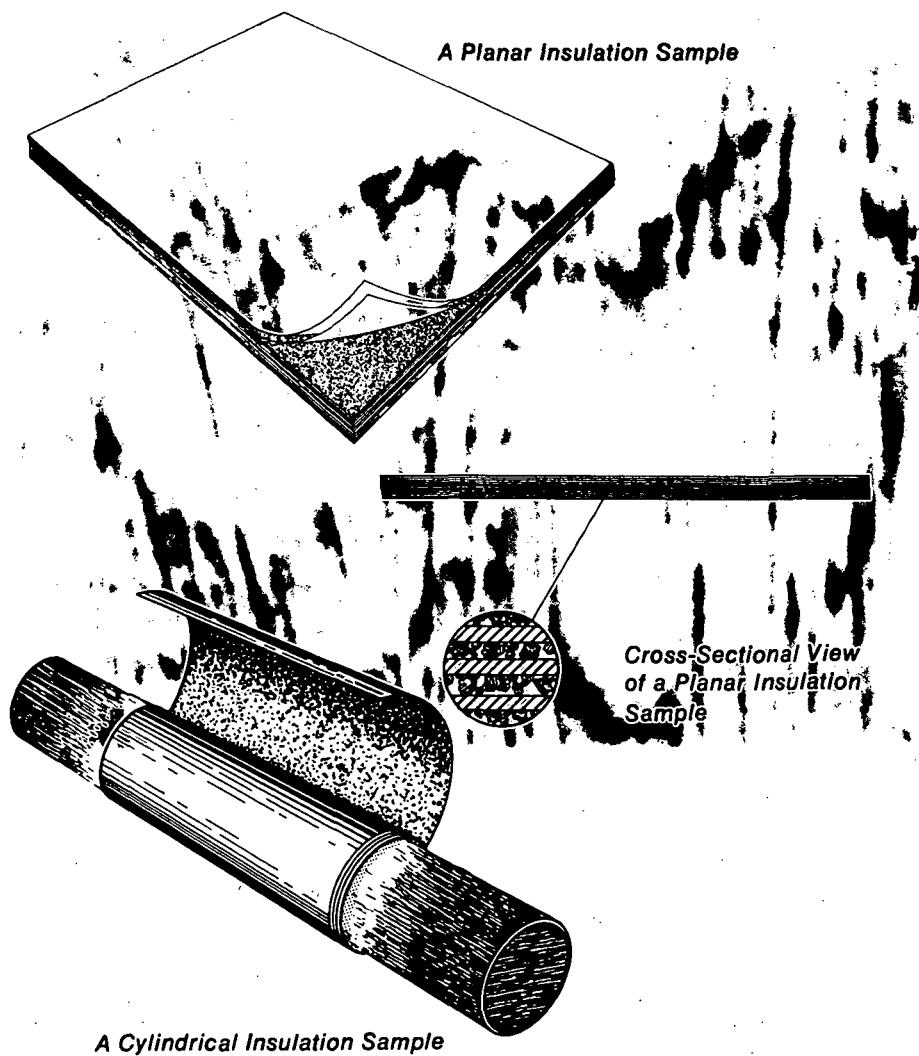
Figure 29.   Planar and Cylindrical Multi-Foil
Insulation
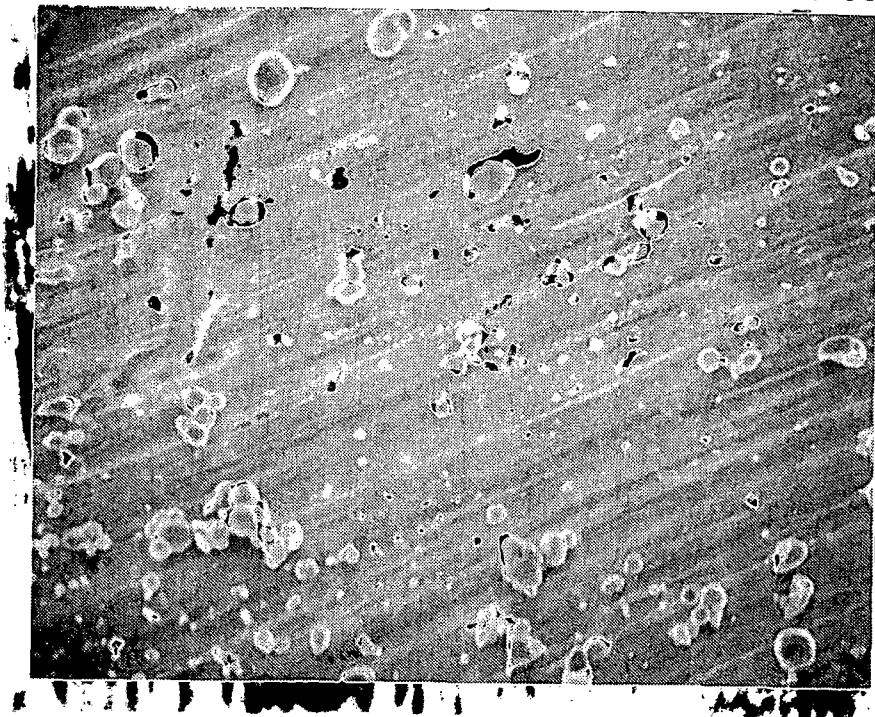
Figure 30.   Scanning Electron Micrograph of
             Zirconia Particles Deposited on
             Nickel Foil (1000X, viewed at
             45 degrees)
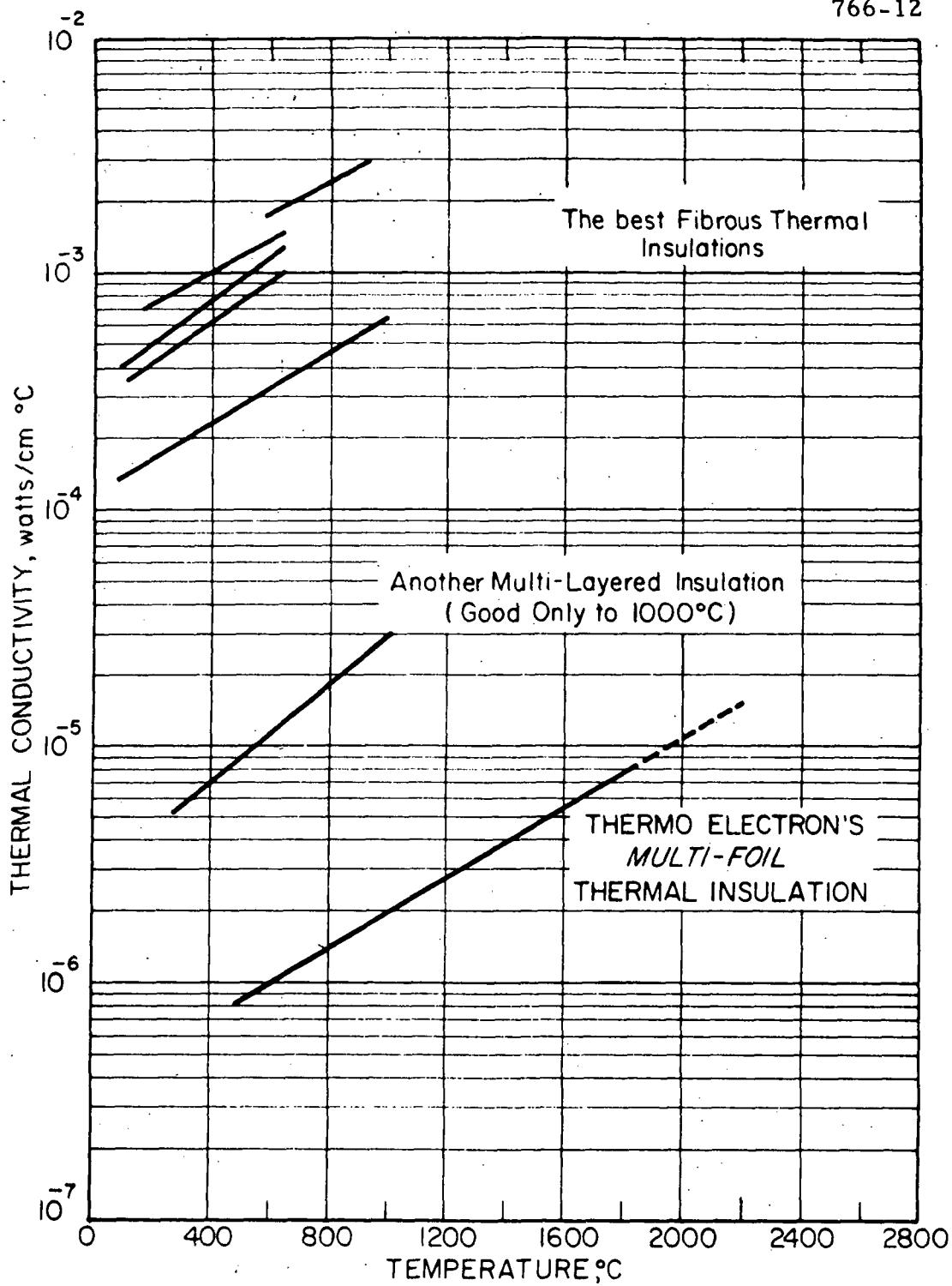
Figure 31.   Thermal Conductivity Comparison

Typical heat flux data for planar Multi-Foil insulation are shown in Figure 32. As typical, these data show a reciprocal dependence on the number of foil layers. Ten layers at 1100 C give a heat loss of 0.2 watt/cm^2. Two layers, corresponding to a thermionic diode, would give an extrapolated loss of about 2 watts/cm^2. The fourth power temperature dependence of these data indicate that the radiation loss component is much greater than the conductive loss component. Thus, the zero loading data in Figure 32 imply an acceptable heat loss through the thoria powder spacer.

In any practical PPD, a loading of several psi will be necessary. The variation of Multi-Foil heat flux as a function of applied pressure is shown in Figure 33. If the pressure dependence for two layers is comparable to those shown in Figure 33, the conductive heat loss through the powder spacer should be tolerable.

Chemical compatibility tests of refractory foil-oxide particle combinations have been investigated as a function of time and operating temperature in vacuum. The combinations most resistant to bonding between foils were W-ThO$_2$ and W(25) Re-ThO$_2$, which exhibited only slight bonding after 2000 hours at 1900 C. Molybdenum and tantalum are unsatisfactory at 1900 C and have limited usefulness at 1700 C. ThO$_2$ is usually superior to Y$_2$O$_3$ in preventing bonding between metal foils. Although some bonding of oxide particles to the emitter might be anticipated after extended periods, essentially zero interaction would be expected between the oxide particles and the collector – provided that these vacuum data are relevant to the cesium atmosphere inside the PPD.

For lower temperature applications, ZrO$_2$ particles are usually deposited on nickel or molybdenum foils. The extremely low thermal conductivity of ZrO$_2$ is attractive.

From the viewpoint of thermionic converter compatibility in a cesium atmosphere, high purity Al$_2$O$_3$ would be desirable. However, the thermal conductivity of Al$_2$O$_3$ is higher than either ThO$_2$ or ZrO$_2$. For initial tests, Al$_2$O$_3$ particles will probably be used.

F. DEVELOPMENT STATUS

Initial steps have been taken to study the feasibility of the PPD. A test diode has been designed, collector membrane bonding techniques have been developed and the pressure required to comply the pillow collector has been investigated.
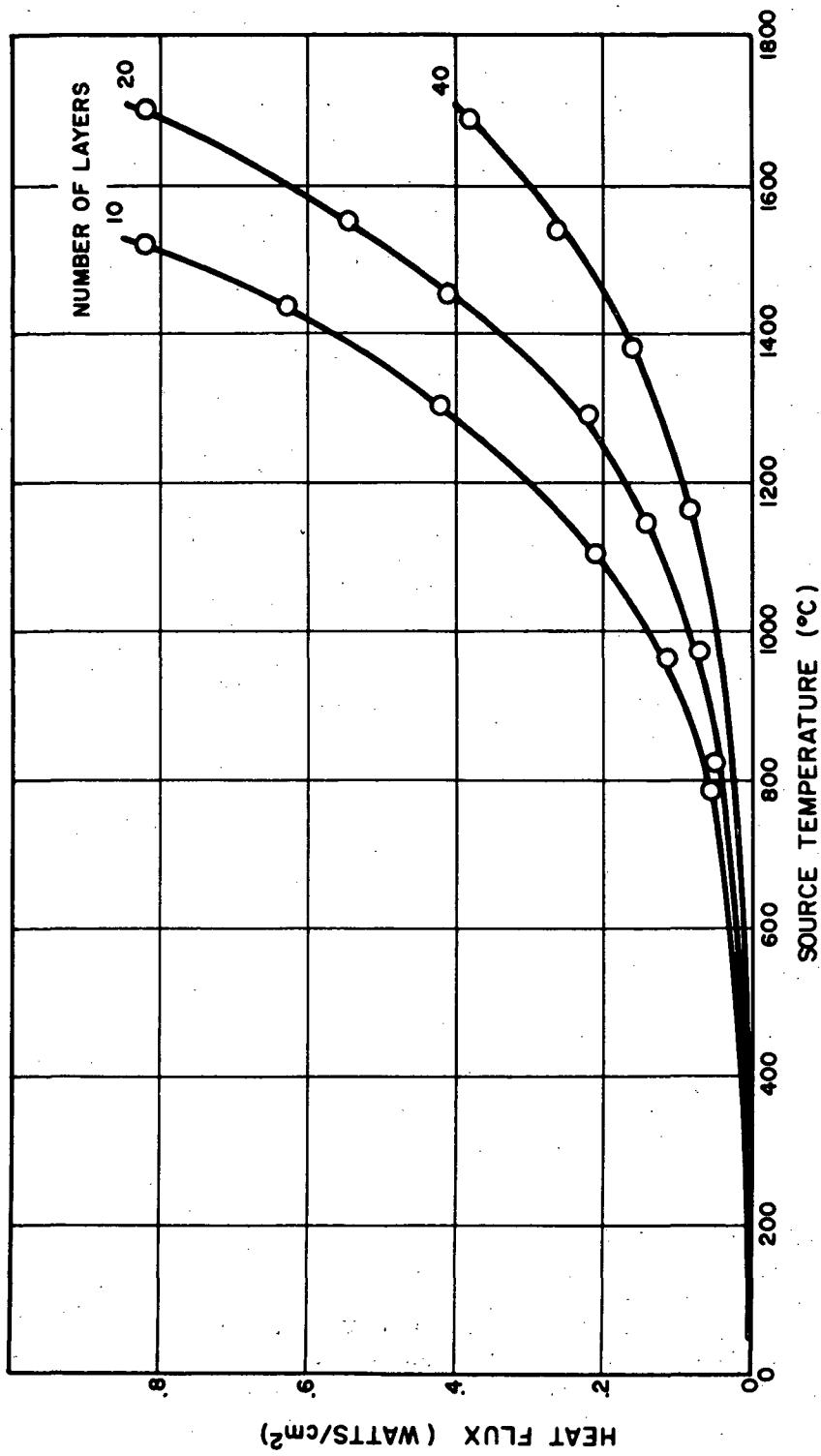
Figure 32. Planar Multi-Foil Heat Flux Test Data (W-ThO$_2$ Insulation, Zero Loading)
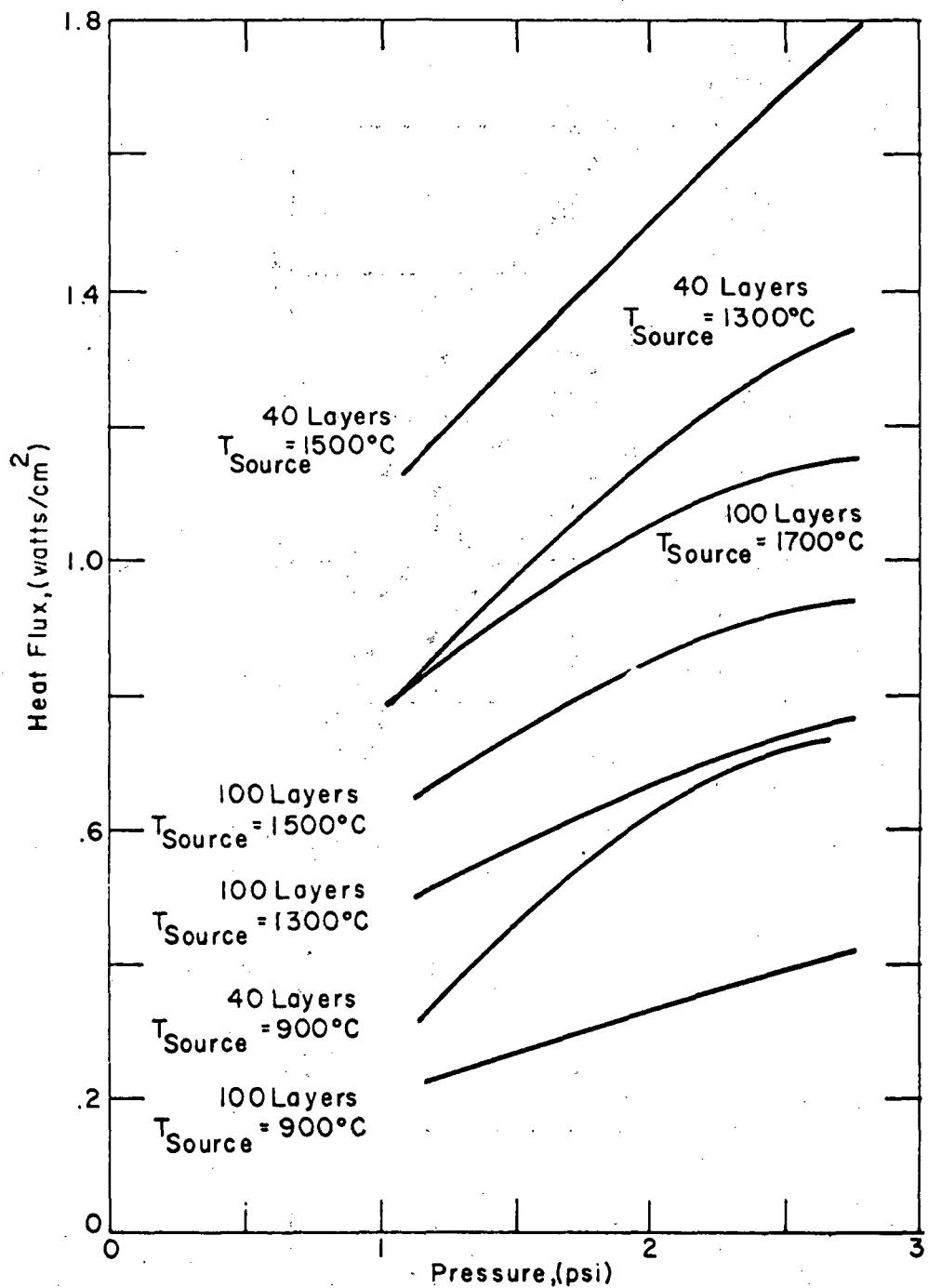
Figure 33. Multi-Foil Heat Flux versus Applied Pressure
(W-ThO$_2$, 40- and 100-Layer Samples)

A prototype PPD has been designed by modifying the standard variable spaced diode. This PPD design is shown in Figure 34. The collector membrane is a 3 mil thick tantalum foil. Heat and electrical conductivity will be provided by molten lead in the collector cavity. The "pillow collector" (i. e., the foil membrane backed by the molten lead) will be pressurized from a nitrogen tank. The PPD pressurization line will be handled in the same manner as the oxygen supply line in diodes using silver tubes in their collectors.

Membrane bonding tests have been performed. Vacuum brazing and electron beam (EB) welding techniques have been evaluated. EB welding has given the best results. Leak tight seals can now be welded reliably.

Because of its low thermal conductivity, zirconia powder is often used in moderate temperature Multi-Foil applications. Since it is a candidate spacer material for the PPD, an experiment was performed in the Activation Chamber to identify any remarkable properties when cesiated.

Zirconia powder (325 mesh) was sprayed onto a RCA-gun by the method used previously for BaO, ZnO, etc. The gun was mounted in the Activation Chamber and baked overnight in the usual way. The gun was heated to 650 C to remove the binder. Cesium vapor was admitted from a "channel" while the ZrO_2 was at about 100 C. This exposure produced low photoemission. At 230 C no thermionic emission could be observed, indicating a work function in excess of 1.5 eV. Repeated cesiation at 100 C increased the photoemission to values comparable to those obtained with other materials, but the thermionic emission remained immeasurably small. Next, cesium-oxygen alternations were investigated. These produced a slight increase in photoemission and a readable thermionic emission. The lowest work function at 230 C was approximately 1.37 eV, but the reading was very unstable.

In order for the PPD to operate without excessive heat loss through the powder spacer, the pillow pressure required to comply the collector to the emitter must be no more than a few psi. A test fixture was set up to study the required pressures. The fixture consisted of an EB welded 3 mil thick tantalum foil pressurized by nitrogen against a dummy transparent emitter. The area of electrode compliance could be observed with the aid of a liquid droplet. Tests gave the encouraging result that nitrogen pressures as low as 1 psi are sufficient to comply the collector over the area of the emitter.
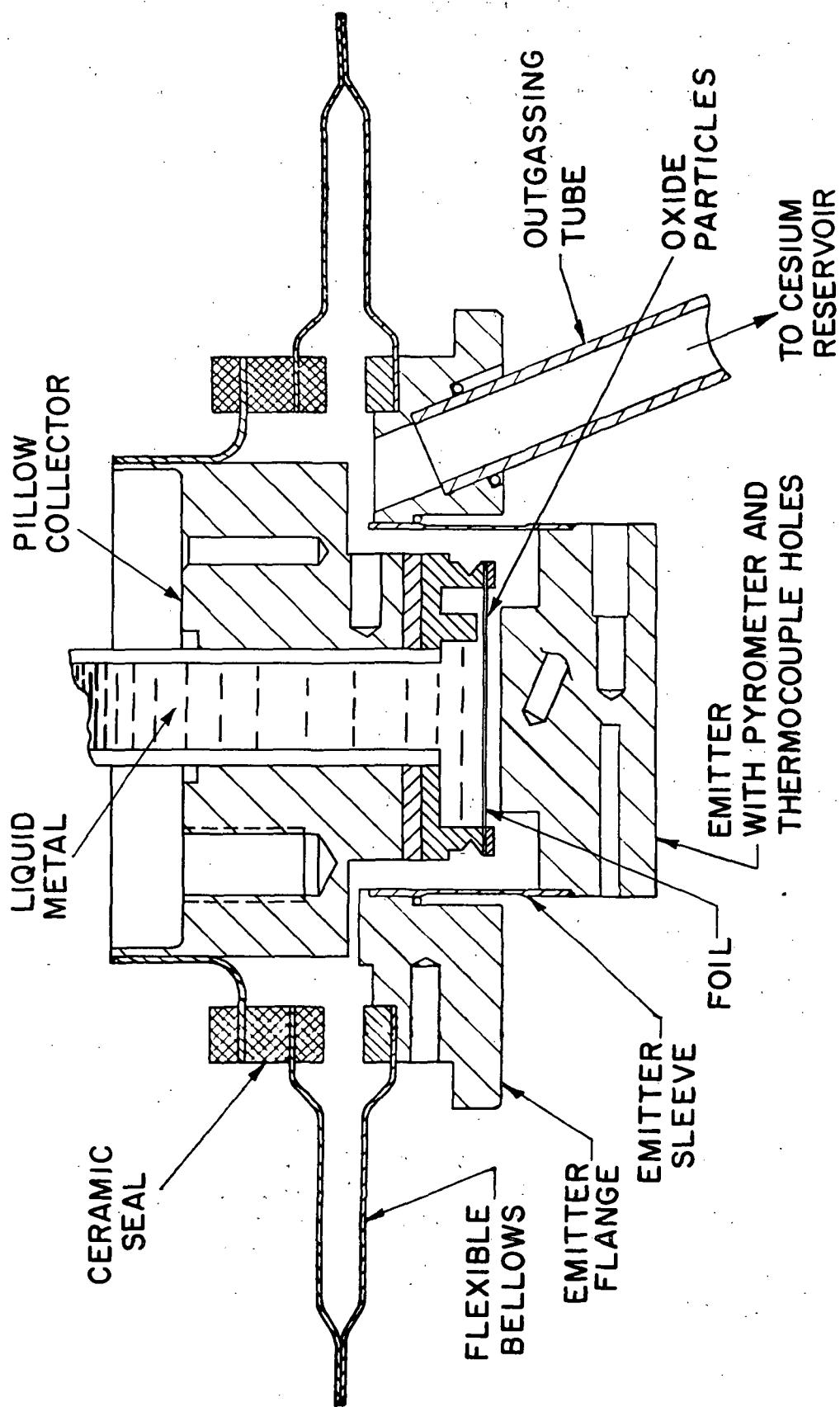
Figure 34. Cross Section of the "Powder Puff" Diode

VI. DISCUSSION OF RESULTS

The foregoing sections have summarized the principal activities devoted to developing high efficiency thermionic converters. This section will discuss the more significant results.

The most interesting electrode material found during the subject reporting period by the screening experiments is ZnO. This material has a combination of properties that recommend it as a collector. Cesiated ZnO has a lower work function than any material yet found which does not require the addition of oxygen. It is also unusual because the cesiated work function of polycrystalline sprayed coatings is lower than that of either the zinc-rich or oxygen-rich single crystal face. The cesiated work function of ZnO is readily reproducible and insensitive to temperature. This reproducibility may be related to its not being hygroscopic (unlike the alkaline earth oxides). Zinc oxide binds cesium tightly. As a consequence, it requires only a low cesium pressure to give its minimum work function. This has the disadvantage that the low cesium pressure which matches ZnO is insufficient for practical current densities from most emitter materials. It also means that the optimum interelectrode spacing for ignited diodes is quite large. However, the low cesium pressure required by ZnO may well be an advantage in auxiliary discharge converters where it should increase the breakdown potential. The greatest disadvantage of ZnO is that it is not a high-temperature material in a cesium atmosphere. Diode data indicate that it will not be useful as high as 750 K. Hence, space applications of ZnO will probably be limited to radioisotope generators.

The ZnO back emission work function of 1.25 eV is the lowest yet measured in a thermionic diode. However, electrical resistance of the thick spray coating and cesium vapor pressure mismatched with the emitter have prevented the realization of the high converter performance potential of ZnO. The electrode resistance problem will be attacked by thin evaporated coatings and the emitter cesium pressure mismatch problem will be attacked by high bare work function materials (e.g., platinum) or dispenser cathodes.

The Surface Characterization Chamber has proven to be quite useful. In particular, the Auger spectral analyses of converter electrodes have provided information about the mechanisms taking place during operation. The study of processing variables on the surface chemistry of tungsten has improved converter fabrication.

Unlike ZnO, LaB_6 requires the addition of oxygen to obtain a low work function in a cesium atmosphere. The addition of oxygen into a converter by means of a heated silver tube exiting through an LaB_6 collector has been studied with an operating diode. It appears that oxygen may be

introduced into the diode in a controlled manner by this technique at low cesium pressure (i. e., reservoir at room temperature). However, during normal diode operation there was no evidence that oxygen could perturb the converter characteristics. Apparently, the cesium vapor in the silver tube reacted with the oxygen before it could diffuse into the interelectrode space.

For space systems, an incremental decrease in plasma arc drop is more desirable than the same decrease in collector work function, since the heat rejection temperature is not lowered. The enhanced mode converter experiments, using a grid interposed between the emitter and collector, have given valuable insight into the constraints of auxiliary ion source devices. Although surface ionization from the heated grid corresponded to an elementary converter model at low output currents, this technique became ineffective at power densities far below practical values. Thermo Electron data are consistent with the interpretation of Rasor Associates; namely, that a positive ion space charge develops around the grid wires and impedes their diffusion into the regions of electron space charge.

Operation of the triode in the plasmatron mode (i. e., with a potential applied to the grid) gave more promising results. This mode of operation provides electron impact ionization throughout the interelectrode space. However, breakdown limited the grid potential to about 10 volts in a low-pressure cesium atmosphere (with or without an inert gas pressure of a few torr). This voltage is well below optimum. In order to circumvent the breakdown problem, high-voltage, short-duration pulses were applied to the grid. Potentials as high as 100 volts could be utilized in this manner. Consequently, the accelerated electrons would encounter more favorable collision cross sections which would improve ionization efficiency and converter output. Equivalent arc drops of less than 0.1 eV have been obtained with the pulsed triode at low power densities. If such low equivalent arc drops could be maintained at practical power densities, it would represent a major breakthrough in thermionic conversion.

A major problem in translating these results to high-power densities is electron-ion scattering of the thermal electrons. This problem can be minimized by closer spacing of the emitter and collector. However, the spacing reduction would appear to preclude any grid structures in the interelectrode space. Thermo Electron is considering two auxiliary electrode design variations to provide significantly closer spacing. One method is to use a ring electrode around the circumference of the emitter and collector. Bell jar experiments in an argon atmosphere indicate that a penetrating discharge can be developed at spacings less than one millimeter. Another technique would be to use an auxiliary electrode embedded in the collector. Hardware implementation of these two design approaches has been initiated.

An alternate means of attacking the arc drop problem in the plasma is to eliminate the need for the plasma by spacing the emitter and collector close enough to overcome the electron space charge. For this purpose, interelectrode spacings of a fraction of a mil are required. Such spacings present difficult mechanical problems. However, Thermo Electron has developed a technique of spacing foil layers (for Multi-Foil thermal insulation) using oxide particles that may be applicable to thermionic diodes. The design concept for the particle spaced diode is described in this report. Initial spacing experiments have been encouraging. If further spacing experiments are successful, a thermionic diode will be fabricated to evaluate the feasibility of this converter concept.

Page
Intentionally
Left Blank

VII. CONCLUSIONS

Since the conclusions to individual topics have been discussed within the body of this report, the items tabulated in this section are somewhat redundant.   The primary conclusions that may be drawn from the program effort during the subject period are:

- Thermionic energy conversion is a viable candidate for space power systems utilizing reactor, radio-isotope and solar heat sources.

- For out-of-core reactor designs, moderate thermionic converter performance improvement is required at lower temperatures to obtain specific powers comparable to the high temperature in-core designs.

- Zinc oxide is a promising collector material for applications with low-temperature heat rejection.

- Oxygen introduction into a thermionic converter via a heated silver tube is feasible only at low cesium pressures.

- Thermionic triodes operating in the plasmatron mode have given more promising results than those using surface ionization from a heated grid.

- Pulsed thermionic triodes operating in the plasmatron mode have provided encouraging data at low power densities. Extension of these results to practical power densities requires much closer emitter-collector spacings.

- The particle spaced diode concept deserves hardware evaluation if planned bell jar spacing tests are successful.

Page
Intentionally
Left Blank

REFERENCES

1. Samsonov, G. V., et al., (in Russian) Ukr. Fiz. Zh, Vol. 21, #2, p. 203 (1976); (Abstract in English) Chemical Abstracts, Vol. 84, #20, 143520q (1976).

2. Taylor, P. A., Leysen, R. and Hopkins, B. J., Solid State Commun., Vol. 17, p. 983 (1975).

3. Leysen, R., Hopkins, B. J. and Taylor, P. A., J. Applied Physics, Vol. 8, p. 907 (1975).

4. Zalm, D., Advan. Electron, Vol. 25, p. 211 (1968).

5. Roberts, R. W., Brit. J. Appl. Phys., Vol. 14, p. 537 (1963).

6. Joyner, R. W., Rickman, J. and Roberts, R. W., Surface Sci., Vol. 34, p. 445 (1973).

7. Tarng, M. L. and Wehner, G. K., J. Applied Phys., Vol. 44, p. 1534 (1973).

8. Brundle, C. R., J. Vac. Sci. Technol., Vol. 11, p. 212 (1974).

9. Dybwad, G. L., J. Appl. Phys., Vol. 42, p. 5192 (1971).

10. Hernqvist, K. G., RCA Review, p. 7, March 1961.

11. Knechtli, R. C. and Fox, M., Adv. Energy Conv., Vol. 3, pp. 333-349 (1963).

12. DeSteese, J. G., "Development of Thermionic Radioisotope Batteries," Proc. 2nd Int'l. Symposium on Power from Radioisotope, Madrid, p. 339 (1972).

13. Dunlay, J., "Development of Foil Thermal Insulation for High Temperature Heat Sources," Proc. 2nd Intersociety Energy Conversion Eng. Conf., p. 171 (1967).

14. Rasor, N. S., Hansen, L. K., Fitzpatrick, G. O., and Britt, E. J., "Practical Aspects of Plasma Processes in Thermionic Energy Converters," Proc. 10th Intersociety Energy Conversion Eng. Conf. (1975).

15. Lam, S. H., _Thermionic Energy Conversion Research Analysis –
    Annual Progress Report_, Princeton Univ. (1975).

16. _Advanced Thermionic Energy Conversion_, Prog. Rpt. No. COO-
    2263-4, Rasor Associates (1975).

17. Webster, H. F. and Beggs, J. E., Bull. Am. Phys. Soc. Ser. II 3,
    p. 266 (1958).

18. Hatsopoulos, G. N. and Kaye, J., "Analysis and Experimental
    Results of a Diode Configuration of a Novel Thermoelectron
    Engine," Proc. of the IRE, Vol. 46, No. 9, p. 1574 (1958).

19. Lam, S. H., _Preliminary Report on Plasma Arc-Drop in Thermionic
    Energy Converters_, Princeton Univ., Rpt. No. COO-2533-3 (March
    1976).

20. Hatsopoulos, G. N., _The Thermo Electron Engine_, Ph. D. Thesis,
    Massachusetts Institute of Technology (June 1976).

21. Moss, H., "Thermionic Diodes as Energy Converters," J. Electron.
    2, p. 305 (1957).

22. Webster, H. F., "Calculation of the Performance of a High-Vacuum
    Thermionic Energy Converter," J. Appl. Phys. 30, p. 488 (1959).

23. Hatsopoulos, G. N. and Gyftopoulos, E. P., _Thermionic Energy
    Conversion - Vol. I: Processes and Devices_, The MIT Press,
    Cambridge (1973).

APPENDIX

BARRIER INDEX

The "barrier index" is a convenient parameter for characterizing thermionic converter development, comparing experimental data, evaluating converter concepts and projecting improvements. The barrier index, V_B, incorporates the diode losses due to scattering, ionization, reflectivity, electrode patches and collector double valued sheath.

The barrier index has the advantage that it can be defined operationally, as illustrated in Figure 35.

For any given emitter temperature and output current, it is possible to adjust cesium pressure, spacing, and collector temperature to maximize the power output. The spacing envelope of the optimized performance curves is shown in Figure 35 for a converter with an emitter temperature of 1800 K. This envelope is shifted by a constant potential difference from the Boltzmann line, which represents the ideal current-voltage characteristics. This potential difference is defined as the "barrier index." In Figure 35 the barrier index, V_B, is 2.1 eV.

The equation for the Boltzmann line is:

$$J_B = AT_E^2 \exp(-eV/kT_E)$$

where:

J_B = ideal current density

A = Richardson constant

T_E = emitter temperature

e = electronic charge

V = output potential

k = Boltzmann constant

Often, sufficient data are not available to establish the envelope curve as in Figure 35. In this case, V_B is given by the minimum potential difference between the Boltzmann line and the measured J-V characteristic for optimized T_C, T_R and d.
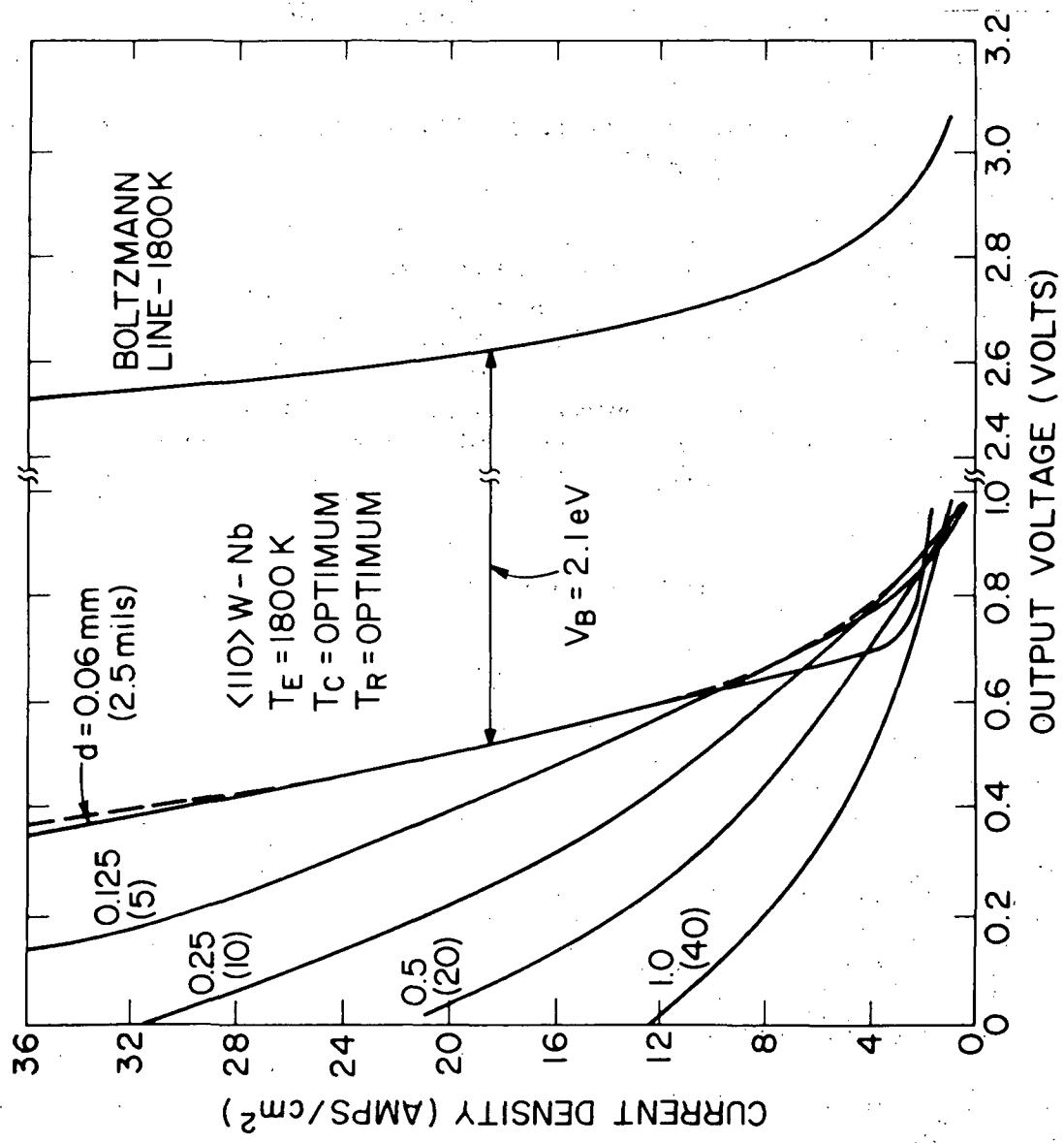
Figure 35. Spacing envelope of the optimized performance curves for a converter at $T_E = 1800\ K$ showing a constant barrier index of 2.1 eV

The Boltzmann line represents the idealized converter output
(up to the emitter saturation current) for zero collector work
function and zero collector temperature. Thus, the "barrier index"
incorporates the sum of the collector work function and the electron
transport losses (due to scattering, not supplied by an auxiliary
power source, electrode reflection, electrode patchiness, ionization
and, possibly, a double valued sheath at the collector) into a single
factor. For a given converter, the value of the barrier index is
independent of emitter temperature over a wide range. This oper-
ational definition of the barrier index gives a convenient means of
characterizing steady state thermionic diode development. Improve-
ments in the barrier index can be translated either into higher
efficiency at a given emitter temperature, or into the same efficiency
at a lower temperature.

For purposes of interpretation and analysis, V_B may be repre-
sented by:

$$V_B = \phi_C + V_d + S + \delta$$

where:

ϕ_C = collector work function

V_d = arc potential drop required to maintain ionization

δ = potential loss due to double valued sheath at the
collector

S = current attenuation index, which is the potential loss
due to all processes which attenuate current flow
through the converter (e.g., scattering, electrode
patchiness and electrode reflection)

$$= KT_E \ln (J_{ESAT}/J_{V_B})$$

where:

J_{ESAT} = emitter saturation current density

and

J_{V_B} = current density at the load potential corresponding to
the V_B determination

Because of the wide range of converter operating conditions and the narrow range of collector work function values of limited accuracy, for many years it had not been possible to discern any correlation between collector work function and converter performance. However, through the use of the measured barrier index and reliable work function determinations (by back emission and retarding data) on a variety of collector materials, it has become possible to develop the correlation shown in Figure 36.

The collector surfaces noted in Figure 36 can be categorized into four sets. The first set consists of a single converter with a polycrystalline tungsten collector. The poor performance of this converter is indicated by the barrier index of 2.2 eV. The high collector work function of 1.83 eV suggests that the collector was contaminated during fabrication. The second set of polycrystalline collectors (molybdenum and niobium) yielded barrier indices close to 2.1 eV. The third set of electropolished single crystal collectors reduced the barrier index to about 2.0 eV. The fourth set consists of tungsten oxide collectors with barrier indices as low as 1.9 eV. Thus, the correlation in Figure 36 demonstrates that a reduction in collector work function is reflected in improved converter performance - at least, for collector work functions down to 1.35 eV.

High performance thermionic converters may require an additional electrode to minimize the arc drop, V_d. Such triodes (ignited and non-ignited) and pulsed diodes which require an auxiliary power input to provide ions for space charge neutralization can be characterized by a "converter barrier index," V_B^* defined by:

$$V_B^* = V_B + V_d^*/\eta_p$$

where:

V_d^* = potential loss due to auxiliary power input required to provide ions for space charge neutralization

$$= \frac{\text{Auxiliary Power Density Input}}{\text{Output Current Density}}$$

η_p = power processing efficiency from converter output to auxiliary power input

Thus V_B^* for triodes is equivalent to V_B for diodes provided that the current densities are comparable.

122
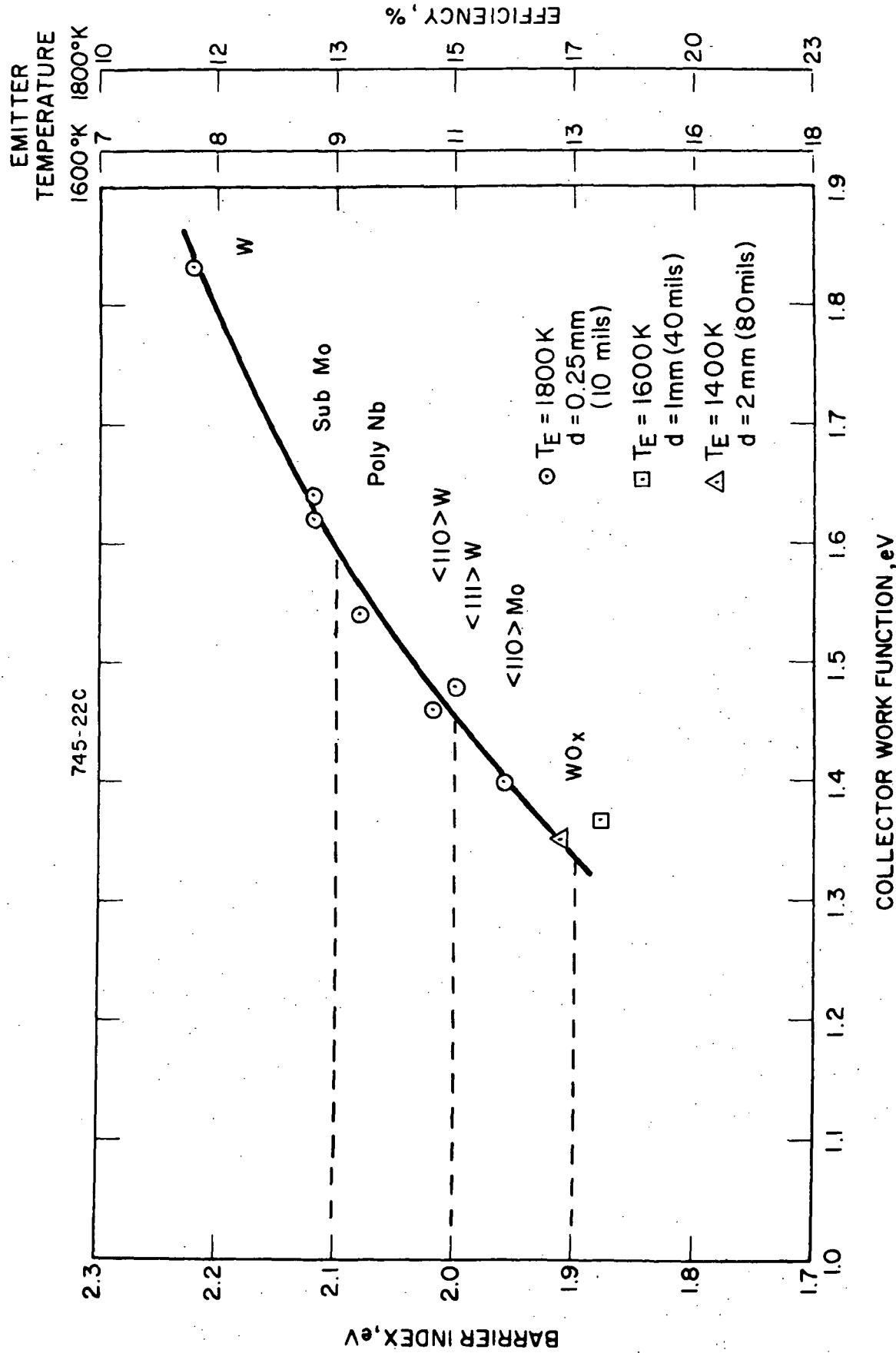
Figure 36. Barrier Index Versus Collector Work Function
for Various Collector Materials

123